

1 RESEARCH ARTICLE

2 **The AREB1 Transcription Factor Influences Histone**
3 **Acetylation to Regulate Drought Responses and Tolerance in**
4 ***Populus trichocarpa***

5 Shuang Li^{a,1}, Ying-Chung Jimmy Lin^{a,b,c,1}, Pengyu Wang^a, Baofeng Zhang^a,
6 Meng Li^a, Su Chen^a, Rui Shi^{b,d}, Sermsawat Tunlaya-Anukit^b, Xinying Liu^a,
7 Zhifeng Wang^a, Xiufang Dai^a, Jing Yu^a, Chenguang Zhou^a, Baoguang Liu^a, Jack
8 P. Wang^{a,b}, Vincent L. Chiang^{a,b,2}, Wei Li^{a,2}

9 ^a State Key Laboratory of Tree Genetics and Breeding, Northeast Forestry University,
10 Harbin 150040, China

11 ^b Forest Biotechnology Group, Department of Forestry and Environmental Resources,
12 North Carolina State University, Raleigh, NC 27695, USA

13 ^c Department of Life Sciences and Institute of Plant Biology, College of Life Science,
14 National Taiwan University, Taipei 10617, Taiwan

15 ^d Department of Crop and Soil Science, North Carolina State University, Raleigh, NC,
16 USA

17 ¹ These authors contributed equally to this work.

18 ² Address correspondence to: vchiang@ncsu.edu or weili2015@nefu.edu.cn

19 **Short title:** AREB1 recruits ADA2b-GCN5 upon drought stress

20 **One-sentence summary:** AREB1 recruits the ADA2b-GCN5 complex to control
21 H3K9ac and RNA polymerase II enrichment on drought-responsive genes, thereby
22 driving high expression of these genes for drought tolerance.

23 The authors responsible for distribution of materials integral to the findings presented
24 in this article in accordance with the policy described in the Instructions for Authors
25 (www.plantcell.org) are: Vincent L. Chiang (vchiang@ncsu.edu) and Wei Li
26 (weili2015@nefu.edu.cn).

27 **ABSTRACT**

28 Plants develop tolerance to drought by activating genes with altered levels of
29 epigenetic modifications. Specific transcription factors (TFs) are involved in this
30 activation, but the molecular connections within the regulatory system are unclear.
31 Here, we analyzed genome-wide H3K9ac enrichment and examined its association
32 with transcriptomes in *Populus trichocarpa* under drought stress. We revealed that
33 ABA-Responsive Element (ABRE) motifs in promoters of the drought-responsive
34 genes *PtrNAC006*, *PtrNAC007*, and *PtrNAC120* are involved in H3K9ac
35 enhancement and activation of these genes. Overexpressing these *PtrNAC* genes in
36 *P. trichocarpa* resulted in strong drought-tolerance phenotypes. We showed that the
37 ABRE binding protein PtrAREB1-2 binds to ABRE motifs associated with these

38 *PtrNAC* genes and recruits the histone acetyltransferase unit ADA2b-GCN5, forming
39 AREB1-ADA2b-GCN5 ternary protein complexes. Moreover, this recruitment enables
40 GCN5-mediated histone acetylation to enhance H3K9ac and enrich RNA polymerase
41 II specifically at these *PtrNAC* genes for the development of drought tolerance.
42 CRISPR-editing or RNAi-mediated downregulation of any of the ternary members
43 results in highly drought-sensitive *P. trichocarpa*. Thus, the combinatorial function of
44 the ternary proteins establishes a coordinated histone acetylation and TF-mediated
45 gene activation for drought response and tolerance in *Populus*.

46

47 **INTRODUCTION**

48 Drought severely affects plant growth, forest productivity, and survival
49 throughout the world. Under drought stress, stem hydraulic conductance and
50 above ground biomass production decrease, causing an up to 45% reduction in
51 radial growth in many forest species (Barber et al., 2000). Severe water
52 deprivation leads to death (Choat et al., 2012). *Populus* species, widely
53 distributed across the northern hemisphere, are among the most
54 drought-sensitive woody species (Monclus et al., 2006), but their wood is a
55 preferred renewable resource for biomaterials and bioenergy production
56 (Ragauskas et al., 2006). Drought-tolerant genotypes of these species could
57 influence the bioeconomy worldwide. Understanding genetic and regulatory
58 mechanisms of drought response and tolerance in *Populus* will enable effective
59 strategic engineering of novel robust genotypes.

60 Plants respond and adapt to drought stress by transcriptionally
61 reprogramming networks of gene expression regulated by a subset of
62 differentially activated or repressed transcription factors (TFs) (Nakashima et
63 al., 2014; Song et al., 2016). The differential expression of such TFs is typically
64 the result of changes in the levels of specific epigenetic modifications on the
65 genes for these TFs through stress signal transduction (Jaenisch and Bird,
66 2003; Kouzarides, 2007). Epigenetic marks are covalent modifications of
67 chromatin, such as histone acetylation and methylation, that initiate and

68 maintain the activities of TFs (Norton et al., 1989; Lee et al., 1993; Shahbazian
69 and Grunstein, 2007; Zentner and Henikoff, 2013).

70 Acetylated (ac) lysine (K) residue 9 of histone H3 (H3K9ac) is one of the
71 most extensively studied epigenetic marks in vascular plants (Kim et al., 2008;
72 Charron et al., 2009; Zhou et al., 2010; Li et al., 2011). Hyperacetylation of
73 H3K9 is almost invariably associated with activation of transcription in all
74 species studied so far, whereas hypoacetylated histones are accompanied by
75 transcriptional repression (Shahbazian and Grunstein, 2007; Zhou et al., 2010;
76 Li et al., 2011; Zentner and Henikoff, 2013). H3K9ac has been considered a
77 general chromatin marker of gene activation. Consistent with this, the
78 euchromatin (where DNA is accessible for transcription) of many eukaryotes,
79 including plants, is marked by H3K9ac (Kurdistani et al., 2004; Kouzarides,
80 2007; Shahbazian and Grunstein, 2007). H3K9ac is enriched in response to
81 drought stress in *Arabidopsis thaliana*, and this enrichment correlates with
82 transcriptional activation for four drought-responsive genes, *RD29A*, *RD29B*,
83 *RD20* and *At2g20880* (Kim et al., 2008, 2012). Importantly, rehydration rapidly
84 removes drought-induced H3K9ac enrichment from regions of these genes
85 (Kim et al., 2012). Chromatin immunoprecipitation sequencing (ChIP-seq)
86 analysis of chromatin modifications in the genome of the moss *Physcomitrella*
87 *patens* similarly demonstrated that H3K9ac patterns respond dynamically to
88 dehydration stress (Widiez et al., 2014).

89 Histone acetylation is catalyzed by histone acetyltransferase (HAT)
90 complexes (Shahbazian and Grunstein, 2007), many of which contain
91 GENERAL CONTROL NON-DEREPRESSIBLE 5 (GCN5) as the catalytic
92 subunit (Brownell et al., 1996) and ALTERATION/DEFICIENCY IN
93 ACTIVATION 2 (ADA2) as an adaptor protein (Grant et al., 1997). ADA2
94 increases the HAT activity of GCN5 (Balasubramanian et al., 2002).
95 *Arabidopsis* contains two related ADA2 factors, ADA2a and ADA2b (Stockinger

96 et al., 2001). *ada2b* mutants are hypersensitive to salt stress and ABA (Hark et
97 al., 2009), suggesting that ADA2b is involved in the abiotic stress response.
98 Mutations in GCN5 and ADA2 affect the expression of several cold-regulated
99 genes leading to reduced tolerance to freezing temperatures (Vlachonasios,
100 2003). GCN5 and ADA2 are required for root meristem development in
101 Arabidopsis and rice (Kornet and Scheres, 2009; Zhou et al., 2017).
102 GCN5-mediated histone acetylation plays important roles in regulating
103 transcriptional responses necessary for growth and adaptation to abiotic stress.

104 Transcriptional responses to drought stress in plants involve TFs, mostly
105 members of the bZIP, NAC, AP2/ERF, MYB, and MYC TF families (Nakashima
106 et al., 2014). **A**BA-**R**esponsive **E**lement **B**inding (AREB, also named ABF)
107 proteins of the bZIP family have been extensively characterized for their roles in
108 regulating drought stress responses. The AREB TF binds to the
109 **A**BA-**R**esponsive **E**lement (ABRE: PyACGTGG/TC) in the promoters of
110 drought-responsive genes, activating expression of these genes for drought
111 tolerance (Fujita et al., 2011). Transgenic Arabidopsis overexpressing
112 *AREB1/ABF2*, *AREB2/ABF4*, and *ABF3* exhibits enhanced drought tolerance
113 (Fujita et al., 2005, 2011). Arabidopsis plants overexpressing TF and other
114 genes with ABRE motif-containing promoters, such as *ANAC002/ATAF1* (Wu
115 et al., 2009), *ANAC019*, *ANAC055* (Tran et al., 2004; Hickman et al., 2013),
116 *ANAC072/RD26* (Fujita et al., 2004; Tran et al., 2004), and *GBF3* (Fujita et al.,
117 2005; Ramegowda et al., 2017), and *HIS1-3* (Ascenzil and Gantt, 1999), *RD20*
118 (Aubert et al., 2010), and *RD29B* (Msanne et al., 2011), also show increased
119 drought tolerance. It is well established that drought tolerance is developed
120 through activation of ABRE-associated genes and that H3K9ac enrichments at
121 such genes are positively correlated with the activation of these genes;
122 however, there has long been a missing link between the two regulatory
123 mechanisms. It remains unclear what system catalyzes the enrichment of

124 H3K9ac modifications and how this system is brought specifically to genes with
125 ABRE-containing promoters. Knowledge of the regulatory mechanisms that
126 initiate and determine drought responses and tolerance is lacking for plants,
127 particularly for tree species.

128 Wood is made up of xylem, the conductive tissue that transports water from
129 soil to leaves and provides mechanical support for the entire plant (Evert, 2006).
130 Stem xylem vessels are highly vulnerable to drought-induced cavitation, which
131 causes interruption of water transport through xylem and stomatal closure
132 leading to a rapid reduction of photosynthesis (Tyree and Sperry, 1989;
133 Arango-Velez et al., 2011). Stem differentiating xylem (SDX) is rich in signaling
134 events and gene transregulation machineries associated with drought
135 response and tolerance (Bogeat-Triboulot et al., 2007; Berta et al., 2010). Stem
136 xylem is therefore a unique biological system in which to learn about regulatory
137 mechanisms of drought response and tolerance.

138 In this study, we used *Populus trichocarpa* for soil-water depletion
139 experiments and analyzed SDX tissue by ChIP-seq and RNA sequencing
140 (RNA-seq) for genome-wide H3K9ac distribution and gene expression. We
141 then identified 76 drought-responsive TF genes whose expression was
142 affected by differential modification of H3K9ac in their promoters, where we
143 found that the ABRE sequence was the most significantly differentially enriched
144 ($P < 10^{-24}$) motif. The 76 ABRE-containing TFs included a subset of NAC genes,
145 among which we focused on three (*PtrNAC006*, *PtrNAC007*, and *PtrNAC120*)
146 and demonstrated that they induce strong drought-tolerant phenotypes when
147 overexpressed in transgenic *P. trichocarpa*. We identified coordinated
148 regulation of histone acetylation and TF-mediated gene activation in drought
149 response and tolerance. Binding of trimeric AREB1-ADA2b-GCN5 protein
150 complexes to ABRE motifs in promoters of drought-responsive genes, such as
151 the three *PtrNAC* genes, elevated their H3K9ac levels and RNA polymerase II

152 recruitment, leading to activation of the *PtrNAC* genes and increasing drought
153 tolerance. This coordinated regulation required the combinatorial function of
154 AREB1, ADA2b, and GCN5 proteins.

155

156 **RESULTS**

157 **The H3K9ac Profile Changes in SDX Tissue of *P. trichocarpa* in** 158 **Response to Drought**

159 To gain insight into the role of H3K9ac modifications in drought response, we
160 generated genome-wide H3K9ac profiles for 3-month-old control and
161 drought-treated *P. trichocarpa* plants maintained in a greenhouse
162 (Supplemental Figure 1). Pilot drought experiments suggested that 5-day (D5)
163 and 7-day (D7) drought treatments together would most likely induce changes
164 in the greatest number of genes most highly responsive to drought stress
165 (Supplemental Figure 1A, B). We therefore applied these two treatments for
166 subsequent ChIP-seq and RNA-seq analyses. We performed ChIP-seq on
167 SDX tissue collected from plants with regular watering (control, no drought
168 (ND); Supplemental Figure 1C, D) and plants under drought treatment
169 (soil-water depletion) for 5 and 7 days (D5, D7; Supplemental Figure 1C, D;
170 Method). The SDX tissue collection from the control (ND) and the
171 drought-treated (D5 and D7) plants was conducted at the same day and at the
172 same time (Supplemental Figure 1C). ChIP-seq was conducted using
173 antibodies against H3K9ac according to the protocol developed for woody
174 species (Lin et al., 2013; Li et al., 2014). We used diffReps (Shen et al., 2013)
175 to identify differential H3K9ac-modified genomic regions (peaks) between
176 5-day drought and control plants (D5/ND) and between 7-day drought and
177 control plants (D7/ND). We found 4578 peaks with increased H3K9ac
178 modification and 5081 peaks with decreased H3K9ac modification for D5/ND,
179 and 5530 increased and 5399 decreased H3K9ac modification regions for

180 D7/ND (P -adj<0.05, Benjamini-Hochberg-adjusted P value in diffReps analysis)
181 (Supplemental Table 1). These results are consistent with the involvement of
182 H3K9ac modifications in drought response in *Physcomitrella patens* (Widiez et
183 al., 2014) and *Arabidopsis* (Kim et al., 2008, 2012; Kim et al., 2008), and
184 provide evidence of such involvement in a tree species.

185 In each of the 19 *P. trichocarpa* chromosomes, these differential H3K9ac
186 peaks were mainly located in genic regions and were relatively rare in
187 intergenic regions (Supplemental Figure 2A, B). The percentage of differential
188 H3K9ac peaks on each chromosome was positively correlated with
189 chromosome size (Supplemental Figure 2C). Fewer differential H3K9ac peaks
190 were identified in chromosomal regions where transposable element (TE)
191 density was high (Supplemental Figure 2C); TEs are particularly common in
192 heterochromatic regions of the genome. Fewer peaks were also distributed in
193 putative centromeric regions of the 19 *P. trichocarpa* chromosomes
194 (Supplemental Figure 2C). Differential H3K9ac peaks were distributed evenly
195 across all chromosomal regions except intergenic, TE, and centromeric
196 regions, indicating that H3K9ac alteration preferentially occurs within gene-rich
197 regions in *P. trichocarpa* under drought stress.

198

199 **Integrative Analysis of ChIP-seq and RNA-seq Data Identifies a Set of** 200 **Drought Stress-Responsive Genes with Differential H3K9ac**

201 Next, we determined whether the differential H3K9ac enrichments were
202 responsible for regulating gene expression changes in response to drought
203 stress. We performed RNA-seq to characterize transcriptome changes in SDX
204 tissues in response to drought stress (Supplemental Figure 1; Methods). RNAs
205 used for constructing the RNA-seq libraries were extracted from the same SDX
206 tissues used for ChIP-seq analyses. Using EdgeR (Robinson et al., 2010) and
207 our analysis pipeline (Lin et al., 2013), we characterized the RNA-seq results

208 to identify differentially expressed genes (DEGs) induced by drought
209 treatments. We found 8341 upregulated and 7118 downregulated genes after
210 5 days of drought stress (D5/ND, False Discovery Rate (FDR)<0.05), and
211 6334 upregulated and 5394 downregulated genes after 7 days of drought
212 treatment (D7/ND, FDR<0.05) (Supplemental Figure 3 and Supplemental
213 Table 2). Gene Ontology (GO) analysis (Supplemental Figure 4) showed that
214 the number of genes in nearly all GO categories at D7 was lower than that at
215 D5. In addition, two classes of genes, “regulation of developmental process”
216 and “regulation of growth” (Supplemental Figure 4), were completely absent
217 from D7 data. The absence of these two classes of genes may be a major
218 reason for the difference in DEG numbers between D5 and D7 treatments.

219 Using BETA (Wang et al., 2013), we integrated the H3K9ac ChIP-seq data
220 with the RNA-seq data (D5/ND; D7/ND) to identify the DEGs exhibiting
221 differential H3K9ac levels (Supplemental Figure 5). We focused on DEGs with
222 differential H3K9ac enrichment in promoter regions (within \pm 2 kb of the
223 transcription start site (TSS); Methods) to identify genes most likely to be
224 directly regulated by H3K9ac modification (Figure 1A, B). There are four
225 possible combinations for the correlation of differential H3K9ac modification
226 and differential gene expression (Figure 1A, B). These combinations are: (1)
227 increased H3K9ac level induces gene downregulation (histone level up-gene
228 down, hUP-gDN; red dots in Figure 1A, B), (2) increased H3K9ac level
229 induces gene upregulation (hUP-gUP) (blue dots), (3) decreased H3K9ac level
230 induces gene upregulation (hDN-gUP) (red dots), and (4) decreased H3K9ac
231 level induces gene downregulation (hDN-gDN) (blue dots). Because H3K9ac
232 is an activating mark (Kurdistani et al., 2004; Shahbazian and Grunstein, 2007;
233 Charron et al., 2009 Zhou et al., 2010; Li et al., 2011; Zentner and Henikoff,
234 2013;), combinations showing hUP-gUP and hDN-gDN are most likely to
235 represent direct effects on gene expression. We therefore focused on the

236 DEGs with the hUP-gUP and hDN-gDN combinations and identified 3,994
237 DEGs (with 4,026 modification sites) that exhibited differential H3K9ac levels
238 in the promoter regions (blue dots; Figure 1A) after 5 days of drought treatment
239 (D5/ND; Supplemental Data set 1) and 3498 such DEGs (with 3527
240 modification sites) after 7 days of drought treatment (blue dots; D7/ND; Figure
241 1B and Supplemental Data set 2).

242 We further analyzed the hUP-gUP and hDN-gDN set of genes by
243 performing GO enrichment analysis of these genes to explore their functional
244 significance. Biological pathways responsive to stimulus, water deprivation,
245 abscisic acid, and abscisic acid-activated signaling pathway were significantly
246 enriched among this hUP-gUP and hDN-gDN set of genes (Supplemental
247 Data set 3). Many other biological processes such as cell wall biogenesis and
248 developmental process were also highly enriched among this gene set. These
249 results suggest that H3K9ac may regulate drought-responsive genes through
250 ABA-dependent regulation and that H3K9ac modifications may systemically
251 influence the expression of the genes with diverse functions associated with
252 drought response and tolerance. Therefore, this gene expression regulation
253 may involve interplay between H3K9ac and TFs.

254

255 **The Abscisic Acid–Responsive Element Was Identified in Promoters of** 256 **Genes with Differential H3K9ac Modifications**

257 TFs are known to regulate their target genes through binding to specific
258 regulatory DNA sequences (*cis*-elements or TF-binding motifs). To investigate
259 whether interplay between H3K9ac and TFs is involved in the transcriptional
260 regulation of drought-response genes, we examined the enrichment of
261 TF-binding motifs within the promoters of the 3994 and 3498 DEGs with
262 differential H3K9ac levels after a 5-day drought (D5/ND) and 7-day drought
263 (D7/ND), respectively, using Analysis of Motif Enrichment (AME) (McLeay and

264 Bailey, 2010) motif searches. This analysis revealed that the ABRE
265 (**ABA-Responsive Element**) motif for the AREB1 (**ABA-Responsive Element**
266 **B**inding 1)-type protein (Fujita et al., 2005, 2011) was most significantly
267 enriched within the H3K9ac-associated promoters for both D5/ND ($P < 10^{-28}$,
268 Fisher's exact test; sequence in red font in Figure 1C, E) and D7/ND ($P < 10^{-24}$,
269 Fisher's exact test; sequence in red, Figure 1D, E). The ABRE is a *cis*-element
270 that controls the expression of many ABA- and drought-responsive genes in
271 *Arabidopsis* and many food crops (Nakashima et al., 2014). Our results
272 indicated that ABRE likely plays a similar role in drought response and
273 resistance in a tree species. Therefore, we focused on the ABRE motif to
274 investigate how AREB1 TF binding to ABRE-containing promoters might
275 interplay and coordinate with H3K9ac in response to drought stress. We first
276 identified the relevant genes with ABRE-containing promoters.

277

278 **ABRE Motifs Mediate H3K9ac Association and Regulation of *PtrNAC*** 279 **Genes**

280 Activating the expression of ABRE-containing genes encoding TF and non-TF
281 proteins has been shown to induce drought tolerance in *Arabidopsis* (Ascenzil
282 and Gantt, 1999; Tran et al., 2004; Fujita et al., 2005; Wu et al., 2009; Aubert
283 et al., 2010; Msanne et al., 2011; Hickman et al., 2013; Nakashima et al., 2014;
284 Ramegowda et al., 2017). The induction is particularly effective with the
285 activation of ABRE-containing TFs (Tran et al., 2004; Fujita et al., 2005; Wu et
286 al., 2009; Hickman et al., 2013; Ramegowda et al., 2017). We analyzed our
287 sequence data, focusing on identifying drought-responsive TF DEGs that had
288 the ABRE motif as well as differential H3K9ac levels in their promoters. We
289 found 60 and 53 such TF genes after 5-day (D5/ND; Supplemental Data set 4)
290 and 7-day (D7/ND; Supplemental Data set 5) drought treatments, respectively.
291 Among these 113 (60+53) TF genes, 37 were common to both the D5 and D7

292 treatments (highlighted in gray in Supplemental Data sets 4 and 5), 23 were
293 specific at D5 (highlighted in yellow in Supplemental Data set 4), and 16 were
294 specific at D7 (highlighted in blue in Supplemental Data set 5). There were
295 thus 76 unique TF genes among these 113 TF genes. While these 76
296 drought-responsive TFs have not previously been reported in a woody species,
297 some of their orthologs in other species have been suggested or demonstrated
298 to play roles in drought response and tolerance (Nakashima et al., 2014).

299 *ANAC002/ATAF1*, *ANAC019*, *ANAC055*, *ANAC072/RD26*, and *GBF3* are
300 so far the only ABRE-containing TFs validated roles in enhancing drought
301 tolerance in transgenic Arabidopsis (Fujita et al., 2004, 2005; Tran et al., 2004;
302 Wu et al., 2009; Hickman et al., 2013; Ramegowda et al., 2017). Sequences of
303 *ANAC019* and *ANAC055* are absent from the *P. trichocarpa* genome, and the
304 *GBF3* ortholog (Potri.002G167100) was also not included in our
305 ABRE-containing TF lists (Supplemental Data sets 4, 5) because its transcript
306 levels were not affected by 5- or 7-day drought treatments (Supplemental Data
307 set 6). Therefore, we focused on identifying orthologs of *ANAC002/ATAF1* and
308 *ANAC072/RD26* in *P. trichocarpa*.

309 *ANAC002/ATAF1* (Hu et al., 2010; Wu et al., 2009) has three *P.*
310 *trichocarpa* orthologs with high protein sequence identity, *PtrNAC005*
311 (Potri.005G069500), *PtrNAC006* (Potri.002G081000), and *PtrNAC007*
312 (Potri.007G099400), and *ANAC072/RD26* (Hu et al., 2010; Tran et al., 2004)
313 has two, *PtrNAC118* (Potri.011G123300) and *PtrNAC120* (Potri.001G404100)
314 (Supplemental Figure 6, and Supplemental Data sets 4 and 5). All these
315 *PtrNAC* genes were highly induced by drought, showing 15- to 400-fold
316 increases in transcript levels determined by reverse-transcription quantitative
317 PCR (RT-qPCR) (Figure 2A). This suggested that these *PtrNAC* genes are
318 strong positive regulators in the ABA-mediated drought signaling pathway,

319 similar to *ANAC002/ATAF1* and *ANAC072/RD26* (Tran et al., 2004; Wu et al.,
320 2009).

321 The five *PtrNAC* genes have one or multiple ABRE motifs in their
322 promoters (2 kb upstream of the TSS) (Figure 2B). We used CHIP with
323 quantitative PCR (CHIP-qPCR) to analyze the influence of drought stress on
324 H3K9ac levels in the ABRE motif regions of the promoters of these five
325 *PtrNAC* genes. Both CHIP-qPCR (Figure 2C) and CHIP-seq (Supplemental
326 Table 1) data consistently demonstrated that as the duration of drought
327 treatment increased, H3K9ac enrichment increased progressively in all the
328 identified ABRE motif regions of the five *PtrNAC* promoters (Figure 2C). The
329 progressive H3K9ac enrichment with drought severity implied that ABRE
330 motifs are significant contributors to the regulation of *PtrNAC* expression in
331 response to drought stress.

332 We then investigated whether the outcome of this regulation of *PtrNAC*
333 expression induces drought tolerance. To do this, we aimed to overexpress
334 these *PtrNAC* genes in *P. trichocarpa* and test the transgenic plants for
335 drought response and tolerance. The five *PtrNAC* genes belong to three
336 sub-groups, with *PtrNAC006* as the sole member of its group, *PtrNAC005* and
337 *PtrNAC007* as homologous members of one sub-group, and *PtrNAC118* and
338 *PtrNAC120* as homologs in another sub-group (Supplemental Figure 6). From
339 each sub-group, we selected the most highly drought-inducible member
340 (Figure 2A), i.e., *PtrNAC006*, *PtrNAC007*, and *PtrNAC120*, for transgenic
341 study.

342

343 **Overexpressing *PtrNAC* Genes Improves Drought Tolerance of *P.*** 344 ***trichocarpa***

345 We overexpressed (OE) *PtrNAC006* (Supplemental Figure 7), *PtrNAC007*,
346 and *PtrNAC120* individually in *P. trichocarpa* under the control of a CaMV 35S

347 promoter. From the plants containing each transgene construct, we selected
348 the line with the highest transgene transcript level (Supplemental Figure 8A).
349 These transgenics, named *OE-PtrNAC006*, *OE-PtrNAC007*, and
350 *OE-PtrNAC120*, were multiplied along with the wild-type and maintained in a
351 walk-in growth chamber (Method) for further analysis. Three-month-old clonal
352 copies of the wild-type and *OE-PtrNAC* plants were used for drought
353 experiments, with a set of these copies being well-watered and another set of
354 these copies (at least 12 for wild-type and for each transgenic type) grown
355 without watering for 12 d. Our screening experiments (Supplemental Figure 1)
356 demonstrated that 12-day drought was lethal to 3-month-old wild-type *P.*
357 *trichocarpa* plants, and this was therefore used for drought tolerance (survival
358 rate) tests. All *OE-PtrNAC* transgenics exhibited drought tolerance, which was
359 particularly strong for *OE-PtrNAC006* plants, while wild-type plants showed
360 severe wilting symptoms (Figure 3A). The growth of *OE-PtrNAC006*
361 transgenics was reduced (Figure 3B), but they wilted to a much lesser extent
362 than the wild-type and the other transgenic types (Figure 3A).

363 After the drought treatment, all plants were rehydrated for 3 days to
364 estimate their survival rates. Most of the wild-type plants did not recover, giving
365 only a 13% survival rate (Figure 3A, C). By contrast, all transgenics recovered
366 rapidly (Figure 3A) with a survival rate of ~76% for *OE-PtrNAC006*, ~56% for
367 *OE-PtrNAC007*, and ~39% for *OE-PtrNAC120* (Figure 3C). The recovered
368 transgenics were maintained in a growth room, where they began to exhibit
369 similar growth and development to their well-watered clonal copies, whereas
370 the drought-stressed wild-type plants grew more slowly than their well-watered
371 controls (Supplemental Figure 8B). Therefore, *OE-PtrNAC* transgenics were
372 both drought tolerant and resilient, particularly the *OE-PtrNAC006* plants.

373 We next examined the effect of *PtrNAC* gene overexpression on alterations
374 in physiology that may contribute to drought survival. Higher stem xylem water

375 potential can prevent drought-induced hydraulic failure and enhance drought
376 resistance (Choat et al., 2012). Consistent with the visible phenotypes,
377 *OE-PtrNAC* plants had higher stem xylem water potential under drought stress
378 (Figure 3D) than did wild-type plants. We then analyzed the morphology of
379 stem xylem cells. Structure and size of stem xylem vessels, the conducting
380 cells, are key factors affecting water transport in plants and are important
381 determinants of drought tolerance (Fisher et al., 2007). The stem xylem
382 vessels in all *OE-PtrNAC* plants, *OE-PtrNAC006* in particular, were smaller
383 than those in wild-type plants (Figure 4A, B, E and *OE-PtrNAC007*,
384 *OE-PtrNAC120* in Supplemental Figure 9). The vessel number per unit area in
385 all *OE-PtrNAC* plants was much greater than that in wild-type plants; a more
386 than 4-fold increase in number was observed in *OE-PtrNAC006* (Figure 4C).
387 Consequently, the area of vessels (void area) in the transverse section of the
388 woody stem was significantly increased in all *OE-PtrNAC* plants (Figure 4D).
389 The increase may contribute to more effective water transport in plants.

390 Our results indicate that *PtrNAC006*, *PtrNAC007*, and *PtrNAC120* are
391 effector genes that transduce key physiological alterations conducive to
392 drought tolerance and resilience. We therefore focused on these genes to
393 investigate whether there is interplay between H3K9ac and AREB1-type TFs
394 and how such interplay regulates the expression of effector genes for drought
395 tolerance in plants. To do this we first examined AREB1 TF homologs in *P.*
396 *trichocarpa* and their responses to drought.

397

398 **PtrAREB1-2 Activates Transcription of the Three *PtrNAC* Genes and** 399 **Directly Binds to the ABRE Motifs in Their Promoters**

400 The AREB1 TF binds to the ABRE motif in promoters of drought-responsive
401 genes to activate expression of these genes for drought tolerance (Fujita et al.,
402 2011). Transgenic *Arabidopsis* overexpressing *AREB1* exhibits enhanced

403 drought tolerance (Fujita et al., 2005, 2011). We identified four *AREB1*
404 homologs in *P. trichocarpa*: *PtrAREB1-1* (Potri.001G371300), *PtrAREB1-2*
405 (Potri.002G125400), *PtrAREB1-3* (Potri.009G101200), and *PtrAREB1-4*
406 (Potri.014G028200). However, the *PtrAREB1-1* transcript could not be
407 detected in RNA-seq of SDX, with and without drought treatment. Both
408 RNA-seq and RT-qPCR analyses revealed that the remaining three *PtrAREB1*
409 genes (*PtrAREB1-2*, -3, and -4) were readily detectable in SDX at ND and
410 highly and similarly induced after D5 or D7 drought treatments (Figure 5A and
411 Supplemental Data set 6). Among these three, *PtrAREB1-2* showed the
412 highest protein sequence identity (Supplemental Figure 10) to the Arabidopsis
413 *AREB1* gene, which mediates a strong drought tolerance in Arabidopsis (Fujita
414 et al., 2005). Thus, we focused on *PtrAREB1-2* to test whether the AREB1 TF
415 coordinates ABRE motif-induced H3K9ac enrichment to regulate expression of
416 drought-tolerance effector genes, such as *PtrNAC006*.

417 In Arabidopsis, AREB1 is a transcriptional activator of ABRE-mediated
418 genes (Fujita et al., 2005). Full activation of AREB1 requires ABA (Fujita et al.,
419 2005; Yoshida et al., 2010), and activation activity is regulated by the
420 ABA-dependent phosphorylation of multiple sites within the conserved
421 domains of AREB1 (Furiihata et al., 2006). We tested whether *PtrAREB1-2* can
422 activate expression of the three *PtrNAC* effector genes, the ABRE-mediated
423 genes, in *P. trichocarpa*. We overexpressed *PtrAREB1-2* in *P. trichocarpa*
424 SDX protoplasts (Lin et al., 2013, 2014) to identify transregulation targets of
425 TFs *in vivo*. RT-qPCR analysis demonstrated a modest effect of *PtrAREB1-2*
426 overexpression on expression of the *PtrNAC* effector genes (Supplemental
427 Figure 11). However, in the presence of external ABA, overexpression of
428 *PtrAREB1-2* induced significant increases in transcript levels of the three
429 *PtrNAC* genes (Figure 5B). These results suggested that *PtrNAC006*,
430 *PtrNAC007*, and *PtrNAC120* are *PtrAREB1-2*-mediated positive regulators in

431 the ABA-dependent signaling pathway for drought tolerance. This mediation
432 further suggests that PtrAREB1-2 binds directly to ABRE motifs in the
433 promoters of *PtrNAC006*, *PtrNAC007*, and *PtrNAC120* enabling gene
434 transactivation.

435 To determine whether PtrAREB1-2 directly binds to ABRE motifs in the
436 promoters of *PtrNAC* genes, anti-GFP antibody CHIP was carried out using
437 SDX protoplasts constitutively expressing a PtrAREB1-2-GFP fusion. We
438 isolated SDX protoplasts and transfected a portion of the protoplasts with a
439 plasmid DNA (pUC19-35S_{pro}-PtrAREB1-2-GFP) for overexpressing Ptr
440 AREB1-2-GFP. Another portion of the SDX protoplasts was transfected with a
441 pUC19-35S_{pro}-sGFP plasmid as a mock control. After 12 h, chromatin was
442 isolated from the transfected protoplasts for CHIP and qPCR analyses. We
443 detected 3- to 6-fold enrichment of ABRE motif sequences from the three
444 *PtrNAC* genes (Figure 5C), confirming that PtrAREB1-2 directly binds to ABRE
445 motifs in the promoters of these *NAC* genes in *P. trichocarpa*. We also used an
446 electrophoretic mobility shift assay (EMSA) to test for direct binding of
447 PtrAREB1-2 to ABRE motifs in promoters of *PtrNAC*s. Retardation of DNA
448 probe mobility and competition analyses demonstrated that PtrAREB1-2 could
449 directly bind to the ABRE motifs in promoters of the three *PtrNAC* genes
450 (Figure 5D, E, F). Furthermore, EMSA competition analyses with ABRE
451 competitors carrying a single nucleotide mutation confirmed that the core
452 ACGTGG/TC sequence is essential for PtrAREB1-2 binding to ABRE motifs
453 (Figure 5D, E, F). We next investigated how such binding mediates increased
454 H3K9ac (Figure 2C) to regulate expression of *NAC* genes (Figure 2A).

455

456 **AREB1 TFs Interact with the HAT Complex ADA2b-GCN5**

457 TFs typically interact with transcriptional co-activators for binding to the
458 specific regions of their target gene promoters for transcriptional regulation

459 (Stockinger et al., 2001; Mao et al., 2006; Weiste and Droge-Laser, 2014;
460 Zhou et al., 2017). The SAGA (Spt-Ada-Gcn5 acetyltransferase) complex is a
461 highly conserved transcriptional co-activator that is involved in the transcription
462 of nearly all active genes in yeast and plants (Koutelou et al., 2010; Bonnet et
463 al., 2014; Zhou et al., 2017). We hypothesized that an ADA2b-GCN5 HAT
464 complex (Vlachonasios, 2003) may be recruited to the promoters of
465 drought-tolerance effector genes, such as the *PtrNAC* genes, by AREB1 to
466 elevate the acetylation of H3K9, leading to activation of these effector genes.
467 To test this hypothesis, we first surveyed the *P. trichocarpa* genome and found
468 an ADA2b-like protein (*PtrADA2b*, Potri.004G135400) with a sequence similar
469 to that of Arabidopsis ADA2b (47% protein sequence identity). Furthermore,
470 *PtrADA2b* was induced by drought stress based on our RT-qPCR (Figure 6A)
471 and RNA-seq analyses (Supplemental Data set 6). We then cloned *PtrADA2b*
472 cDNAs to study their transcriptional functions. The *PtrADA2b* gene has five
473 exons and four introns, encoding cDNAs of ~0.5 kb. The cDNAs were
474 PCR-amplified from SDX of *P. trichocarpa*, and three products of ~0.5, ~0.8,
475 and ~1.0 kb were obtained (Supplemental Figure 12A). Sequence analysis of
476 the three products showed that pre-mRNAs from the *PtrADA2b* gene
477 underwent alternative splicing events in the fourth exon and third intron,
478 generating three splice variants (*PtrADA2b-1*, *PtrADA2b-2*, and *PtrADA2b-3*;
479 Supplemental Figure 12B). Among the three splice variants of *PtrADA2b*,
480 *PtrADA2b-3* showed the highest protein sequence identity to the Arabidopsis
481 *ADA2b* gene. Therefore, we focused on *PtrADA2b-3* for further study.

482 We also found two GCN5 homologs, *PtrGCN5-1* (Potri.002G045900) and
483 *PtrGCN5-2* (Potri.005G217400), in the *P. trichocarpa* genome (Supplemental
484 Data set 6). The two homologs share 84% protein sequence identity. Although
485 *PtrGCN5-1* was not a DEG in RNA-seq (Supplemental Data set 6), RT-qPCR
486 results demonstrated that *PtrGCN5-1* was drought-inducible and expressed

487 abundantly in xylem tissue (Figure 6B). However, *PtrGCN5-2* was expressed
488 at very low levels under both well-watered and drought conditions (Figure 6B).
489 We selected *PtrGCN5-1* together with *PtrADA2b-3* to test our hypothesis that
490 an ADA2b-GCN5 HAT complex can be recruited by AREB1 for
491 hyperacetylating H3K9 to activate the ABRE-mediated genes. Therefore, in *P.*
492 *trichocarpa*, there should be a ternary protein complex,
493 PtrADA2b-PtrGCN5-PtrAREB1, that binds to ABRE motifs of *PtrNAC* genes,
494 such as *PtrNAC006*, to elevate their H3K9ac.

495 Having already demonstrated that PtrAREB1 binds directly to the ABRE
496 motifs of *PtrNAC006*, *PtrNAC007*, and *PtrNAC120* (Figure 5C-F), we next
497 tested the potential interactions among PtrADA2b-3, PtrGCN5-1, and
498 PtrAREB1-2 *in vitro* and *in vivo*. We first tested the pairwise interaction
499 between PtrADA2b-3 and PtrGCN5-1. Pull-down assays using *Escherichia*
500 *coli*-produced PtrGCN5-1:6xHis-tag and PtrADA2b-3:S-tag, or
501 PtrGCN5-1:6xHis-tag and GFP:S-tag fusion proteins showed that
502 PtrADA2b-3:S-tag, but not GFP:S-tag, was retained by the PtrGCN5-1:6xHis
503 protein, indicating that PtrGCN5-1 interacts with PtrADA2b-3 (Figure 6C). We
504 then tested pairwise interactions between PtrADA2b-3 and PtrAREB1-2, and
505 between PtrAREB1-2 and PtrGCN5-1. *In vitro* pull-down demonstrated
506 interactions between the S-tagged PtrADA2b-3 and the His-tagged
507 PtrAREB1-2 (Figure 6D) and between the S-tagged PtrAREB1-2 and the
508 His-tagged PtrGCN5-1 (Figure 6E). These pairwise (PtrADA2b-3:PtrGCN5-1,
509 PtrADA2b-3:PtrAREB1-2, and PtrAREB1-2:PtrGCN5-1) interactions suggest
510 the involvement of ternary protein complexes made from PtrADA2b, PtrGCN5,
511 and PtrAREB1. We then performed bimolecular fluorescence
512 complementation (BiFC) assays to confirm the presence of these pairwise
513 interactions *in vivo* using *P. trichocarpa* SDX protoplasts.

514 PtrADA2b-3:YFP^N, where PtrADA2b-3 was fused to the N-terminus of YFP
515 (aa 1-174), and PtrGCN5-1:YFP^C (PtrGCN5-1 fused to the C-terminus of YFP
516 (aa 175-239)) were co-expressed together with the H2A-1:mCherry nuclear
517 marker in SDX protoplasts. The presence of the two fusion proteins
518 reconstituted YFP signals, which were colocalized with H2A-1:mCherry
519 exclusively in the nucleus, confirming that PtrADA2b-3 interacts with
520 PtrGCN5-1 forming dimers *in vivo* (Figure 6F and Supplemental Figure 13A, J).
521 Nuclear-localized YFP signals were also observed for moieties representing
522 dimers of PtrADA2b-3 and PtrAREB1-2 (Figure 6G and Supplemental Figure
523 13B, K) and of PtrAREB1-2 and PtrGCN5-1 (Figure 6H and Supplemental
524 Figure 13C, L). Empty plasmids and PtrMYB021, an unrelated TF expressed in
525 the nucleus (Li et al., 2012), were used as negative controls. Co-transfection of
526 each protein of interest with empty plasmid did not yield any YFP signal
527 (Figure 6I-K and Supplemental Figure 13D-F and M-O). Co-expression of the
528 PtrADA2b-3:YFP^N fusion and PtrMYB021:YFP^C (Figure 6L and Supplemental
529 Figure 13G, P), of PtrMYB021:YFP^N and PtrAREB1-2:YFP^C (Figure 6M and
530 Supplemental Figure 13H, Q), or of PtrMYB021:YFP^N and PtrGCN5-1:YFP^C
531 (Figure 6N and Supplemental Figure 13I, R) with H2A-1:mCherry resulted in
532 the detection of only H2A-1:mCherry signals in the nucleus, demonstrating the
533 interaction specificity between the paired proteins tested. The observed YFP
534 signals (Figure 6F-H and Supplemental Figure 13A-C and J-L) were therefore
535 the consequence of dimerization of the paired proteins tested. These results
536 are consistent with the *in vitro* evidence (Figure 6C-E) suggesting ternary
537 protein complexes involving PtrADA2b-3, PtrGCN5-1, and PtrAREB1-2.

538

539 **PtrADA2b-3 and PtrGCN5-1 Together Enhance PtrAREB1-Mediated**
540 **Transcriptional Activation of *PtrNAC* Genes by Increasing H3K9ac Level**
541 **and RNA Polymerase II Recruitment at Their Promoters**

542 The *in vitro* and *in vivo* protein interaction assays and CHIP-qPCR validated
543 our hypothesis that PtrADA2b-3, PtrGCN5-1, and PtrAREB1-2, form dimeric or
544 ternary protein complexes (Figure 6C-N and Supplemental Figure 13A-R) for
545 binding to ABRE motifs in promoters of the *PtrNAC* genes (Figure 5C). Binding
546 is through the complex's PtrAREB1-2 member, creating a *PtrNAC*
547 gene-specific HAT system to mediate enhanced H3K9ac of *NAC* genes for
548 their elevated expression. However, we demonstrated that PtrAREB1-2 alone
549 (in the presence of external ABA) can mediate elevated expression of the
550 three *PtrNAC* genes (Figure 5B). We therefore tested whether the formation of
551 dimeric or trimeric protein complexes is necessary for enhancing the
552 PtrAREB1-2-mediated transcriptional activation of the three *PtrNAC* genes.
553 We overexpressed (1) *PtrAREB1-2*, (2) *PtrGCN5-1*, (3) *PtrADA2b-3*, (4) the
554 *PtrAREB1-2:PtrGCN5-1* fusion gene, (5) the *PtrAREB1-2:PtrADA2b-3* fusion,
555 (6) the *PtrADA2b-3:PtrGCN5-1* fusion, and (7) the
556 *PtrAREB1-2:PtrADA2b-3:PtrGCN5-1* fusion, individually, in *P. trichocarpa*
557 SDX protoplasts and compared the overexpression effects on the transcript
558 levels of the three *PtrNAC* genes, using *GFP* expression as a control. ABA
559 was applied when the transfected protoplasts were incubated.

560 As already demonstrated (Figure 5B), in the presence of external ABA,
561 overexpression of PtrAREB1-2 alone effectively activated expression of the
562 three *NAC* genes (Figure 7A). Other individual (PtrGCN5-1 and PtrADA2b-3)
563 or dimeric (PtrAREB1-2:PtrGCN5-1, PtrAREB1-2:PtrADA2b-3, and
564 PtrADA2b-3:PtrGCN5-1) proteins could also activate the three *NAC* genes, but
565 with similar or lower activation efficiency as PtrAREB1-2 alone (Figure 7A).
566 Therefore, PtrAREB1-2 alone through its binding to the ABRE motif
567 establishes a basic transregulation system for activating *NAC* genes.
568 Dimerization of PtrGCN5-1 or PtrADA2b-3 with PtrAREB1-2 is not necessary

569 for this basic transregulation system because such dimers had no effect on
570 *NAC* gene activation mediated by PtrAREB1-2 alone (Figure 7A).

571 By contrast, the ternary complex, PtrAREB1-2:PtrADA2b-3:PtrGCN5-1
572 strongly induced activation of the three *NAC* genes, nearly doubling the
573 activation levels mediated by PtrAREB1-2 alone (Figure 7A). Based on our
574 RNA-seq and ChIP-seq data, we selected five drought-responsive *PtrNAC*
575 genes without ABRE motifs in their promoters as negative controls. Two
576 (*PtrNAC071*, Potri.019G099900; and *PtrNAC091*, Potri.019G099800) of the
577 five have neither an ABRE motif nor a H3K9ac mark in their promoters. The
578 remaining three (*PtrNAC047*, Potri.013G054000; *PtrNAC083*,
579 Potri.017G063300; and *PtrNAC100*, Potri.017G086200) also have no ABRE
580 motif but do have H3K9ac marks in their promoters. Members of the ternary
581 complex, individually or in any dimeric or trimeric combination, could not
582 activate any of these five negative control genes (Figure 7A).

583 We also repeated the SDX protoplast overexpression experiments in the
584 absence of external ABA for all seven transgenes described above, and found
585 that the transregulation effects were nearly identical to those in the presence of
586 ABA, but the activation of the three *NAC* genes was significantly lower
587 (Supplemental Figure 14). We concluded that PtrADA2b and PtrGCN5
588 together could enhance PtrAREB1-mediated transcriptional activation of
589 *PtrNAC* genes. The results also support our hypothesis that a
590 PtrADA2b-PtrGCN5 HAT complex is recruited by AREB1 to *PtrNAC* gene
591 promoters that must have the ABRE motif, elevating their H3K9ac level and
592 leading to the activation of these *NAC* genes. We next tested whether the
593 enhancement of the PtrAREB1-mediated *PtrNAC* gene activation is a result of
594 increasing H3K9ac level at their promoters.

595 The complete set of monomeric and oligomeric proteins used for verifying
596 their effects on *PtrNAC* gene activation (Figure 7A) was also used in SDX

597 protoplast-based ChIP-qPCR to test their influence on the enrichment of
598 H3K9ac in promoters of the *PtrNAC* genes that they bind to. Therefore, SDX
599 protoplasts were transfected with (1) $35S_{pro}:PtrAREB1-2$, (2)
600 $35S_{pro}:PtrGCN5-1$, (3) $35S_{pro}:PtrADA2b-3$, (4) $35S_{pro}:PtrAREB1-2:PtrGCN5-1$,
601 (5) $35S_{pro}:PtrAREB1-2:PtrADA2b-3$, (6) $35S_{pro}:PtrADA2b-3:PtrGCN5-1$, and (7)
602 $35S_{pro}:PtrAREB1-2:PtrADA2b-3:PtrGCN5-1$ constructs, with $35S_{pro}:GFP$ as
603 the control, and assayed by anti-H3K9ac antibody ChIP following our
604 previously described protocol (Li et al., 2014). All tested monomeric and
605 dimeric proteins induced a nearly identical level of H3K9ac at the ABRE motif
606 regions (Figure 2B) in the promoters of the *PtrNAC* genes (Figure 7B). This
607 H3K9ac level was drastically elevated in the presence of the ternary protein
608 complex derived from the $35S_{pro}:PtrAREB1-2:PtrADA2b-3:PtrGCN5-1$
609 transgene (Figure 7B). None of the monomeric, dimeric, or trimeric proteins
610 could induce any H3K9ac enrichment in promoters of the five *PtrNAC* control
611 genes lacking the ABRE motif (Figure 7B). The results suggest that
612 *PtrAREB1-2* alone induces a basal level of H3K9ac for transcriptional
613 activation of the *PtrNAC* genes (Figure 7A).

614 Levels of H3K9ac can be readily augmented by recruiting the effective HAT
615 complex (*PtrADA2b-3:PtrGCN5-1* dimers) to *PtrAREB1-2*, which binds to the
616 promoters (ABRE motifs) of *PtrNAC* genes enhancing transcription. Because
617 gene transcription, particularly of TF genes, is also mediated by RNA
618 polymerase II (Pol II) binding to the upstream promoter of the genes (Roeder,
619 1996), we then asked if the increase in *PtrAREB1*-mediated transcriptional
620 activation of *PtrNAC* genes correlates with their enhanced RNA Pol II
621 recruitment. We examined the occupancy of total RNA Pol II at the promoters
622 of the three *PtrNAC* genes in SDX protoplasts transfected with the same set of
623 seven transgene constructs plus control described above; transfected
624 protoplasts were assayed by anti-Pol II antibody ChIP followed by qPCR.

625 The effects of the different transgenic proteins on levels of RNA Pol II
626 enrichment at promoters of the three *PtrNAC* genes were similar to those on
627 levels of H3K9ac enrichment. PtrAREB1-2 alone binding to the *NAC* gene was
628 accompanied by a basal level of RNA Pol II enrichment (Figure 7C), which was
629 strongly enhanced when PtrADA2b-3:PtrGCN5-1 formed a complex with
630 PtrAREB1-2 (Figure 7C). Again, none of the five negative control genes had
631 enhanced RNA Pol II levels at their promoters (Figure 7C). The results suggest
632 that the enhancement of PtrAREB1-mediated transcriptional activation of
633 *PtrNAC* genes is a result of increasing H3K9ac level (hyperacetylation) at their
634 promoters creating a more “open” chromatin (Lee et al., 1993; Norton et al.,
635 1989; Kouzarides, 2007; Zentner and Henikoff, 2013), thereby facilitating
636 high-level accumulation of RNA Pol II.

637 The protoplast results demonstrated that the ternary complex
638 PtrAREB1-2:PtrADA2b-3:PtrGCN5-1 is necessary for establishing a regulatory
639 machinery with enhanced H3K9ac and RNA Pol II enrichment for activating
640 expression of the three *PtrNAC* drought-tolerance effector genes (Figure 7).
641 We then tested, *in planta*, the necessity of PtrAREB1-2, PtrADA2b-3, and
642 PtrGCN5-1 and their effects on transcriptional regulation of the *PtrNAC* genes
643 and on drought tolerance through RNAi and knockout transgenesis.

644

645 **Reduced or Deleted Expression of *PtrAREB1-2*, *PtrADA2b-3*, or**
646 ***PtrGCN5-1* in *P. trichocarpa* Decreases (1) H3K9ac and RNA Polymerase**
647 **II Enrichment on *PtrNAC* Genes, (2) Expression of These *NAC* Genes,**
648 **and (3) Plant Drought Tolerance**

649 We first generated 13 and eight lines of transgenic *P. trichocarpa* in which
650 *PtrAREB1-2* and *PtrGCN5-1*, respectively, were suppressed through RNAi.
651 From each of these transgenic types, we selected two lines with distinct levels
652 (highest and intermediate suppression) of target gene knock-down

653 (RNAi6-*PtrAREB1-2* and RNAi9-*PtrAREB1-2*; RNAi2-*PtrGCN5-1* and
654 RNAi5-*PtrGCN5-1* in Supplemental Figure 15A). In parallel, we modified our *P.*
655 *trichocarpa* genetic transformation protocol (Song et al., 2006) to allow
656 genome editing using CRISPR-Cas9. We generated four lines of transgenic *P.*
657 *trichocarpa* and identified two biallelic mutants, *ada2b-3-1* and *ada2b-3-2*
658 (Supplemental Figure 15B), which were named KO1-*PtrADA2b-3* and
659 KO2-*PtrADA2b-3*, respectively. These selected transgenics were propagated
660 and maintained in a walk-in growth chamber for further characterization.

661 We characterized the transgenics and mutants as well as the wild-type
662 under drought stress (withholding water for 5 days). We performed RT-qPCR
663 on transcripts of the three *PtrNAC* genes in SDX to reveal the impact of
664 *PtrAREB1-2*, *PtrADA2b-3*, and *PtrGCN5-1* on the expression of these *NAC*
665 genes, which were drastically activated under drought stress (Figure 2A). The
666 activation state of these three *NAC* genes was substantially diminished if the
667 expression of any one of the *PtrAREB1-2*, *PtrADA2b-3*, or *PtrGCN5-1* genes
668 was reduced (Figure 8A-C). The results suggest that simultaneous high
669 expression levels of *PtrAREB1-2*, *PtrADA2b-3*, and *PtrGCN5-1* are essential
670 to activate drought-tolerant effector genes (*NAC*).

671 Next we examined the effects of *PtrAREB1-2*, *PtrADA2b-3*, and *PtrGCN5-1*
672 on the enrichment of H3K9ac at promoters of the three *PtrNAC* genes. We
673 carried out CHIP-qPCR to quantify H3K9ac enrichment using the same SDX
674 used for the RT-qPCR experiments above. The results demonstrated that the
675 significantly elevated H3K9ac enrichments at the promoters of the three *NAC*
676 genes under drought stress (Figure 2C) were greatly reduced when the
677 expression of any of the *PtrAREB1-2*, *PtrADA2b-3*, or *PtrGCN5-1* genes was
678 reduced (Figure 8D-F). Similarly, using the same SDX tissue as above, the
679 enrichment of RNA Pol II at the three *PtrNAC* gene promoters was significantly
680 decreased in the transgenics compared to wild-type plants (Figure 8G-I).

681 Finally, we examined the transgenics and mutants for their drought
682 tolerance and survival (Figure 8J). Preliminary examinations demonstrated
683 that they were hypersensitive to drought and none of them could survive the
684 12-day drought + 3-day rehydration cycle normally used for testing wild-type *P.*
685 *trichocarpa* (Figure 3A). Therefore, we applied a milder drought (10 days)
686 stress to these transgenics and wild-type. After 10 days of drought and 3 days
687 of rehydration (Method), RNAi9-*PtrAREB1-2*, RNAi5-*PtrGCN5-1*, and
688 KO2-*PtrADA2b-3* had ~19, ~20, and ~30% survival rates, respectively,
689 contrasting with a survival rate of ~76% for wild-type plants (Figure 8K). We
690 concluded that *PtrADA2b-3*, *PtrGCN5-1*, and *PtrAREB1-2* together control the
691 level of H3K9ac and the recruitment of RNA Pol II to promoters of
692 drought-responsive genes, e.g., the *PtrNAC* genes, thereby conferring high
693 expression levels of the effector gene for tolerance and survival in *P.*
694 *trichocarpa*.

695

696 **DISCUSSION**

697 In this study, we reported on a regulatory system involving coordinated
698 regulation of H3K9 acetylation and AREB1 TF functions for activating many
699 drought-responsive genes (or drought-tolerant effector genes) (Supplemental
700 Data sets 4 and 5), such as some *NAC* genes, for enhanced drought tolerance
701 in *P. trichocarpa*. It has long been known that AREBs can transactivate
702 drought-responsive genes through binding to ABRE motifs in the promoters of
703 these target genes to induce drought tolerance (Fujita et al., 2005; Yoshida et
704 al., 2010; Nakashima et al., 2014). It is also known that levels of H3K9ac
705 modification increase under drought stress. What has not been clear is the
706 type of acetylation modifiers involved and whether such modifications induce
707 specific drought-responsive genes to confer drought tolerance. Our current
708 study helps fill this important knowledge gap, allowing a fuller understanding of

709 regulatory mechanisms underlying a process that is critical to plant growth and
710 adaptation.

711 We integrated transcriptomic and epigenomic analyses to show that
712 drought stress affects H3K9ac modifications genome-wide in *P. trichocarpa*
713 and that the level of H3K9ac enrichment is associated with the transcriptional
714 activity of drought stress-responsive genes (Figure 1A, B and Supplemental
715 Figure 5). Such an association includes four unique sets of genes, i.e., the
716 hUP-gDN, hUP-gUP, hDN-gUP, and hDN-gDN gene sets (Figure 1A, B).
717 Because H3K9ac is an activating mark, the hUP-gUP and hDN-gDN set of
718 genes are most likely to represent direct effects of differential H3K9ac
719 enrichments on the gene expression. Therefore, the analysis of the hUP-gUP
720 and hDN-gDN gene set is a more logical data reduction approach to start with
721 for a more focused objective. The GO term and motif enrichment search
722 analyses of this gene set revealed that H3K9ac likely regulates
723 drought-responsive genes through ABA-dependent pathway (Figure 1;
724 Supplemental Data set 3). These analyses led to the identification of 76 key TF
725 genes with ABRE motifs in their promoters, including 11 *NAC* homologs
726 (Supplemental Data sets 4 and 5). Overexpression of three of these *NAC*
727 genes (*PtrNAC006*, *007*, and *120*) in *P. trichocarpa* resulted in much improved
728 drought tolerance, consistent with the phenotypes of transgenic *Arabidopsis*
729 and rice where genes with ABRE motif-containing promoters were
730 overexpressed (Fujita et al., 2005; Barbosa et al., 2013).

731 *In vivo* CHIP, EMSA, and *in vivo* transactivation assays demonstrated that
732 *PtrAREB1* binds directly to ABRE motifs of *PtrNAC006*, *PtrNAC007*, and
733 *PtrNAC120* and is a transactivator of these ABRE-mediated *NAC* genes
734 (Figure 5). Overexpressing *PtrAREB1-2* in *P. trichocarpa* induced strong
735 drought tolerance in transgenics with a 100% survival rate (Supplemental
736 Figure 16A, C). Therefore, either activating *PtrAREB1-2*, which enhances

737 expression of ABRE-mediated drought-responsive genes, or directly activating
738 genes with ABRE motif-containing promoters induces drought tolerance in
739 transgenic *P. trichocarpa* (Figure 3). These results suggest that plants activate
740 either AREB1 or ABRE-mediated genes in response to drought stress to
741 develop tolerance for survival. However, knowledge about the activation
742 mechanism has been previously lacking.

743 We now reveal that, while binding to the ABRE motifs of
744 drought-responsive genes (*PtrNACs*) (Figures 5B and 7A), PtrAREB1-2
745 recruits the SAGA-like HAT complex PtrADA2b-3:PtrGCN5-1, forming ternary
746 protein complexes (Figures 6C-N and 9, Supplemental Figure 13). The
747 formation of ternary proteins brings HAT modifiers (Figure 9), and thus high
748 levels of H3K9ac, specifically to drought-responsive genes for increased
749 transcriptional activation (Figure 7A). The intrinsic ABRE-mediated expression
750 of drought-responsive genes can only be effectively activated by ternary
751 proteins—PtrAREB1-2:PtrADA2b-3:PtrGCN5-1 (Figure 7A). In addition, only
752 the ternary complex containing PtrGCN5-1 can boost the enrichment of
753 H3K9ac at the promoter of drought-responsive genes (Figure 7B), creating
754 “open” chromatin states (Berger, 2007) for elevated gene expression. Such
755 chromatin states allow enhanced recruitment of RNA Pol II at *PtrNAC* gene
756 promoters for transcription. This enhanced recruitment also needs the ternary
757 complex (Figure 9).

758 TFs that recruit members of SAGA-like protein complexes for
759 transcriptional regulation in plant development have been reported previously
760 (Mao et al., 2006; Weiste and Droge-Laser, 2014; Zhou et al., 2017). The
761 SAGA complex is a highly conserved transcriptional co-activator in plants and
762 other organisms (Brownell et al., 1996; Grant et al., 1997; Koutelou et al., 2010;
763 Bonnet et al., 2014; Zhou et al., 2017). Arabidopsis TF bZIP11 interacts with
764 ADA2b, activating auxin-induced transcription (Weiste and Droge-Laser, 2014).

765 A recent study showed that the rice homeodomain protein WOX11 recruits the
766 ADA2-GCN5 HAT module to regulate crown root cell proliferation (Zhou et al.,
767 2017). We uncovered a coordinated regulation of histone modifications and
768 regulatory TFs requiring a combinatorial function of the regulatory TF and two
769 SAGA members for transcriptional activation of drought-responsive genes.
770 This combinatorial function is supported by *in planta* evidence. RNAi or
771 CRISPR-mediated mutation of any one of the ternary members reduces the
772 drought-activated states of the drought-responsive *PtrNAC* genes and the
773 H3K9ac and RNA Pol II enrichment levels at the promoters of these *NAC*
774 genes (Figure 8A-I). As a result, the drought survival rates of these RNAi
775 transgenics and CRISPR mutants reduced drastically from ~76% (wild type,
776 with very mild drought treatment) down to ~19-30% (Figure 8J, K).

777 Under drought conditions, plants alter their physiology to reduce growth
778 and enhance drought tolerance for adaptation (Skirycz and Inze, 2010). Such
779 adaptation includes adjustments of stomatal closure (Hu et al., 2006), root
780 architecture (Lee et al., 2017), and hydraulic conductance (Hochberg et al.,
781 2017). Hydraulic conductivity in xylem is related to xylem water potential
782 (Choat et al., 2012) and vessel diameter (Tyree and Sperry, 1989; Fisher et al.,
783 2007). Decrease in water potential reduces hydraulic conductivity (Tyree and
784 Sperry, 1989; Choat et al., 2012) and leads to failure in upward water transport
785 through xylem, known as xylem cavitation or embolism (Tyree and Sperry,
786 1989). Plants with smaller vessel diameter can endure lower water potential to
787 prevent xylem cavitation (Fisher et al., 2007). All the *OE-PtrNAC* transgenics
788 produced here have higher stem water potential (Figure 3D), smaller vessel
789 lumen area (Figure 4A, B, E), and more vessel cells (Figure 4A, C) than
790 wild-type controls. These cellular phenotypes indicate that coordinated
791 regulation of histone modifications and TFs may link to signaling pathways
792 leading to reprogrammed cell differentiation to minimize xylem cavitation for

793 survival. Thus, our work uncovers a potential molecular mechanism involved in
794 regulating plant hydraulic conductance in response to drought stress.

795 For the coordinated regulatory system discovered in this study, we only
796 focused on a set of key factors (*AREB1*, *ADA2b*, and *GCN5*). In the genome of
797 *P. trichocarpa* there are four *AREB1*, three *ADA2b*, and two *GCN5* homologs
798 (Supplemental Data set 6). We also discovered that the regulation activates
799 many other TF genes and genes with promoters containing ABRE motifs (at
800 least 76 key TF genes). We do not know the roles of these other genes. They
801 may also be directly involved in drought response and tolerance, or in other
802 traits such as cellular activities, that may additionally contribute to
803 development of drought tolerance.

804 In addition to the unique cellular development, we also observed retarded
805 growth (Supplemental Figure 16A, B) in transgenics overexpressing *Ptr*
806 *AREB1-2*. However, these transgenics are completely drought tolerant after a
807 continuous dehydration of 12 days (100% survival rate, Supplemental Figure
808 16A, C). Slight growth reduction also occurred in transgenic *OE-PtrNAC006*
809 plants, which too exhibited a high survival rate (76%, Figure 3A, C). After the
810 12-day drought (water withholding) experiments, the potting soil in which these
811 two types of transgenics were grown remained sufficiently moist, whereas the
812 soil of wild-type control plants was dried out. Therefore, these transgenics
813 have reprogrammed their growth to allow reduced transpiration and increased
814 water use efficiency to maintain a level of stem hydraulic conductivity
815 conducive to growth. These drought-tolerant plants are also highly drought
816 resilient and grow normally after drought stress, with a growth rate similar to
817 that of normal wild-type *P. trichocarpa*. Such transgenics should grow well on
818 marginal land not suitable for conventional agriculture. Field testing of these
819 transgenics/mutants will reveal additional regulation, enabling further strategic
820 re-engineering to maximize growth and other beneficial traits while minimizing

821 the negative effects of drought stress. The approaches reported here need to
822 be explored in other tree species. A sustainable and abundant woody
823 feedstock continues to be an essential renewable resource worldwide.

824

825 **METHODS**

826

827 **Plant Materials and Growth Conditions**

828 *P. trichocarpa* genotype Nisqually-1 was used for all experiments. Wild-type
829 and transgenic plants were grown in a walk-in growth chamber (21–25 °C, 16 h
830 light/8 h dark cycle with supplemental light of ~ 300 $\mu\text{E m}^{-2} \text{s}^{-1}$, three-band linear
831 fluorescent lamp T5 28W 6400K, 60-80% humidity) as previously described
832 (Song et al., 2006). Soil was composed of peat moss and Metro-Mix200 in a 2:1
833 ratio at identical dry weight per pot, and was watered daily to maintain a water
834 content of ~0.75 g water/g dry soil. In ChIP-seq and RNA-seq experiments,
835 3-month-old clonally propagated wild-type *P. trichocarpa* plants in 15-cm pots
836 (1 plant/pot) having the same size and vigor were used for drought treatments
837 (soil water depletion), following established procedures (Arango-Velez et al.,
838 2011). *P. trichocarpa* plants were divided into three groups: (1) control, (2)
839 5-day drought treatment (no watering), and (3) 7-day drought treatment (no
840 watering). All plants were equally well-watered prior to drought treatment.
841 Watering of group 3 plants ceased first, for 7 days (D7). Two days later,
842 watering of group 2 plants ceased for 5 days (D5). Watering of group 1 control
843 plants was continued on a daily basis (ND) for the entire period of the drought
844 treatments for groups 3 and 2. In this way, all plants were harvested on the
845 same day (day 7) and at the same time (~10 am) for SDX tissue collection
846 (Supplemental Figure 1C). SDX tissue for ChIP-seq was collected from
847 debarked stem, treated with formaldehyde to stabilize protein–DNA

848 interactions, and then frozen in liquid nitrogen and stored at -80°C until use, as
849 described previously (Lin et al., 2013; Li et al., 2014). SDX tissue for RNA-seq
850 was collected directly into liquid nitrogen and stored in liquid nitrogen (Li et al.,
851 2012; Lin et al., 2013).

852

853 **ChIP Assays in *P. trichocarpa* Differentiating Xylem**

854 ChIP was carried out on the SDX of 3-month-old *P. trichocarpa* plants
855 following an established protocol (Lin et al., 2013; Li et al., 2014). Briefly, ~5 g
856 SDX tissue was cross-linked in 1% formaldehyde and used to isolate nuclei
857 and chromatin. The chromatin was sheared into 200- to 1000-bp fragments,
858 subjected to immunoprecipitation using 5 μg anti-H3K9ac (Abcam, ab10812)
859 or anti-RNA polymerase II (ab817) antibodies, and collected with protein G
860 magnetic beads (Invitrogen). Precipitated chromatin was de-cross-linked to
861 release the ChIP-DNA, which was purified and quantified (Qubit® Fluorometer)
862 for ChIP-qPCR detection or ChIP-seq library construction. Primers for
863 ChIP-qPCR are listed in Supplemental Table 3. For ChIP-seq, 12 libraries (2
864 DNA samples (ChIP-DNA and input DNA) \times 2 biological replicates
865 (independent pools of *P. trichocarpa* SDX tissue) \times 3 (1 control, ND + 2
866 treatments, D5 and D7)) were prepared using a library preparation kit (New
867 England Biolabs) according to the manufacturer's instructions and sequenced
868 using an Illumina Genome Analyzer.

869

870 **ChIP-seq Data Analysis**

871 Reads with an average length of 100 bp were obtained. After removing the
872 library index sequences from each read, the remaining sequence reads were
873 mapped to the *P. trichocarpa* genome v.3.0 using Bowtie2 (version 2.1.0;
874 parameters: bowtie2 -p 8 -x P.trichocarpa.index -1 read1.fq.gz -2 read2.fq.gz
875 -S mapping.sam) (Langmead and Salzberg, 2012). The alignments with no

876 more than three mismatches were remained for further analysis. The quality of
877 the raw data was evaluated with FastQC
878 (<http://www.bioinformatics.bbsrc.ac.uk/projects/fastqc/>), and low-quality reads
879 were filtered by Sickle (<https://github.com/najoshi/sickle/>). Peak calling to
880 identify the range and pattern of H3K9ac and detection of differential
881 modification between the drought-treated and well-watered samples were
882 performed using diffReps (Shen et al., 2013) with default parameters
883 (diffReps.pl --meth nb --pval 0.0001 --treatment D5/D7_IP.bed --control
884 ND_IP.bed --btr D5/D7_input.bed --bco ND_input.bed --report diffReps_peaks
885 --chrLen PtrChrLen.txt --nproc 7). The replicate reproducibility was evaluated
886 by the negative binomial test. The Benjamini-Hochberg-adjusted P value
887 ($P\text{-adj} < 0.05$) in diffReps analysis was used to select differential H3K9ac peaks
888 between the drought-treated and well-watered samples.

889

890 **Total RNA Extraction**

891 Total RNA from SDX or SDX protoplasts of *P. trichocarpa* plants was extracted
892 using a Qiagen RNeasy Mini Kit (Invitrogen) as previously described (Lin et al.,
893 2013, 2014). RNA quality was examined using a Bioanalyzer 2100 (Agilent).
894 The RNA was used for RNA-seq, gene cloning, and RT-qPCR.

895

896 **RNA-seq Analysis**

897 RNA-seq was performed for SDX tissues isolated from the same *P. trichocarpa*
898 plants used for ChIP-seq. Total RNA (1 µg) of each sample was used for library
899 construction using an Illumina TruSeq RNA sample preparation kit. The quality
900 and concentration of libraries were examined using a Bioanalyzer 2100
901 (Agilent). A total of 12 libraries (4 biological replicates (independent pools of *P.*
902 *trichocarpa* SDX tissue)) × 3 (1 control, ND + 2 treatments, D5 and D7)) were
903 sequenced using an Illumina Genome Analyzer, and 100-bp average read

904 lengths were obtained. After removing the library index sequences from each
905 read, the remaining RNA-seq reads were mapped to the *P. trichocarpa*
906 genome v.3.0 using TopHat (Kim et al., 2013) with default parameters (tophat
907 --read-mismatches 2 -p 8 P.trichocarpa.index sample_1.fq.gz
908 sample_reads_2.fq.gz). The frequency of raw counts was determined by
909 BEDtools (Quinlan and Hall, 2010) for all annotated genes. DEGs between the
910 drought-treated and well-watered samples were identified using EdgeR
911 (Robinson et al., 2010) based on raw counts of mapped RNA-seq reads to
912 annotated genes and following an established analysis pipeline (Lin et al.,
913 2013) with an FDR<0.05. Gene ontology (GO) analyses were conducted using
914 the online tool PANTHER (<http://www.pantherdb.org/geneListAnalysis.do>; Mi
915 et al., 2013) by Fisher's exact test with FDR multiple test correction
916 (FDR<0.05).

917

918 **Integrative Analysis of ChIP-seq and RNA-seq**

919 BETA (Wang et al., 2013) was used to integrate ChIP-seq and RNA-seq data
920 for *P. trichocarpa* with minor modifications. BETA uses a Rank Product
921 algorithm to screen for target genes of histone modification based on both the
922 proximity of the modification to the TSS of the gene and the differential
923 expression level of the gene. Drought-responsive DEGs with differential
924 H3K9ac peaks (FDR<0.05) within ± 2 kb of the TSS of the drought-responsive
925 DEGs were identified by the modified BETA (BETA minus -p diffReps_peaks -r
926 Ptr.refgene -d 2000 -n diffReps_gene.results). Gene expression information
927 and the differential H3K9ac peaks for the identified drought-responsive DEGs
928 were integrated to reveal correlations between H3K9ac (hUP or hDN) and
929 gene expression (gUP or gDN) using R scripts (Wickham, 2009). The
930 abundance of consensus motifs in the 2-kb promoters of the identified
931 drought-responsive DEGs with differential H3K9ac was assessed using AME

932 (Analysis of Motif Enrichment) (McLeay and Bailey, 2010) with Fisher's exact
933 test.

934

935 **Phylogenetic Analysis**

936 A phylogenetic tree was reconstructed using MEGA 5 with the neighbor-joining
937 method and 1000 bootstrap replicates. Alignments used to produce
938 phylogenies are provided as Supplemental Data sets 7 and 8.

939

940 **RT- quantitative PCR**

941 RT-quantitative PCR was performed as previously described (Li et al., 2012) to
942 detect gene expression in SDX tissue or SDX protoplasts of *P. trichocarpa*
943 plants. cDNAs were synthesized by reverse transcription with SuperScript III
944 Reverse Transcriptase (Invitrogen) according to the manufacturer's protocol.
945 Quantitative RT-PCR was carried out using FastStart Universal SYBR Green
946 Master (Roche) on an Agilent Mx3000P Real-time PCR System. PCR
947 amplification was in the logarithmic phase for each DNA molecule being
948 analyzed.

949

950 **Generation and Analysis of *P. trichocarpa* Transgenic and Mutant Plants**

951 Coding regions of *PtrNAC006*, *007*, *120*, and *PtrAREB1-2* were amplified from
952 *P. trichocarpa* plants and, after sequence confirmation, inserted into the pBI121
953 vector under control of the CaMV 35S promoter to generate overexpression
954 constructs. RNAi constructs were designed for downregulation of *PtrAREB1-2*
955 and *PtrGCN5-1* genes. Specific sequences of the two RNAi target genes were
956 amplified and assembled with a 600-bp GUS linker sequence to form RNAi
957 transgene sequences and then cloned into pCR2.1 vector. After sequencing,
958 the assembled RNAi transgene fragments were subcloned into the pBI121
959 vector to obtain RNAi constructs. Knockout mutants of *PtrADA2b-3* were

960 generated using the CRISPR-Cas9 system (Ueta et al., 2017). The sgRNA
961 sequence (Supplemental Table 3) targeting *PtrADA2b-3* was selected using
962 CRISPR-P 2.0 (<http://crispr.hzau.edu.cn/cgi-bin/CRISPR2/CRISPR>). sgRNA
963 target sequences with sticky ends created by *Bsal* were synthesized and
964 inserted into pEgP237-2A-GFP vector digested with *Bsal* (Ueta et al., 2017).
965 All plasmids were introduced into *Agrobacterium tumefaciens* strain C58 for *P.*
966 *trichocarpa* transformation as previously described (Song et al., 2006).

967 The expression of *PtrNAC* genes, *PtrAREB1-2* and *PtrGCN5-1*, in
968 transgenic plants was determined by RT-qPCR as described above. For
969 detection of the *PtrADA2b-3* mutation, PCR amplification was carried out using
970 primers flanking the sgRNA target sequence. The PCR products (300-500 bp)
971 were inserted into pMD18-T vector (Takara, 6011), and 20 colonies were
972 selected for sequencing. Primers for vector construction, mutation detection,
973 and RT-qPCR are listed in Supplemental Table 3. The transgenic *P.*
974 *trichocarpa* lines with the highest transgene transcript levels for *PtrNAC* genes
975 and *PtrAREB1-2*, and with two distinct levels (highest and intermediate
976 suppression) of target gene knockdown for *PtrAREB1-2* and *PtrGCN5-1* were
977 selected and maintained in a walk-in growth chamber for further analysis.
978 Transgenic, mutant, and wild-type plants were grown in 15-cm pots (1 plant/pot)
979 with the same amount of soil as described above. Drought treatment was
980 applied to 3-month-old plants of ~50 cm height by withholding water. To allow
981 drought-treated plants to recover, plants overexpressing *PtrNAC* genes and
982 *PtrAREB1-2*, and wild-type control plants were re-watered after 12 days of
983 drought treatment, and RNAi-*PtrAREB1-2*, RNAi-*PtrGCN5-1*, KO-*PtrADA2b-3*,
984 and wild-type plants were re-watered after 10 days. Survival rates were
985 calculated based on the plants that survived after re-watering for 3 days. At
986 least 12 transgenic plants for each gene construct and 12 wild-type plants were
987 tested in each drought treatment experiment. Water potential was measured

988 under well-watered conditions and with drought treatment for 5 days,
989 respectively. Six transgenic plants for each gene construct and six wild-type
990 plants were used in each test. A SAPS II Water Potential System (SEC) was
991 used for measurement of stem water potential according to the manufacturer's
992 instructions. Statistical analyses were performed based on data from three
993 independent experiments.

994

995 **Histochemical and Histological Analysis**

996 Stem segments were harvested from the 10th internode of *OE-PtrNAC006*,
997 *OE-PtrNAC007*, and *OE-PtrNAC120* transgenic and wild-type plants. Each
998 segment was cut into 2-mm fragments and fixed with 4% paraformaldehyde in
999 1× PBS buffer at 4 °C for 12 h. Fixed materials were washed with 1× PBS,
1000 dehydrated in a graded ethanol series, incubated sequentially in
1001 ethanol/xylene 75:25, 50:50, 25:75, and 0:100%, and embedded in paraffin
1002 (Sigma). The embedded fragments were sectioned to a thickness of 16 µm
1003 using a rotary microtome (Leica RM2245) and deparaffinized using xylene.
1004 Sections were stained with safranin O and fast green, and observed under a
1005 microscope (Leica DM6B). The parameters of individual vessels were
1006 measured using LAS V4.8 and LAS X V2.0 software (Leica). More than 30
1007 measurements for each transgenic line and wild-type with three independent
1008 replicates were performed for statistical analysis.

1009

1010 **Scanning Electron Micrograph Analysis**

1011 Fresh stem segments of the 10th internode of *OE-PtrNAC006*, *OE-PtrNAC007*,
1012 and *OE-PtrNAC120* transgenic and wild-type plants were harvested and
1013 coated with gold (Au) at 10 mA for 60 s. The samples were transferred to a
1014 scanning electron microscopy chamber and imaged under high vacuum at 15
1015 kV using a Nanotech JCM-5000.

1016

1017 **Gene Expression Analysis in SDX Protoplasts**

1018 The full coding sequences of *PtrAREB1-2*, *PtrGCN5-1*, and *PtrADA2b-3* were
1019 cloned into pENTR/D-TOPO vector (Invitrogen), respectively, and were then
1020 recombined into the pUC19-35S_{pro}-RfA-35S_{pro}-sGFP (Li et al., 2012)
1021 destination vector, generating pUC19-35S_{pro}-*PtrAREB1-2*-35S_{pro}-sGFP,
1022 pUC19-35S_{pro}-*PtrGCN5-1*-35S_{pro}-sGFP, and
1023 pUC19-35S_{pro}-*PtrADA2b-3*-35S_{pro}-sGFP. *PtrAREB1-2* without stop codon was
1024 inserted into the pUC19-35S_{pro}-sGFP (Li et al., 2012) vector, generating
1025 pUC19-35S_{pro}-*PtrAREB1-2*-sGFP. *PtrADA2b-3* was then cloned into
1026 pUC19-35S_{pro}-*PtrAREB1-2*-sGFP, giving
1027 pUC19-35S_{pro}-*PtrAREB1-2*-*PtrADA2b-3*. The constructs
1028 pUC19-35S_{pro}-*PtrAREB1-2*-*PtrGCN5-1* and
1029 pUC19-35S_{pro}-*PtrADA2b-3*-*PtrGCN5-1* were generated in a similar way.
1030 *PtrAREB1-2* without stop codon was cloned into
1031 pUC19-35S_{pro}-*PtrADA2b-3*-*PtrGCN5-1*, generating
1032 pUC19-35S_{pro}-*PtrAREB1-2*-*PtrADA2b-3*-*PtrGCN5-1*. The plasmids were
1033 prepared using a CsCl gradient and transfected into SDX protoplasts as
1034 described previously (Lin et al., 2013, 2014). After culturing for 12 h,
1035 protoplasts were collected for RNA extraction and RT-qPCR analysis as
1036 described above. Three biological replicates for each transfection and three
1037 technical repeats for each biological replicate were performed. Primers for
1038 construct generation and RT-qPCR are listed in Supplemental Table 3.

1039

1040 **ChIP Assays in SDX Protoplasts**

1041 Plasmids as described above were prepared using a CsCl gradient and
1042 transfected into SDX protoplasts as described previously (Lin et al., 2013,
1043 2014) for ChIP assays. Approximately 6 mg plasmid DNA and $\sim 1 \times 10^7$ SDX

1044 protoplasts were used for each transfection. CHIP assays in SDX protoplasts
1045 were performed as described previously (Lin et al., 2013; Li et al., 2014) with a
1046 few modifications. In brief, protoplasts were collected for cross-linking with 1%
1047 formaldehyde in WI buffer (0.2 M MES pH 5.7, 0.8 M mannitol, 2 M KCl) for 10
1048 min at room temperature. The cross-linked protoplasts were collected for
1049 chromatin extraction and sonication using a Bioruptor (Diagenode) for three
1050 rounds of five cycles. Sonicated chromatin was immunoprecipitated using 5 µg
1051 anti-GFP (Abcam, ab290), anti-H3K9ac (ab10812), or anti-RNA polymerase II
1052 (ab817) antibodies. Purified CHIP-DNAs were analyzed by CHIP-qPCR as
1053 previously described (Li et al., 2014). Three biological replicates for each
1054 transfection and three technical repeats for each biological replicate were
1055 performed. Primers for CHIP-qPCR are listed in Supplemental Table 3.

1056

1057 **Pull-Down Assays**

1058 For pull-down assays, pETDuet-1 vector (Novagen) was used to co-express
1059 two target genes driven by two independent T7 promoters. The coding
1060 sequences of *PtrAREB1-2* and *PtrADA2b-3* were cloned into pETDuet-1
1061 vector at the first multiple cloning site with 6xHis tag and the second multiple
1062 cloning site with S tag, respectively, to generate a construct harboring
1063 *PtrAREB1-2:6xHis-tag* and *PtrADA2b-3:S-tag*. In the same way, constructs
1064 harboring *PtrGCN5-1:6xHis-tag* and *PtrADA2b-3:S-tag*, *PtrGCN5-1:6xHis-tag*
1065 and *PtrAREB1-2:S-tag*, *PtrAREB1-2:6xHis-tag* and *GFP:S-tag*, and
1066 *PtrGCN5-1:6xHis-tag* and *GFP:S-tag* were assembled, respectively, and *GFP*
1067 was used as a negative control. Primers for construct generation are listed in
1068 Supplemental Table 3. The constructs were transferred into *E. coli* BL21 to
1069 produce fusion proteins. Briefly, bacteria were cultured in LB medium at 37 °C
1070 until OD₆₀₀ reached 0.4~0.6 and then continuously cultured at 25 °C for 6 h
1071 after adding 0.5 mM isopropyl β-d-thiogalactopyranoside (IPTG). Cells were

1072 collected and lysed in Lysis Buffer (50 mM Tris-HCl, pH 8.0, 500 mM NaCl, 10
1073 mM imidazole, 10% glycerol, 0.1% Tween-20, and 2 mM PMSF) by sonication.
1074 The supernatants from the cell lysates were collected and incubated with
1075 HisPur Ni-NTA Resin (Thermo Scientific) for 2 h at 4 °C. After washing the
1076 beads eight times with Wash Buffer (50 mM Tris-HCl, pH 8.0, 500 mM NaCl,
1077 15 mM imidazole, 10% glycerol, 1.5 mM β -mercaptoethanol), the bound
1078 proteins were eluted with Elution Buffer (50 mM Tris-HCl, pH 8.0, 500 mM
1079 imidazole, 1.5 mM β -mercaptoethanol) and collected using Centrifugal Filter
1080 Devices (Millipore). His- and S-tagged proteins were detected using anti-His
1081 (Abcam, ab1187) and anti-S (ab184223) antibodies, respectively.

1082

1083 **Immunoblotting**

1084 Proteins were separated by 10% SDS-PAGE gel and subsequently blotted
1085 onto a PVDF membrane (Thermo scientific). The membrane was blocked
1086 using non-fat dry milk and then probed with the indicated antibodies (anti-His
1087 antibody, Abcam, ab1187; anti-S antibody, ab184223). Signals were detected
1088 using SuperSignal West Pico Chemiluminescent Substrate (Thermo Scientific)
1089 and X-Ray film (Sigma).

1090

1091 **EMSA Assays**

1092 The full-length coding sequence of *PtrAREB1-2* was cloned into pETDuet-1
1093 vector (Novagen) with a 6xHis tag at its N-terminus using *Bam*HI/*Hind*III
1094 restriction enzymes. The construct was transferred into *E. coli* BL21 for
1095 recombinant protein production. Recombinant protein was purified using
1096 HisPur Ni-NTA Resin (Thermo Scientific) as described for pull-down assays
1097 and collected in concentration buffer (50 mM Tris-HCl, pH 8.0, 100 mM NaCl)
1098 using Centrifugal Filter Devices (Millipore). An empty pETDuet-1 vector was
1099 used as a negative control. DNA fragments from *PtrNAC006*, *PtrNAC007*, and

1100 *PtrNAC120* promoters, harboring the ABRE motif, were biotin-labeled at the 3'
1101 end using a Biotin 3' End DNA labeling kit (Thermo Scientific). All ABRE motifs
1102 in the promoter fragments were also mutated by changing the first T to A for
1103 synthesis of mutated probes. Primers for construct generation and probe
1104 preparation are listed in Supplemental Table 3.

1105 EMSA was performed using a Lightshift Chemiluminescent EMSA kit
1106 (Thermo Scientific) according to the manufacturer's instructions. Briefly,
1107 biotin-labeled probes were mixed with 100 ng purified proteins for 20 min in
1108 binding buffer (10 mM Tris-HCl, pH 7.5, 50 mM KCl, 1 mM DTT, 2.5% glycerol,
1109 5 mM MgCl₂, 0.05% Nonidet P-40, and 100 ng/μL poly (dl-dC)) at room
1110 temperature. Wild-type or mutated unlabeled probes were used as competitors
1111 in competition analyses in 50-, 100-, and 150-fold molar excess relative to the
1112 labeled probes. Protein–DNA mixtures were separated on a 6.5% native
1113 PAGE gel and transferred to a nylon membrane (Thermo Scientific). Signals
1114 were detected by chemiluminescence.

1115

1116 **BiFC Assays**

1117 The coding sequences of *PtrADA2b-3*, *PtrAREB1-2*, and *PtrGCN5-1* were
1118 cloned into pENTR/D-TOPO vector (Invitrogen), and sequence-confirmed
1119 PCR fragments were recombined into a BiFC destination vector. Primers for
1120 BiFC vector construction are listed in Supplemental Table 3. Each pair of
1121 vectors (*ADA2b-3:YFP^N/GCN5-1:YFP^C*, *ADA2b-3:YFP^N/AREB1-2:YFP^C*, and
1122 *AREB1-2:YFP^N/GCN5-1:YFP^C*) was cotransfected into SDX protoplasts with
1123 *H2A-1:mCherry* following an established protocol (Lin et al., 2014).
1124 Cotransfection of each protein of interest with empty plasmid was performed
1125 as a negative control. An unrelated nuclear protein, PtrMYB021, was used as
1126 another negative control. *ADA2b-3:YFP^N/MYB021:YFP^C*,
1127 *MYB021:YFP^N/AREB1-2:YFP^C*, and *MYB021:YFP^N/GCN5-1:YFP^C* were

1128 independently cotransfected with *H2A-1:mCherry* into SDX protoplasts. After
1129 incubation for 12 h, SDX protoplasts were collected and examined under a
1130 confocal laser scanning microscope (Zeiss LSM 700). One entire run of BiFC
1131 therefore included nine experiments for three pairs of the tested dimers and
1132 two sets of negative controls. The entire run was repeated three times using
1133 three different batches of SDX protoplasts (i.e., 3 biological replicates). The
1134 SDX protoplast system typically has a transformation rate of 30 to 40% (Lin et
1135 al., 2014). In each of the nine experiments (in one biological replicate), 50 to
1136 60 individual protoplast cells were examined and at least 12 individual
1137 protoplast cells with the specific fluorescent signals from co-transfected
1138 proteins could normally be identified. One image was selected, such as shown
1139 in Figure 6F, from these ~12 cells from each experiment. The images of a set
1140 of nine experiments for one biological replicate are shown in Figure 6F-N.
1141 Images from the other two biological replicates are shown in Supplemental
1142 Figure 13A-R.

1143

1144 **Statistical Analysis**

1145 Student's *t* test was performed using SPSS software (v.19.0) to determine
1146 significance, which was defined as **P*<0.05, ***P*<0.01. Detailed results of
1147 statistical analyses are available as Supplemental File 1.

1148

1149 **Accession Numbers**

1150 The ChIP-seq and RNA-seq data for this work have been deposited in the
1151 NCBI GEO database under accession number GSE81048. Sequence data
1152 from this article can be found in *Populus trichocarpa* v3.0 (Poplar) of
1153 Phytozome 12 under the following accession numbers: *PtrNAC005*
1154 (Potri.005G069500), *PtrNAC006* (Potri.002G081000), *PtrNAC118*
1155 (Potri.011G123300), *PtrNAC007* (Potri.007G099400), *PtrNAC120*

1156 (Potri.001G404100), *PtrAREB1-2* (Potri.002G125400), *PtrAREB1-3*
1157 (Potri.009G101200), *PtrAREB1-4* (Potri.014G028200), *PtrADA2b-3*
1158 (Potri.004G135400), *PtrGCN5-1* (Potri.002G045900), *PtrMYB021*
1159 (Potri.009G053900), *PtrNAC047* (Potri.013G054000), *PtrNAC071*
1160 (Potri.019G099900), *PtrNAC083* (Potri.017G063300), *PtrNAC091*
1161 (Potri.019G099800), *PtrNAC100* (Potri.017G086200).

1162

1163 **Supplemental Data**

1164 **Supplemental Figure 1.** Drought Treatment of *P. trichocarpa* Followed by
1165 Genome-Wide Investigation of H3K9ac and Transcriptomic Analysis in SDX
1166 Tissues.

1167 **Supplemental Figure 2.** Genome-Wide Analysis of H3K9ac in SDX Tissues of
1168 *P. trichocarpa* under Well-Watered and Drought Conditions.

1169 **Supplemental Figure 3.** RNA-seq Volcano Plots for D5/ND and D7/ND.

1170 **Supplemental Figure 4.** Main Enriched Gene Ontology (GO) Categories
1171 among Upregulated or Downregulated Genes Identified from D5 and D7
1172 treatments.

1173 **Supplemental Figure 5.** Integration of ChIP-seq and RNA-seq Data to Identify
1174 Drought Stress-Responsive Genes Associated with H3K9ac at Promoter
1175 and/or Gene Body Regions.

1176 **Supplemental Figure 6.** Phylogenetic Tree of *NAC* Genes in *P. trichocarpa*
1177 and *Arabidopsis*.

1178 **Supplemental Figure 7.** Phenotypes and transgene expression levels in the
1179 stem developing xylem of four independent *PtrNAC006* transgenic lines.

1180 **Supplemental Figure 8.** Transcript Levels of *PtrNAC006*, *PtrNAC007*, and
1181 *PtrNAC120* and Growth Data for Wild-Type and Transgenic Plants under
1182 Well-Watered and Drought Conditions.

1183 **Supplemental Figure 9.** Scanning Electron Micrographs of Wild-Type,
1184 *OE-PtrNAC007*, and *OE-PtrNAC120* Transgenic Plants.

1185 **Supplemental Figure 10.** Phylogenetic Tree of *AREB1* Genes in *P.*
1186 *trichocarpa* and *Arabidopsis*.

1187 **Supplemental Figure 11.** Relative Transcript Level of *PtrNAC006*,
1188 *PtrNAC007*, and *PtrNAC120* in SDX Protoplasts Overexpressing *PtrAREB1-2*
1189 or *GFP* in the Absence of External ABA.

1190 **Supplemental Figure 12.** Cloning of the *PtrADA2b* Gene and Schematic
1191 Diagram of Its Splice Variants.

1192 **Supplemental Figure 13.** Biological Replicates of the BiFC Assay Data.

1193 **Supplemental Figure 14.** *PtrAREB1-2:PtrADA2b-3:PtrGCN5-1* Induces
1194 Activation of the Three *NAC* Genes in the Absence of External ABA.

1195 **Supplemental Figure 15.** Identification RNAi-*PtrAREB1-2*, RNAi-*PtrGCN5-1*,
1196 and Knockout-*PtrADA2b-3* Plants.

1197 **Supplemental Figure 16.** Overexpressing the *PtrAREB1-2* Gene Improves
1198 Drought Stress Tolerance of *P. trichocarpa*.

1199 **Supplemental Table 1.** ChIP-seq for Identification of Differential H3K9ac
1200 Peaks under Drought Stress.

1201 **Supplemental Table 2.** RNA-seq for Identification of Differentially Expressed
1202 Genes under Drought Stress.

1203 **Supplemental Table 3.** Primer List.

1204 **Supplemental Data set 1.** Integrative Analysis of ChIP-seq and RNA-seq
1205 Data for D5/ND.

1206 **Supplemental Data set 2.** Integrative Analysis of ChIP-seq and RNA-seq
1207 Data for D7/ND.

1208 **Supplemental Data set 3.** Gene Ontology (GO) Enrichment Analysis of the
1209 hUP-gUP and hDN-gDN Set of Genes in D5 and D7.

1210 **Supplemental Data set 4.** ABRE-Containing Transcription Factor Genes for
1211 D5/ND.
1212 **Supplemental Data set 5.** ABRE-Containing Transcription Factor Genes for
1213 D7/ND.
1214 **Supplemental Data set 6.** RNA-seq Data of *PtrGCN5*, *PtrADA2b*, *PtrAREB1*,
1215 *PtrNACs* and *PtrGBF3* Genes.
1216 **Supplemental Data set 7.** Alignments Used to Produce Phylogenies of NACs.
1217 **Supplemental Data set 8.** Alignments Used to Produce Phylogenies of
1218 AREB1s.
1219 **Supplemental File 1.** Statistical analysis.

1220

1221 **ACKNOWLEDGMENTS**

1222 We thank Keishi Osakabe for CRISPR/Cas9 constructs. This work was
1223 supported by the National Key Research and Development Program of China
1224 (no. 2016YFD0600106), the National Natural Science Foundation of China
1225 Grants 31522014, 31570663, and 31430093, the Fundamental Research
1226 Funds for the Central Universities (2572018CL02), and the Innovation Project
1227 of State Key Laboratory of Tree Genetics and Breeding (Northeast Forestry
1228 University) (to W.L.). We are also grateful for financial support from the
1229 ‘1000-talents Plan’ for young researchers from China and Longjiang Young
1230 Scholar Program of Heilongjiang Provincial Government (to W.L.), the US
1231 Office of Science (Biological and Environmental Research), Department of
1232 Energy Grant DE-SC000691 (to V.L.C.), Taiwan Ministry of Science and
1233 Technology MOST 106-2311-B-002-001-MY2 and 107-2636-B-002-003 (to
1234 Y.-C.J.L.), and the 111 Project (B16010).

1235

1236 **AUTHOR CONTRIBUTIONS**

1237 W.L., V.L.C., Y.-C.J.L. and J.P.W. conceived the research and designed the
1238 experiments. S.L., Y.-C.J.L., P.W., B.Z., M.L., X.L., Z.W., X.D., J.Y., C.Z. and
1239 B.L. performed the experiments. S.C., R.S., and S.T.-A. contributed new
1240 analytic/computational tools. W.L., V.L.C., Y.-C.J.L., and S.L. analyzed the
1241 data and wrote the manuscript with input from all co-authors.

1242

1243 REFERENCES

1244 **Arango-Velez, A., Zwiazek, J.J., Thomas, B.R., and Tyree, M.T.** (2011).

1245 Stomatal factors and vulnerability of stem xylem to cavitation in poplars.

1246 *Physiol. Plant.* **143**: 154-165.

1247 **Ascenzil, R., and Gantt, J.S.** (1999). Molecular genetic analysis of the

1248 drought-inducible linker histone variant in *Arabidopsis thaliana*. *Plant Mol. Biol.*

1249 **41**: 159–169.

1250 **Aubert, Y., Vile, D., Pervent, M., Aldon, D., Ranty, B., Simonneau, T.,**

1251 **Vavasseur, A., and Galaud, J.P.** (2010). RD20, a stress-inducible caleosin,

1252 participates in stomatal control, transpiration and drought tolerance in

1253 *Arabidopsis thaliana*. *Plant Cell Physiol.* **51**: 1975-1987.

1254 **Balasubramanian, R., Pray-Grant, M.G., Selleck, W., Grant, P.A., and Tan,**

1255 **S.** (2002). Role of the Ada2 and Ada3 transcriptional coactivators in histone

1256 acetylation. *J. Biol. Chem.* **277**: 7989-7995.

1257 **Barber, V.A., Juday, G.P., and Finney, B.P.** (2000). Reduced growth of

1258 Alaskan white spruce in the twentieth century from temperature-induced

1259 drought stress. *Nature.* **405**: 668-673.

1260 **Barbosa, E.G.G., Leite, J.P., Marin, S.R.R., Marinho, J.P., Carvalho, J.D.C.,**

1261 **Fuganti-Pagliarini, R., Farias, J.R.B., Neumaier, N.,**

1262 **Marcelino-Guimaraes, F.C., de Oliveira, M.C.N., Yamaguchi-Shinozaki,**

1263 **K., Nakashima, K., Maruyama, K., Kanamori, N., Fujita, Y., Yoshida, T.,**

1264 **and Nepomuceno, A.L.** (2013). Overexpression of the ABA-Dependent

1265 AREB1 Transcription Factor from *Arabidopsis thaliana* Improves Soybean
1266 Tolerance to Water Deficit. *Plant. Mol. Biol. Rep.* **31**: 719-730.

1267 **Berger, S.L.** (2007). The complex language of chromatin regulation during
1268 transcription. *Nature.* **447**: 407-412.

1269 **Berta, M., Giovannelli, A., Sebastiani, F., Camussi, A., and Racchi, M.L.**
1270 (2010). Transcriptome changes in the cambial region of poplar (*Populus*
1271 *alba L.*) in response to water deficit. *Plant biology.* **12**: 341-354.

1272 **Bogeat-Triboulot, M.B., Brosche, M., Renaut, J., Jouve, L., Le Thiec, D.,**
1273 **Fayyaz, P., Vinocur, B., Witters, E., Laukens, K., Teichmann, T., Altman,**
1274 **A., Hausman, J.F., Polle, A., Kangasjarvi, J., and Dreyer, E.** (2007).
1275 Gradual soil water depletion results in reversible changes of gene
1276 expression, protein profiles, ecophysiology, and growth performance in
1277 *Populus euphratica*, a poplar growing in arid regions. *Plant Physiol.* **143**:
1278 876-892.

1279 **Bonnet, J., Wang, C.Y., Baptista, T., Vincent, S.D., Hsiao, W.C., Stierle, M.,**
1280 **Kao, C.F., Tora, L., and Devys, D.** (2014). The SAGA coactivator complex
1281 acts on the whole transcribed genome and is required for RNA polymerase II
1282 transcription. *Genes Dev.* **28**: 1999-2012.

1283 **Brownell, J.E., Zhou, J., Ranalli, T., Kobayashi, R., Edmondson, D.G.,**
1284 **Roth, S.Y., and Allis, C.D.** (1996). Tetrahymena histone acetyltransferase
1285 A: a homolog to yeast Gcn5p linking histone acetylation to gene activation.
1286 *Cell.* **84**: 843-851.

1287 **Charron, J.B., He, H., Elling, A.A., and Deng, X.W.** (2009). Dynamic
1288 landscapes of four histone modifications during deetiolation in *Arabidopsis*.
1289 *Plant Cell.* **21**: 3732-3748.

1290 **Choat, B., Jansen, S., Brodribb, T.J., Cochard, H., Delzon, S., Bhaskar, R.,**
1291 **Bucci, S.J., Feild, T.S., Gleason, S.M., Hacke, U.G., Jacobsen, A.L.,**
1292 **Lens, F., Maherali, H., Martinez-Vilalta, J., Mayr, S., Mencuccini, M.,**

1293 **Mitchell, P.J., Nardini, A., Pittermann, J., Pratt, R.B., Sperry, J.S.,**
1294 **Westoby, M., Wright, I.J., and Zanne, A.E.** (2012). Global convergence in
1295 the vulnerability of forests to drought. *Nature*. **491**: 752-755.

1296 **Evert, R.F.** (2006). *Esau's Plant Anatomy: Meristems, Cells, and Tissues of*
1297 *the Plant Body: Their Structure, Function, and Development*, 3rd ed.
1298 (Hoboken, NJ: John Wiley & Sons).

1299 **Fisher, J.B., Goldstein, G., Jones, T.J., and Cordell, S.** (2007). Wood vessel
1300 diameter is related to elevation and genotype in the Hawaiian tree
1301 *Metrosideros polymorpha* (Myrtaceae). *Am. J. Bot.* **94**: 709-715.

1302 **Fujita, M., Fujita, Y., Maruyama, K., Seki, M., Hiratsu, K., Ohme-Takagi, M.,**
1303 **Tran, L.S., Yamaguchi-Shinozaki, K., and Shinozaki, K.** (2004). A
1304 dehydration-induced NAC protein, RD26, is involved in a novel
1305 ABA-dependent stress-signaling pathway. *Plant J.* **39**: 863-876.

1306 **Fujita, Y., Fujita, M., Satoh, R., Maruyama, K., Parvez, M.M., Seki, M.,**
1307 **Hiratsu, K., Ohme-Takagi, M., Shinozaki, K., and Yamaguchi-Shinozaki,**
1308 **K.** (2005). AREB1 is a transcription activator of novel ABRE-dependent ABA
1309 signaling that enhances drought stress tolerance in *Arabidopsis*. *Plant Cell.*
1310 **17**: 3470-3488.

1311 **Fujita, Y., Fujita, M., Shinozaki, K., and Yamaguchi-Shinozaki, K.** (2011).
1312 ABA-mediated transcriptional regulation in response to osmotic stress in
1313 plants. *J. Plant Res.* **124**: 509-525.

1314 **Furihata, T., Maruyama, K., Fujita, Y., Umezawa, T., Yoshida, R.,**
1315 **Shinozaki, K., and Yamaguchi-Shinozaki, K.** (2006). Abscisic
1316 acid-dependent multisite phosphorylation regulates the activity of a
1317 transcription activator AREB1. *Proc. Natl. Acad. Sci. USA.* **103**: 1988-1993.

1318 **Grant, P.A., Duggan, L., Cote, J., Roberts, S.M., Brownell, J.E., Candau, R.,**
1319 **Ohba, R., Owen-Hughes, T., Allis, C.D., Winston, F., Berger, S.L., and**
1320 **Workman, J.L.** (1997). Yeast Gcn5 functions in two multisubunit complexes

1321 to acetylate nucleosomal histones: characterization of an Ada complex and
1322 the SAGA (Spt/Ada) complex. *Genes Dev.* **11**: 1640-1650.

1323 **Hark, A.T., Vlachonasios, K.E., Pavangadkar, K.A., Rao, S., Gordon, H.,**
1324 **Adamakis, I.D., Kaldis, A., Thomashow, M.F., and Triezenberg, S.J.**
1325 (2009). Two *Arabidopsis* orthologs of the transcriptional coactivator ADA2
1326 have distinct biological functions. *Biochim. Biophys. Acta.* **1789**: 117-124.

1327 **Hickman, R., Hill, C., Penfold, C.A., Breeze, E., Bowden, L., Moore, J.D.,**
1328 **Zhang, P., Jackson, A., Cooke, E., Bewicke-Copley, F., Mead, A.,**
1329 **Beynon, J., Wild, D.L., Denby, K.J., Ott, S., and Buchanan-Wollaston, V.**
1330 (2013). A local regulatory network around three NAC transcription factors in
1331 stress responses and senescence in *Arabidopsis* leaves. *Plant J.* **75**: 26-39.

1332 **Hochberg, U., Bonel, A.G., David-Schwartz, R., Degu, A., Fait, A., Cochard,**
1333 **H., Peterlunger, E., and Herrera, J.C.** (2017). Grapevine acclimation to
1334 water deficit: the adjustment of stomatal and hydraulic conductance differs
1335 from petiole embolism vulnerability. *Planta.* **245**: 1091-1104.

1336 **Hu, H., Dai, M., Yao, J., Xiao, B., Li, X., Zhang, Q., and Xiong, L.** (2006).
1337 Overexpressing a NAM, ATAF, and CUC (NAC) transcription factor
1338 enhances drought resistance and salt tolerance in rice. *Proc. Natl. Acad. Sci.*
1339 *USA.* **103**: 12987-12992.

1340 **Hu, R., Qi, G., Kong, Y., Kong, D., Gao, Q., and Zhou, G.** (2010).
1341 Comprehensive analysis of NAC domain transcription factor gene family in
1342 *Populus trichocarpa*. *BMC Plant Biol.* **10**: 145.

1343 **Jaenisch, R., and Bird, A.** (2003). Epigenetic regulation of gene expression:
1344 how the genome integrates intrinsic and environmental signals. *Nat. Genet.*
1345 **33**: 245-254.

1346 **Kim, D., Pertea, G., Trapnell, C., Pimentel, H., Kelley, R., and Salzberg, S.L.**
1347 (2013). TopHat2: accurate alignment of transcriptomes in the presence of
1348 insertions, deletions and gene fusions. *Genome Biol.* **14**: R36.

1349 **Kim, J.M., To, T.K., Ishida, J., Matsui, A., Kimura, H., and Seki, M.** (2012).
1350 Transition of chromatin status during the process of recovery from drought
1351 stress in *Arabidopsis thaliana*. *Plant Cell Physiol.* **53**: 847-856.

1352 **Kim, J.M., To, T.K., Ishida, J., Morosawa, T., Kawashima, M., Matsui, A.,**
1353 **Toyoda, T., Kimura, H., Shinozaki, K., and Seki, M.** (2008). Alterations of
1354 lysine modifications on the histone H3 N-tail under drought stress conditions
1355 in *Arabidopsis thaliana*. *Plant Cell Physiol.* **49**: 1580-1588.

1356 **Kornet, N., and Scheres, B.** (2009). Members of the GCN5 histone
1357 acetyltransferase complex regulate PLETHORA-mediated root stem cell
1358 niche maintenance and transit amplifying cell proliferation in *Arabidopsis*.
1359 *Plant cell.* **21**: 1070-1079.

1360 **Koutelou, E., Hirsch, C.L., and Dent, S.Y.** (2010). Multiple faces of the SAGA
1361 complex. *Curr. Opin. Cell Biol.* **22**: 374-382.

1362 **Kouzarides, T.** (2007). Chromatin modifications and their function. *Cell.* **128**:
1363 693-705.

1364 **Kurdistani, S.K., Tavazoie, S., and Grunstein, M.** (2004). Mapping global
1365 histone acetylation patterns to gene expression. *Cell.* **117**: 721-733.

1366 **Langmead, B., and Salzberg, S.L.** (2012). Fast gapped-read alignment with
1367 Bowtie 2. *Nat. Methods.* **9**: 357-U354.

1368 **Lee, D.K., Chung, P.J., Jeong, J.S., Jang, G., Bang, S.W., Jung, H., Kim,**
1369 **Y.S., Ha, S.H., Choi, Y.D., and Kim, J.K.** (2017). The rice OsNAC6
1370 transcription factor orchestrates multiple molecular mechanisms involving
1371 root structural adaptations and nicotianamine biosynthesis for drought
1372 tolerance. *Plant Biotechnol. J.* **15**: 754-764.

1373 **Lee, D.Y., Hayes, J.J., Dmitry., P., and Wolffe, A.P.** (1993). A positive role
1374 for histone acetylation in transcription factor access to nucleosomal DNA.
1375 *Cell.* **72**: 73-84.

1376 **Li, Q., Lin, Y.C., Sun, Y.H., Song, J., Chen, H., Zhang, X.H., Sederoff, R.R.,**
1377 **and Chiang, V.L.** (2012). Splice variant of the SND1 transcription factor is a
1378 dominant negative of SND1 members and their regulation in *Populus*
1379 *trichocarpa*. Proc. Natl. Acad. Sci. USA. **109**: 14699-14704.

1380 **Li, W., Lin, Y.C., Li, Q., Shi, R., Lin, C.Y., Chen, H., Chuang, L., Qu, G.Z.,**
1381 **Sederoff, R.R., and Chiang, V.L.** (2014). A robust chromatin
1382 immunoprecipitation protocol for studying transcription factor-DNA
1383 interactions and histone modifications in wood-forming tissue. Nat. Protoc. **9**:
1384 2180-2193.

1385 **Li, W., Liu, H., Cheng, Z.J., Su, Y.H., Han, H.N., Zhang, Y., and Zhang, X.S.**
1386 (2011). DNA methylation and histone modifications regulate *de novo* shoot
1387 regeneration in *Arabidopsis* by modulating *WUSCHEL* expression and auxin
1388 signaling. PLoS Genet. **7**: e1002243.

1389 **Lin, Y.C., Li, W., Chen, H., Li, Q., Sun, Y.H., Shi, R., Lin, C.Y., Wang, J.P.,**
1390 **Chen, H.C., Chuang, L., Qu, G.Z., Sederoff, R.R., and Chiang, V.L.**
1391 (2014). A simple improved-throughput xylem protoplast system for studying
1392 wood formation. Nat. Protoc. **9**: 2194-2205.

1393 **Lin, Y.C., Li, W., Sun, Y.H., Kumari, S., Wei, H., Li, Q., Tunlaya-Anukit, S.,**
1394 **Sederoff, R.R., and Chiang, V.L.** (2013). SND1 transcription factor-directed
1395 quantitative functional hierarchical genetic regulatory network in wood
1396 formation in *Populus trichocarpa*. Plant Cell. **25**: 4324-4341.

1397 **Mao, Y., Pavangadkar, K.A., Thomashow, M.F., and Triezenberg, S.J.**
1398 (2006). Physical and functional interactions of *Arabidopsis* ADA2
1399 transcriptional coactivator proteins with the acetyltransferase GCN5 and
1400 with the cold-induced transcription factor CBF1. Biochim. Biophys. Acta.
1401 **1759**: 69-79.

1402 **McLeay, R.C., and Bailey, T.L.** (2010). Motif Enrichment Analysis: a unified
1403 framework and an evaluation on ChIP data. BMC Bioinformatics. **11**: 165.

1404 **Mi, H., Muruganujan, A., Casagrande, J.T., and Thomas, P.D.** (2013).
1405 Large-scale gene function analysis with the PANTHER classification system.
1406 Nat. Protoc. **8**: 1551-1566.

1407 **Monclus, R., Dreyer, E., Villar, M., Delmotte, F.M., Delay, D., Petit, J.M.,**
1408 **Barbaroux, C., Le Thiec, D., Brechet, C., and Brignolas, F.** (2006).
1409 Impact of drought on productivity and water use efficiency in 29 genotypes
1410 of *Populus deltoides* x *Populus nigra*. New Phytol. **169**: 765-777.

1411 **Msanne, J., Lin, J., Stone, J.M., and Awada, T.** (2011). Characterization of
1412 abiotic stress-responsive *Arabidopsis thaliana* RD29A and RD29B genes
1413 and evaluation of transgenes. Planta. **234**: 97-107.

1414 **Nakashima, K., Yamaguchi-Shinozaki, K., and Shinozaki, K.** (2014). The
1415 transcriptional regulatory network in the drought response and its crosstalk
1416 in abiotic stress responses including drought, cold, and heat. Front Plant Sci.
1417 **5**: 170.

1418 **Norton, V.G., Imai, B.S., Yau, P., and Bradbury, E.M.** (1989). Histone
1419 acetylation reduces nucleosome core particle linking number change. Cell.
1420 **57**: 449-457.

1421 **Quinlan, A.R., and Hall, I.M.** (2010). BEDTools: A flexible suite of utilities for
1422 comparing genomic features. Bioinformatics. **26**: 841-842.

1423 **Ragauskas, A.J., Williams, C.K., Davison, B.H., Britovsek, G., Cairney, J.,**
1424 **Eckert, C.A., Frederick, W., Hallett, J., Leak, D., Liotta, C., Mielenz, J.,**
1425 **Murphy, R., Templer, R., and Tschaplinski, T.** (2006). The path forward
1426 for biofuels and biomaterials. Science. **311**: 484-489.

1427 **Ramegowda, V., Gill, U.S., Sivalingam, P.N., Gupta, A., Gupta, C., Govind,**
1428 **G., Nataraja, K.N., Pereira, A., Udayakumar, M., Mysore, K.S., and**
1429 **Senthil-Kumar, M.** (2017). GBF3 transcription factor imparts drought
1430 tolerance in *Arabidopsis thaliana*. Sci. Rep. **7**: 9148.

1431 **Robinson, M.D., McCarthy, D.J., and Smyth, G.K.** (2010). edgeR: a
1432 Bioconductor package for differential expression analysis of digital gene
1433 expression data. *Bioinformatics*. **26**: 139-140.

1434 **Roeder, R.G.** (1996). The role of general initiation factors in transcription by
1435 RNA polymerase II. *Trends Biochem Sci*. **21**: 327-335.

1436 **Shahbazian, M.D., and Grunstein, M.** (2007). Functions of site-specific
1437 histone acetylation and deacetylation. *Annu. Rev. Biochem.* **76**: 75-100.

1438 **Shen, L., Shao, N.Y., Liu, X., Maze, I., Feng, J., and Nestler, E.J.** (2013).
1439 diffReps: detecting differential chromatin modification sites from ChIP-seq
1440 data with biological replicates. *PLoS One*. **8**: e65598.

1441 **Skiryycz, A., and Inze, D.** (2010). More from less: plant growth under limited
1442 water. *Curr. Opin. Biotechnol.* **21**: 197-203.

1443 **Song, J., Lu, S., Chen, Z.Z., Lourenco, R., and Chiang, V.L.** (2006). Genetic
1444 transformation of *Populus trichocarpa* genotype Nisqually-1: a functional
1445 genomic tool for woody plants. *Plant Cell Physiol.* **47**: 1582-1589.

1446 **Song, L., Huang, S.C., Wise, A., Castanon, R., Nery, J.R., Chen, H.,**
1447 **Watanabe, M., Thomas, J., Bar-Joseph, Z., and Ecker, J.R.** (2016). A
1448 transcription factor hierarchy defines an environmental stress response
1449 network. *Science*. **354**: aag1550.

1450 **Stockinger, E.J., Mao, Y., Regier, M.K., Triezenberg, S.J., and**
1451 **Thomashow, M.F.** (2001). Transcriptional adaptor and histone
1452 acetyltransferase proteins in *Arabidopsis* and their interactions with CBF1, a
1453 transcriptional activator involved in cold-regulated gene expression. *Nucleic*
1454 *acids research*. **29**: 1524-1533.

1455 **Tran, L.S., Nakashima, K., Sakuma, Y., Simpson, S.D., Fujita, Y.,**
1456 **Maruyama, K., Fujita, M., Seki, M., Shinozaki, K., and**
1457 **Yamaguchi-Shinozaki, K.** (2004). Isolation and functional analysis of
1458 *Arabidopsis* stress-inducible NAC transcription factors that bind to a

1459 drought-responsive cis-element in the early responsive to dehydration stress
1460 1 promoter. *Plant Cell*. **16**: 2481-2498.

1461 **Tyree, M.T., and Sperry, J.S.** (1989). Vulnerability of Xylem to Cavitation and
1462 Embolism. *Annu. Rev. Plant Physiol. Plant Mol. Biol.* **1**: 19-36.

1463 **Ueta, R., Abe, C., Watanabe, T., Sugano, S.S., Ishihara, R., Ezura, H.,**
1464 **Osakabe, Y., and Osakabe, K.** (2017). Rapid breeding of parthenocarpic
1465 tomato plants using CRISPR/Cas9. *Sci. Rep.* **7**: 507.

1466 **Vlachonasios, K.E.** (2003). Disruption mutations of ADA2b and GCN5
1467 transcriptional adaptor genes dramatically affect *Arabidopsis* growth,
1468 development, and gene expression. *Plant Cell*. **15**: 626-638.

1469 **Wang, S., Sun, H., Ma, J., Zang, C., Wang, C., Wang, J., Tang, Q., Meyer,**
1470 **C.A., Zhang, Y., and Liu, X.S.** (2013). Target analysis by integration of
1471 transcriptome and ChIP-seq data with BETA. *Nat. Protoc.* **8**: 2502-2515.

1472 **Weiste, C., and Droge-Laser, W.** (2014). The *Arabidopsis* transcription factor
1473 bZIP11 activates auxin-mediated transcription by recruiting the histone
1474 acetylation machinery. *Nat. Commun.* **5**: 3883.

1475 **Wickham, H.** (2009). *ggplot2: Elegant Graphics for Data Analysis*. Springer
1476 Science & Business Media.

1477 **Widiez, T., Symeonidi, A., Luo, C., Lam, E., Lawton, M., and Rensing, S.A.**
1478 (2014). The chromatin landscape of the moss *Physcomitrella patens* and its
1479 dynamics during development and drought stress. *Plant J.* **79**: 67-81.

1480 **Wu, Y., Deng, Z., Lai, J., Zhang, Y., Yang, C., Yin, B., Zhao, Q., Zhang, L.,**
1481 **Li, Y., Yang, C., and Xie, Q.** (2009). Dual function of *Arabidopsis* ATAF1 in
1482 abiotic and biotic stress responses. *Cell Res.* **19**: 1279-1290.

1483 **Yoshida, T., Fujita, Y., Sayama, H., Kidokoro, S., Maruyama, K., Mizoi, J.,**
1484 **Shinozaki, K., and Yamaguchi-Shinozaki, K.** (2010). AREB1, AREB2, and
1485 ABF3 are master transcription factors that cooperatively regulate

1486 ABRE-dependent ABA signaling involved in drought stress tolerance and
1487 require ABA for full activation. *Plant J.* **61**: 672-685.

1488 **Zentner, G.E., and Henikoff, S.** (2013). Regulation of nucleosome dynamics
1489 by histone modifications. *Nature Struct. Mol. Biol.* **20**: 259-266.

1490 **Zhou, J., Wang, X., He, K., Charron, J.B., Elling, A.A., and Deng, X.W.**
1491 (2010). Genome-wide profiling of histone H3 lysine 9 acetylation and
1492 dimethylation in *Arabidopsis* reveals correlation between multiple histone
1493 marks and gene expression. *Plant. Mol. Biol.* **72**: 585-595.

1494 **Zhou, S., Jiang, W., Long, F., Cheng, S., Yang, W., Zhao, Y., and Zhou,**
1495 **D.X.** (2017). Rice homeodomain protein WOX11 recruits a histone
1496 acetyltransferase complex to establish programs of cell proliferation of
1497 crown root meristem. *Plant Cell.* **29**: 1088-1104.

1498

1499 **Figure Legends**

1500 **Figure 1. Integration of ChIP-seq and RNA-seq Data to Identify Drought**
1501 **Stress-Responsive Genes with Differential H3K9ac of Promoters and**
1502 **Identification of Transcription Binding Motifs.**

1503 **(A)** and **(B)** Plots for \log_2 fold change of gene expression and H3K9ac
1504 enrichment at promoters for D5/ND **(A)** and D7/ND **(B)**; hUP, increased
1505 H3K9ac level; hDN, decreased H3K9ac level; gUP, gene upregulation; gDN,
1506 gene downregulation. **(C)** and **(D)** Analysis of motif enrichment of the
1507 promoters with differential H3K9ac for D5/ND **(C)** and D7/ND **(D)**; H represents
1508 A or C or T, N represents any base, K represents G or T, and M represents A
1509 or C. **(E)** The top-ranked motif in the promoters with differential H3K9ac for
1510 both D5/ND and D7/ND was the ABRE consensus motif for the AREB1
1511 transcription factor.

1512

1513 **Figure 2. ABRE Motifs Mediate H3K9ac Association and Regulation of**
1514 ***PtrNAC* Genes.**

1515 **(A)** RT-qPCR detection of *PtrNAC005*, *PtrNAC006*, *PtrNAC007*, *PtrNAC118*,
1516 and *PtrNAC120* in wild-type *P. trichocarpa* plants without (ND) or with drought
1517 treatment for 5 (D5) and 7 (D7) days. Error bars indicate one SE of three
1518 biological replicates from independent pools of *P. trichocarpa* stem
1519 differentiating xylem (SDX) tissues. Asterisks indicate significant difference
1520 between control (ND) and drought-treated samples (D5; D7) for each gene
1521 (** $P < 0.01$, Student's *t*-test). **(B)** Schematic diagram of ABRE motifs in five
1522 *PtrNAC* gene promoters. **(C)** ChIP quantitative PCR (ChIP-qPCR) detection of
1523 H3K9ac in ABRE motif regions of *PtrNAC* promoters in wild-type *P. trichocarpa*
1524 plants without (ND) or with drought treatment for 5 (D5) and 7 (D7) days.
1525 Numbers indicate ABRE motif sites in each gene. ChIP assays were performed
1526 using antibodies against H3K9ac, and the precipitated DNA was quantified by

1527 qPCR. Enrichment values represent the relative fold change from ND, and
1528 error bars indicate one SE of three biological replicates from independent pools
1529 of *P. trichocarpa* SDX tissues. Asterisks indicate significant difference between
1530 control (ND) and drought-treated samples (D5; D7) for each fragment
1531 containing the ABRE motif (* P <0.05; ** P <0.01, Student's *t*-test).

1532

1533 **Figure 3. Overexpressing *PtrNAC* Genes Improves Drought Tolerance of**
1534 ***P. trichocarpa*.**

1535 **(A)** Drought tolerance phenotype of *OE-PtrNAC006* (*OE-N6*), *OE-PtrNAC007*
1536 (*OE-N7*), and *OE-PtrNAC120* (*OE-N12*) transgenic plants. Three-month-old
1537 plants (before drought, upper panel) were dehydrated for 12 days (D12, middle
1538 panel) and then rehydrated for 3 days (D12 + Rehydrated for 3 d, lower panel).
1539 Bars=10 cm. **(B)** Statistical analysis of height and stem basal diameter of
1540 wild-type (WT) and *OE-PtrNAC* transgenic plants before drought, at D12, and
1541 D12 + Rehydrated for 3 d. Error bars represent one SE of three independent
1542 experiments with 12 *P. trichocarpa* plants for each genotype in each replicate.
1543 Asterisks indicate significant difference between the transgenics harboring
1544 each gene construct and WT plants for each time point (* P <0.05; ** P <0.01,
1545 Student's *t*-test). **(C)** Statistical analysis of survival rates after drought treatment
1546 and recovery (D12 + Rehydrated for 3 d). The average percentage of survival
1547 and standard errors were calculated from three independent experiments with
1548 at least 12 plants of each genotype in each replicate. Asterisks indicate
1549 significant difference between the transgenics harboring each gene construct
1550 and WT plants (* P <0.05; ** P <0.01, Student's *t*-test). **(D)** Statistical analysis of
1551 stem water potential of WT and *OE-PtrNACs* transgenic plants with no drought
1552 treatment and drought treatment for 5 days. Error bars represent one SE of
1553 three independent experiments with six *P. trichocarpa* plants of each genotype
1554 in each replicate, and asterisks indicate significant difference between the

1555 transgenics harboring each gene construct and WT plants for each condition
1556 (** $P < 0.01$, Student's t -test).

1557

1558 **Figure 4. Overexpressing *PtrNAC* Genes Affects the Size and Number of**
1559 **Vessels in Xylem Tissue of *P. trichocarpa*.**

1560 **(A)** Stem cross-sections of wild-type (WT) and *OE-PtrNAC* transgenic plants
1561 with the 10th internode. Bars=200 μm . **(B)**, **(C)** and **(D)** Statistical analysis of
1562 mean lumen area of individual vessels (μm^2) **(B)**, number of vessels per
1563 cross-sectional area (mm^2) **(C)**, and area of vessels (μm^2) per cross-sectional
1564 area (mm^2) **(D)** using vessel cells from **(A)**. Error bars represent one SE of three
1565 independent replicates with at least 200 vessel cells for each genotype in each
1566 replicate, and asterisks indicate significant difference between the transgenics
1567 harboring each gene construct and WT plants. * $P < 0.05$, ** $P < 0.01$ (Student's
1568 t -test). **(E)** Scanning electron micrographs (SEM) of WT and *OE-PtrNAC006*
1569 transgenic plants with the 10th internode imaged at $\times 500$, $\times 1000$, and $\times 2000$
1570 magnification. Bars=20 μm .

1571

1572 **Figure 5. *PtrAREB1-2* Activates Transcription of *PtrNAC* Genes and**
1573 **Binds Directly to the ABRE Motifs in Their Promoters.**

1574 **(A)** Expression patterns of *PtrAREB1-2*, *PtrAREB1-3*, and *PtrAREB1-4* genes
1575 in response to drought stress detected by RT-qPCR. Expression was highly
1576 induced by drought treatment. Error bars indicate one SE of three biological
1577 replicates from independent pools of *P. trichocarpa* stem differentiating xylem
1578 (SDX) tissues. Asterisks indicate significant difference between control (ND)
1579 and drought-treated samples (D5; D7) for each gene (** $P < 0.01$, Student's
1580 t -test). **(B)** RT-qPCR to detect transcript abundance of *PtrNAC006*,
1581 *PtrNAC007*, and *PtrNAC120* in SDX protoplasts overexpressing *GFP* (control)
1582 or *PtrAREB1-2* in the presence of external 50 μM ABA. Control values were

1583 set as 1. Error bars indicate one SE of three biological replicates (three
1584 independent batches of SDX protoplast transfections). Asterisks indicate
1585 significant difference for each gene between control protoplasts and those
1586 overexpressing *PtrAREB1-2* samples for each gene (** $P < 0.01$, Student's
1587 *t*-test). **(C)** *PtrAREB1-2* ChIP assays showing that *PtrAREB1-2* binds directly
1588 to the promoters of *PtrNAC* genes. *P. trichocarpa* SDX protoplasts
1589 overexpressing *PtrAREB1-2-GFP* or *GFP* (control) were used for ChIP assay
1590 with anti-GFP antibody, and the precipitated DNA was quantified by qPCR.
1591 Enrichment of DNA was calculated as the ratio between
1592 $35S_{pro}:PtrAREB1-2-GFP$ and $35S_{pro}:GFP$ (control), normalized to that of the
1593 *PtrACTIN* gene. Numbers indicate ABRE motif sites in *PtrNAC120*. Error bars
1594 represent one SE of three biological replicates (three independent batches of
1595 SDX protoplast transfections). Asterisks indicate significant difference between
1596 the control fragment (*PtrACTIN*) and each fragment containing an ABRE motif
1597 (** $P < 0.01$, Student's *t*-test). **(D-F)** Nucleotide sequences of the wild-type
1598 ABRE and a mutated ABRE motif (mABRE) (upper panel). Core sequences
1599 are shaded in black, and the mutated nucleotide is shaded in gray. EMSA
1600 analysis of *PtrAREB1-2* binding to ABRE motifs in *PtrNAC006* **(D)**, *PtrNAC007*
1601 **(E)**, and *PtrNAC120* **(F)** promoters (lower panel). The arrow shows the shifted
1602 band representing the protein–DNA complex. *PtrNAC006* **(D)**, *PtrNAC007* **(E)**,
1603 and *PtrNAC120* **(F)** promoter fragments were labeled with biotin. Fragments
1604 without biotin labeling were used as competitors. Wild-type or mutated ABRE
1605 competitors were used in a molar excess of 50x, 100x, or 150x.

1606

1607 **Figure 6. *PtrAREB1-2* Interacts with the Histone Acetyltransferase**
1608 **Complex *PtrADA2b-3-PtrGCN5-1*.**

1609 **(A)** and **(B)** Abundance of alternatively spliced transcripts of *PtrADA2b-1*,
1610 *PtrADA2b-2*, and *PtrADA2b-3* **(A)**, and *PtrGCN5-1* and *PtrGCN5-2* **(B)**

1611 determined by RT-qPCR in the xylem of *P. trichocarpa* under well-watered and
1612 drought conditions. Error bars indicate one SE of three biological replicates in
1613 **(A)**, and six biological replicates in **(B)** from independent pools of *P. trichocarpa*
1614 stem differentiating xylem (SDX) tissues. Asterisks indicate significant
1615 difference between control (ND) and the drought-treated (D5; D7) samples for
1616 each gene ($*P<0.05$; $**P<0.01$, Student's *t*-test), and n.s. denotes no significant
1617 difference. **(C-E)** Interactions of PtrADA2b-3, PtrGCN5-1, and PtrAREB1-2
1618 with each other determined by pull-down. His-tagged PtrGCN5-1 and
1619 PtrAREB1-2, and S-tagged PtrADA2b-3 and PtrAREB1-2 purified from *E. coli*
1620 were used for pull-down assays, and GFP was used as a negative control.
1621 **(F-N)** BiFC assays in *P. trichocarpa* SDX protoplasts showing that PtrADA2b-3,
1622 PtrGCN5-1, and PtrAREB1-2 proteins interact with each other in the nucleus
1623 **(F-H)**. Cotransfection of each protein of interest with empty plasmid was
1624 served as a control **(I-K)**. PtrMYB021, an unrelated TF expressed in the
1625 nucleus (Li et al., 2012), was used as another negative control **(L-N)**. Neither
1626 negative control gave any YFP signal. Green shows the YFP signals from
1627 protein interaction, red indicates the nuclear marker H2A-1:mCherry, and
1628 yellow represents the merged signals from YFP and mCherry. Bars=10 μ m.
1629 Images from two other biological replicates are shown in Supplemental Figure
1630 13.

1631

1632 **Figure 7. PtrADA2b-3 and PtrGCN5-1 Together Enhance**
1633 **PtrAREB1-2-Mediated Transcriptional Activation of *PtrNAC* Genes by**
1634 **Increasing H3K9ac Level and RNA Polymerase II Recruitment at Their**
1635 **Promoters.**

1636 **(A)** Quantitative PCR detection of *PtrNAC006*, *PtrNAC007*, and *PtrNAC120*
1637 transcripts in *P. trichocarpa* stem differentiating xylem (SDX) protoplasts
1638 overexpressing *GFP* (control), *PtrAREB1-2*, *PtrGCN5-1*, *PtrADA2b-3*,

1639 *PtrAREB1-2:PtrGCN5-1*, *PtrAREB1-2:PtrADA2b-3*, *PtrADA2b-3:PtrGCN5-1*,
1640 or *PtrAREB1-2:PtrADA2b-3:PtrGCN5-1* in the presence of external 50 μ M
1641 ABA. Five genes without ABRE motifs were used as negative controls, none of
1642 which had activated expression. The control values in **(A)** were set as 1. Error
1643 bars represent one SE of three biological replicates (three independent
1644 batches of SDX protoplast transfections). Asterisks indicate significant
1645 difference between the ternary complex and each monomeric or dimeric
1646 protein for each gene (** P <0.01, Student's t -test), and n.s. denotes no
1647 significant difference. **(B)** and **(C)** ChIP-qPCR showing that co-overexpression
1648 of *PtrAREB1-2*, *PtrADA2b-3*, and *PtrGCN5-1* increased H3K9ac **(B)** and RNA
1649 polymerase II (Pol II) **(C)** enrichment at the promoters of *PtrNAC006*,
1650 *PtrNAC007*, and *PtrNAC120*. SDX protoplasts overexpressing *PtrAREB1-2*,
1651 *PtrGCN5-1*, *PtrADA2b-3*, *PtrAREB1-2:PtrGCN5-1*, *PtrAREB1-2:PtrADA2b-3*,
1652 *PtrADA2b-3:PtrGCN5-1*, *PtrAREB1-2:PtrADA2b-3:PtrGCN5-1*, or *GFP*
1653 (control) were used for ChIP assay with anti-H3K9ac **(B)** and anti-RNA Pol II
1654 **(C)** antibodies, and the precipitated DNA was quantified by qPCR. None of the
1655 five negative control genes had enhanced H3K9ac **(B)** or RNA Pol II **(C)** levels
1656 at their promoters. Enrichment values represent the relative fold change
1657 compared to the protoplasts overexpressing *PtrAREB1-2*. Error bars indicate
1658 one SE of three biological replicates (three independent batches of SDX
1659 protoplast transfections). Asterisks in **(B)** and **(C)** indicate significant difference
1660 between the ternary complex and each monomeric or dimeric protein for each
1661 fragment containing the ABRE motif (** P <0.01, Student's t -test), and n.s.
1662 denotes no significant difference.

1663

1664 **Figure 8. Reduced or Deleted Expression of *PtrAREB1-2*, *PtrADA2b-3*, or**
1665 ***PtrGCN5-1* in *P. trichocarpa* Decreases H3K9ac and RNA Polymerase II**

1666 **Enrichment on *PtrNAC* Genes, Expression of These *NAC* Genes, and**
1667 **Plant Drought Tolerance.**

1668 **(A-C)** Quantitative PCR detection of *PtrNAC006*, *PtrNAC007*, and *PtrNAC120*
1669 transcripts in wild-type (WT), RNAi-*PtrAREB1-2* (R6 and R9 = lines 6 and 9)
1670 **(A)**, KO-*PtrADA2b-3* (KO1 and KO2 = knock-out mutants 1 and 2) **(B)** and
1671 RNAi-*PtrGCN5-1* (R2 and R5 = lines 2 and 5) **(C)** transgenic plants following
1672 drought treatment for 5 days. Error bars in **(A-C)** indicate one SE of three
1673 biological replicates from independent pools of *P. trichocarpa* stem
1674 differentiating xylem (SDX) tissues, and asterisks indicate significant difference
1675 between each transgenic line and WT plants for each *PtrNAC* gene, * $P < 0.05$,
1676 ** $P < 0.01$ (Student's *t*-test). **(D-F)** ChIP quantitative PCR (ChIP-qPCR)
1677 detection of H3K9ac at promoters of *PtrNAC* genes in WT, RNAi-*PtrAREB1-2*
1678 **(D)**, KO-*PtrADA2b-3* **(E)** and RNAi-*PtrGCN5-1* **(F)** transgenic plants following
1679 drought treatment for 5 days. **(G-I)** ChIP-qPCR detection of RNA polymerase II
1680 (Pol II) enrichment at promoters of *PtrNAC* genes in WT, RNAi-*PtrAREB1-2*
1681 **(G)**, KO-*PtrADA2b-3* **(H)**, and RNAi-*PtrGCN5-1* **(I)** transgenic plants following
1682 drought treatment for 5 days. ChIP assays were performed using antibodies
1683 against H3K9ac **(D-F)** and RNA Pol II **(G-I)**, and the precipitated DNA was
1684 quantified by qPCR. Enrichment values represent the relative fold change
1685 compared to WT plants. Numbers in **(D-I)** indicate ABRE motif sites in
1686 *PtrNAC120*. Each experiment had three biological replicates showing similar
1687 results. Error bars indicate one SE of three technical replicates, and asterisks
1688 indicate significant difference from WT plants, ** $P < 0.01$ (Student's *t*-test). **(J)**
1689 Drought-sensitive phenotype of RNAi9-*PtrAREB1-2*, RNAi5-*PtrGCN5-1*, and
1690 KO2-*PtrADA2b-3* transgenic plants. Three-month-old plants (before drought,
1691 upper panel) were dehydrated for 10 days and then rehydrated for 3 days (D10
1692 + Rehydrated for 3 d, lower panel). Bars=10 cm. **(K)** Statistical analysis of
1693 survival rates after drought treatment and recovery (D10 + Rehydrated for 3 d).

1694 Error bars represent one SE of three independent experiments with at least 12
1695 plants of each genotype in each replicate, and asterisks indicate significant
1696 difference between the transgenics of each gene construct and WT plants.
1697 ** $P < 0.01$ (Student's *t*-test).

1698

1699 **Figure 9. Proposed Model of AREB1-Mediated Histone Acetylation in**
1700 **Regulation of Drought Stress-Responsive *PtrNAC* Genes.**

1701 Under drought stress conditions, the expression of the AREB1 transcription
1702 factor is induced. AREB1 interacts with the ADA2b-GCN5 histone
1703 acetyltransferase complex and recruits the proteins to *PtrNAC006*, *PtrNAC007*,
1704 and *PtrNAC120* genes through binding to ABRE motifs, resulting in enhanced
1705 H3K9ac and RNA polymerase II (Pol II) enrichment for activating expression of
1706 the *PtrNAC006*, *PtrNAC007*, and *PtrNAC120* genes.

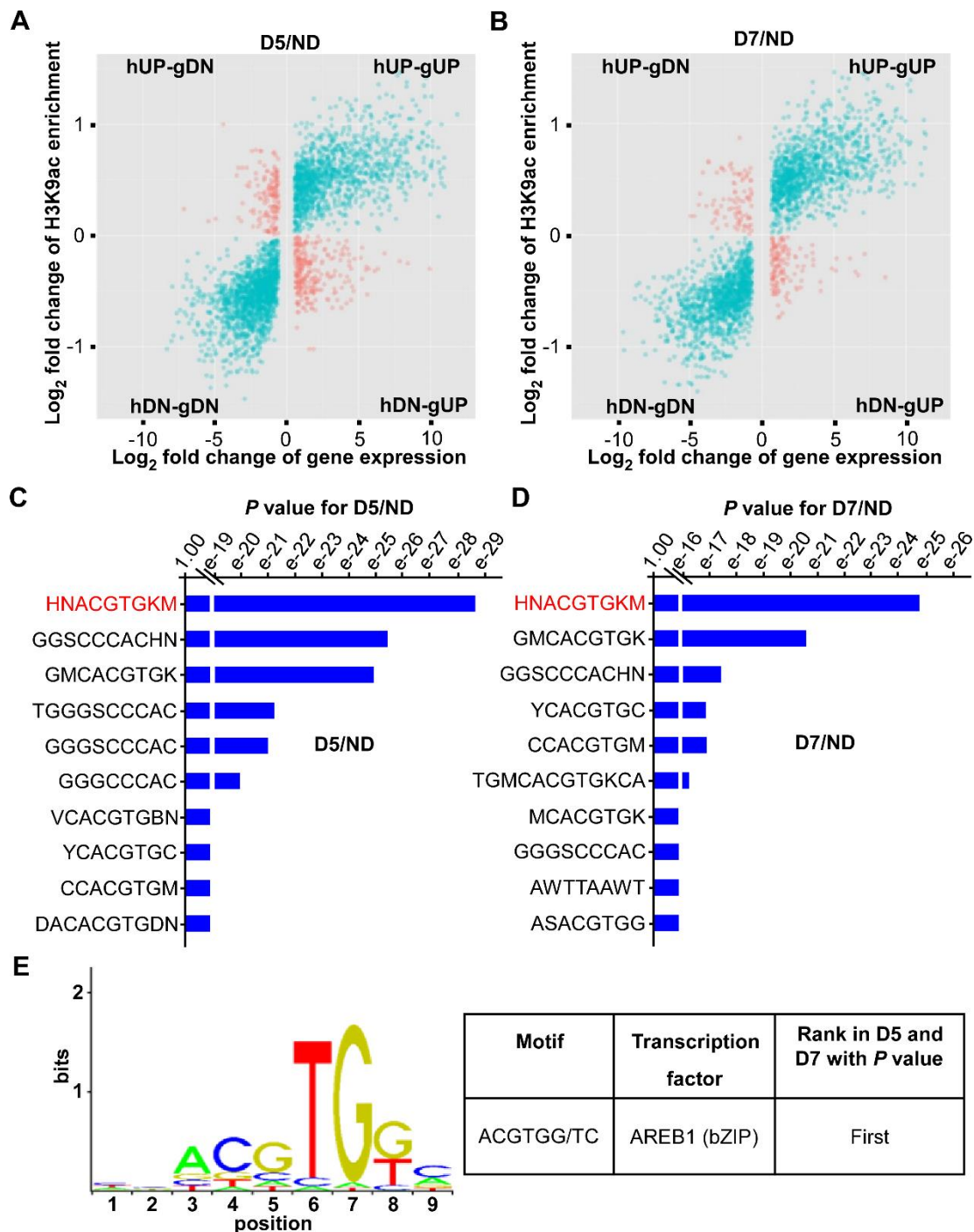


Figure 1. Integration of ChIP-seq and RNA-seq Data to Identify Drought Stress-Responsive Genes with Differential H3K9ac of Promoters and Identification of Transcription Binding Motifs.

(A) and (B) Plots for \log_2 fold change of gene expression and H3K9ac enrichment at promoters for D5/ND (A) and D7/ND (B); hUP, increased H3K9ac level; hDN, decreased H3K9ac level; gUP, gene upregulation; gDN, gene downregulation. (C) and (D) Analysis of motif enrichment of the promoters with differential H3K9ac for D5/ND (C) and D7/ND (D); H represents A or C or T, N represents any base, K represents G or T, and M represents A or C. (E) The top-ranked motif in the promoters with differential H3K9ac for both D5/ND and D7/ND was the ABRE consensus motif for the AREB1 transcription factor.

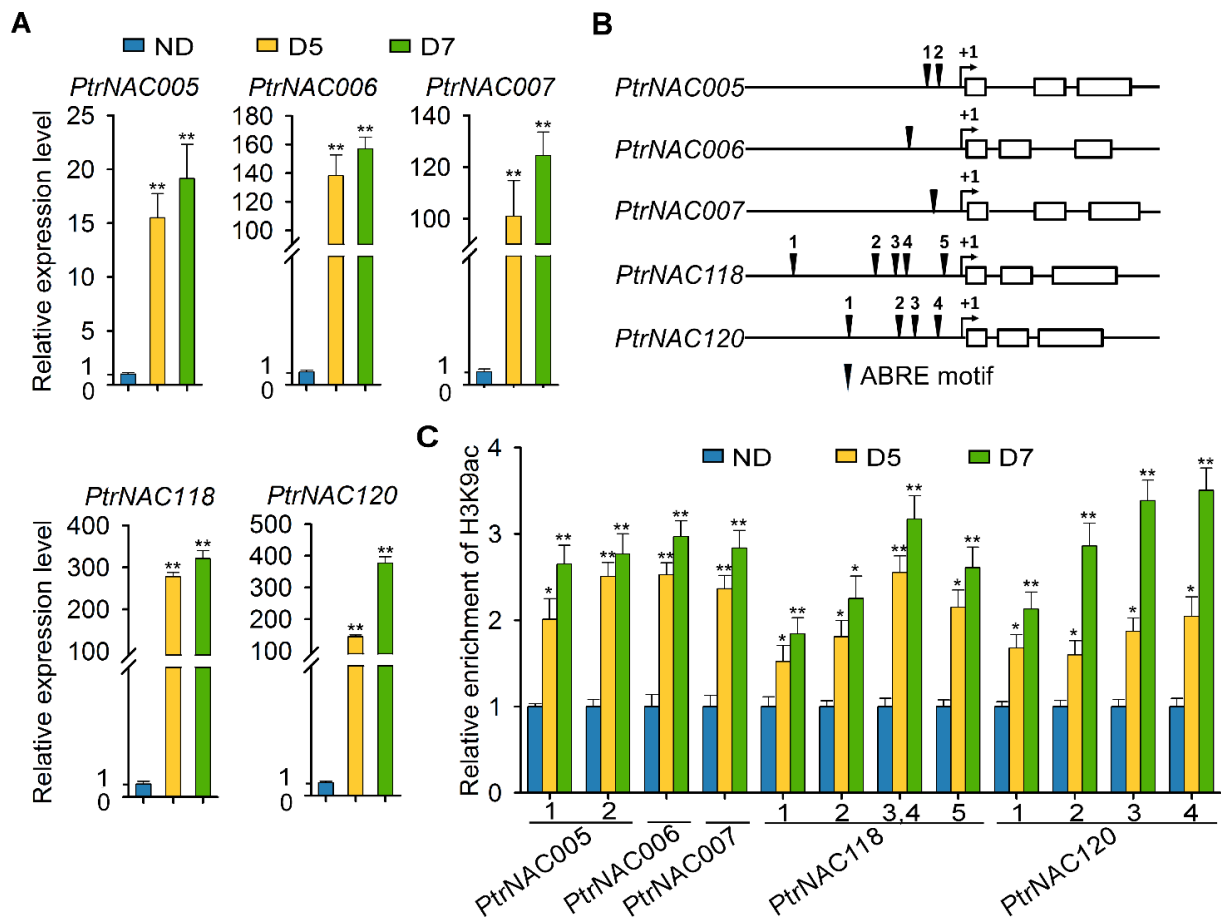


Figure 2. ABRE Motifs Mediate H3K9ac Association and Regulation of *PtrNAC* Genes.

(A) RT-qPCR detection of *PtrNAC005*, *PtrNAC006*, *PtrNAC007*, *PtrNAC118*, and *PtrNAC120* in wild-type *P. trichocarpa* plants without (ND) or with drought treatment for 5 (D5) and 7 (D7) days. Error bars indicate one SE of three biological replicates from independent pools of *P. trichocarpa* stem differentiating xylem (SDX) tissues. Asterisks indicate significant difference between control (ND) and drought-treated samples (D5; D7) for each gene (** $P < 0.01$, Student's *t*-test). **(B)** Schematic diagram of ABRE motifs in five *PtrNAC* gene promoters. **(C)** ChIP quantitative PCR (ChIP-qPCR) detection of H3K9ac in ABRE motif regions of *PtrNAC* promoters in wild-type *P. trichocarpa* plants without (ND) or with drought treatment for 5 (D5) and 7 (D7) days. Numbers indicate ABRE motif sites in each gene. ChIP assays were performed using antibodies against H3K9ac, and the precipitated DNA was quantified by qPCR. Enrichment values represent the relative fold change from ND, and error bars indicate one SE of three biological replicates from independent pools of *P. trichocarpa* SDX tissues. Asterisks indicate significant difference between control (ND) and drought-treated samples (D5; D7) for each fragment containing the ABRE motif (* $P < 0.05$; ** $P < 0.01$, Student's *t*-test).

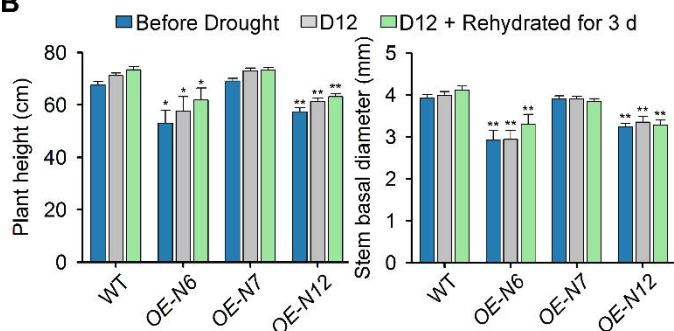
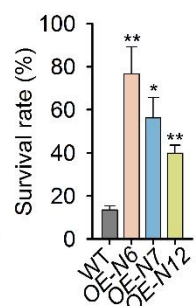
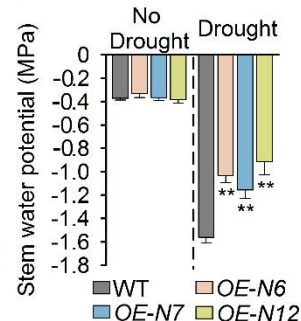
A**B****C****D**

Figure 3. Overexpressing *PtrNAC* Genes Improves Drought Tolerance of *P. trichocarpa*.

(A) Drought tolerance phenotype of *OE-PtrNAC006* (*OE-N6*), *OE-PtrNAC007* (*OE-N7*), and *OE-PtrNAC120* (*OE-N12*) transgenic plants. Three-month-old plants (before drought, upper panel) were dehydrated for 12 days (D12, middle panel) and then rehydrated for 3 days (D12 + Rehydrated for 3 d, lower panel). Bars=10 cm. **(B)** Statistical analysis of height and stem basal diameter of wild-type (WT) and *OE-PtrNAC* transgenic plants before drought, at D12, and D12 + Rehydrated for 3 d. Error bars represent one SE of three independent experiments with 12 *P. trichocarpa* plants for each genotype in each replicate. Asterisks indicate significant difference between the transgenics harboring each gene construct and WT plants for each time point (* $P < 0.05$; ** $P < 0.01$, Student's *t*-test). **(C)** Statistical analysis of survival rates after drought treatment and recovery (D12 + Rehydrated for 3 d). The average percentage of survival and standard errors were calculated from three independent experiments with at least 12 plants of each genotype in each replicate. Asterisks indicate significant difference between the transgenics harboring each gene construct and WT plants (* $P < 0.05$; ** $P < 0.01$, Student's *t*-test). **(D)** Statistical analysis of stem water potential of WT and *OE-PtrNACs* transgenic plants with no drought treatment and drought treatment for 5 days. Error bars represent one SE of three independent experiments with six *P. trichocarpa* plants of each genotype in each replicate, and asterisks indicate significant difference between the transgenics harboring each gene construct and WT plants for each condition (** $P < 0.01$, Student's *t*-test).

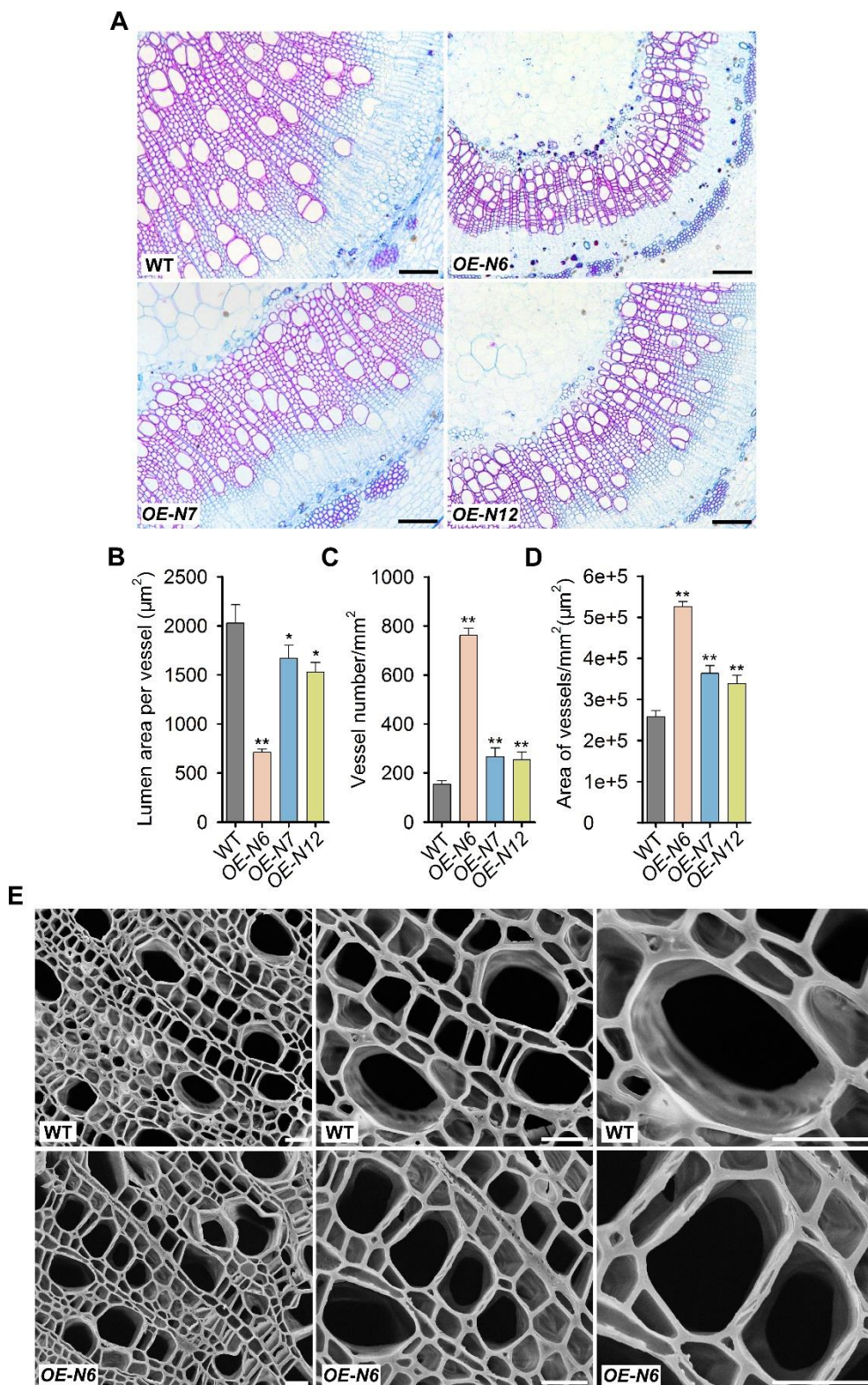


Figure 4. Overexpressing *PtrNAC* Genes Affects the Size and Number of Vessels in Xylem Tissue of *P. trichocarpa*.

(A) Stem cross-sections of wild-type (WT) and *OE-PtrNAC* transgenic plants with the 10th internode. Bars=200 μm . (B), (C) and (D) Statistical analysis of mean lumen area of individual vessels (μm^2) (B), number of vessels per cross-sectional area (mm^2) (C), and area of vessels (μm^2) per cross-sectional area (mm^2) (D) using vessel cells from (A). Error bars represent one SE of three independent replicates with at least 200 vessel cells for each genotype in each replicate, and asterisks indicate significant difference between the transgenics harboring each gene construct and WT plants. * $P < 0.05$, ** $P < 0.01$ (Student's *t*-test). (E) Scanning electron micrographs (SEM) of WT and *OE-PtrNAC006* transgenic plants with the 10th internode imaged at $\times 500$, $\times 1000$, and $\times 2000$ magnification. Bars=20 μm .

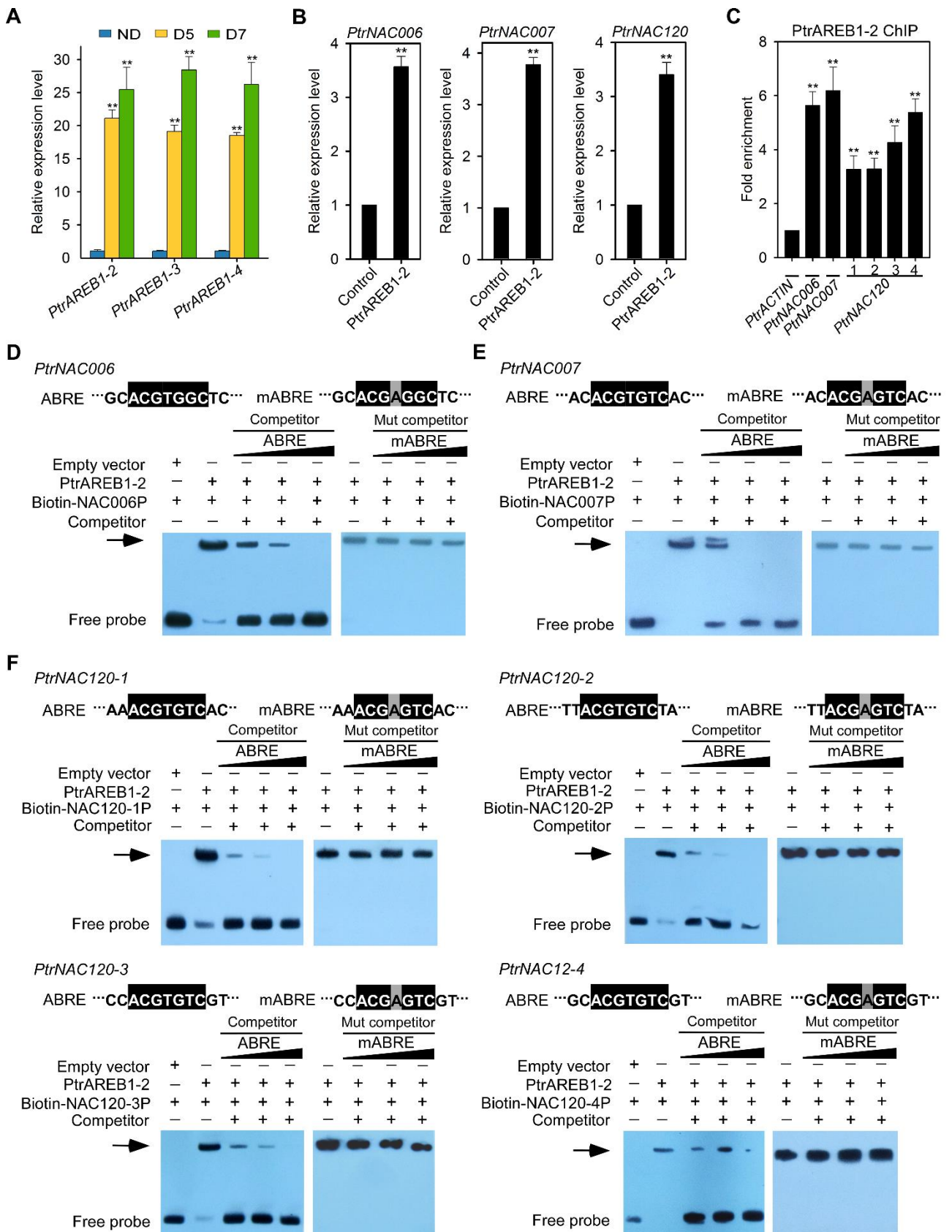


Figure 5. PtrAREB1-2 Activates Transcription of *PtrNAC* Genes and Binds Directly to the ABRE Motifs in Their Promoters.

(A) Expression patterns of *PtrAREB1-2*, *PtrAREB1-3*, and *PtrAREB1-4* genes in response to drought stress detected by RT-qPCR. Expression was highly induced by drought treatment. Error bars indicate one SE of three biological replicates from independent pools of *P. trichocarpa* stem differentiating xylem (SDX) tissues. Asterisks indicate significant difference between control (ND) and drought-treated samples (D5; D7) for each gene (** $P < 0.01$, Student's *t*-test).

(B) RT-qPCR to detect transcript abundance of *PtrNAC006*, *PtrNAC007*, and *PtrNAC120* in SDX protoplasts overexpressing *GFP* (control) or *PtrAREB1-2* in the presence of external 50 μ M ABA. Control values were set as 1. Error bars indicate one SE of three biological replicates (three independent batches of SDX protoplast transfections). Asterisks indicate significant difference for each gene between control protoplasts and those overexpressing *PtrAREB1-2* samples for each gene (** $P < 0.01$, Student's *t*-test). **(C)** *PtrAREB1-2* ChIP assays showing that *PtrAREB1-2* binds directly to the promoters of *PtrNAC* genes. *P. trichocarpa* SDX protoplasts overexpressing *PtrAREB1-2-GFP* or *GFP* (control) were used for ChIP assay with anti-GFP antibody, and the precipitated DNA was quantified by qPCR. Enrichment of DNA was calculated as the ratio between $35S_{pro}:PtrAREB1-2-GFP$ and $35S_{pro}:GFP$ (control), normalized to that of the *PtrACTIN* gene. Numbers indicate ABRE motif sites in *PtrNAC120*. Error bars represent one SE of three biological replicates (three independent batches of SDX protoplast transfections). Asterisks indicate significant difference between the control fragment (*PtrACTIN*) and each fragment containing an ABRE motif (** $P < 0.01$, Student's *t*-test). **(D-F)** Nucleotide sequences of the wild-type ABRE and a mutated ABRE motif (mABRE) (upper panel). Core sequences are shaded in black, and the mutated nucleotide is shaded in gray. EMSA analysis of *PtrAREB1-2* binding to ABRE motifs in *PtrNAC006* **(D)**, *PtrNAC007* **(E)**, and *PtrNAC120* **(F)** promoters (lower panel). The arrow shows the shifted band representing the protein–DNA complex. *PtrNAC006* **(D)**, *PtrNAC007* **(E)**, and *PtrNAC120* **(F)** promoter fragments were labeled with biotin. Fragments without biotin labeling were used as competitors. Wild-type or mutated ABRE competitors were used in a molar excess of 50 \times , 100 \times , or 150 \times .

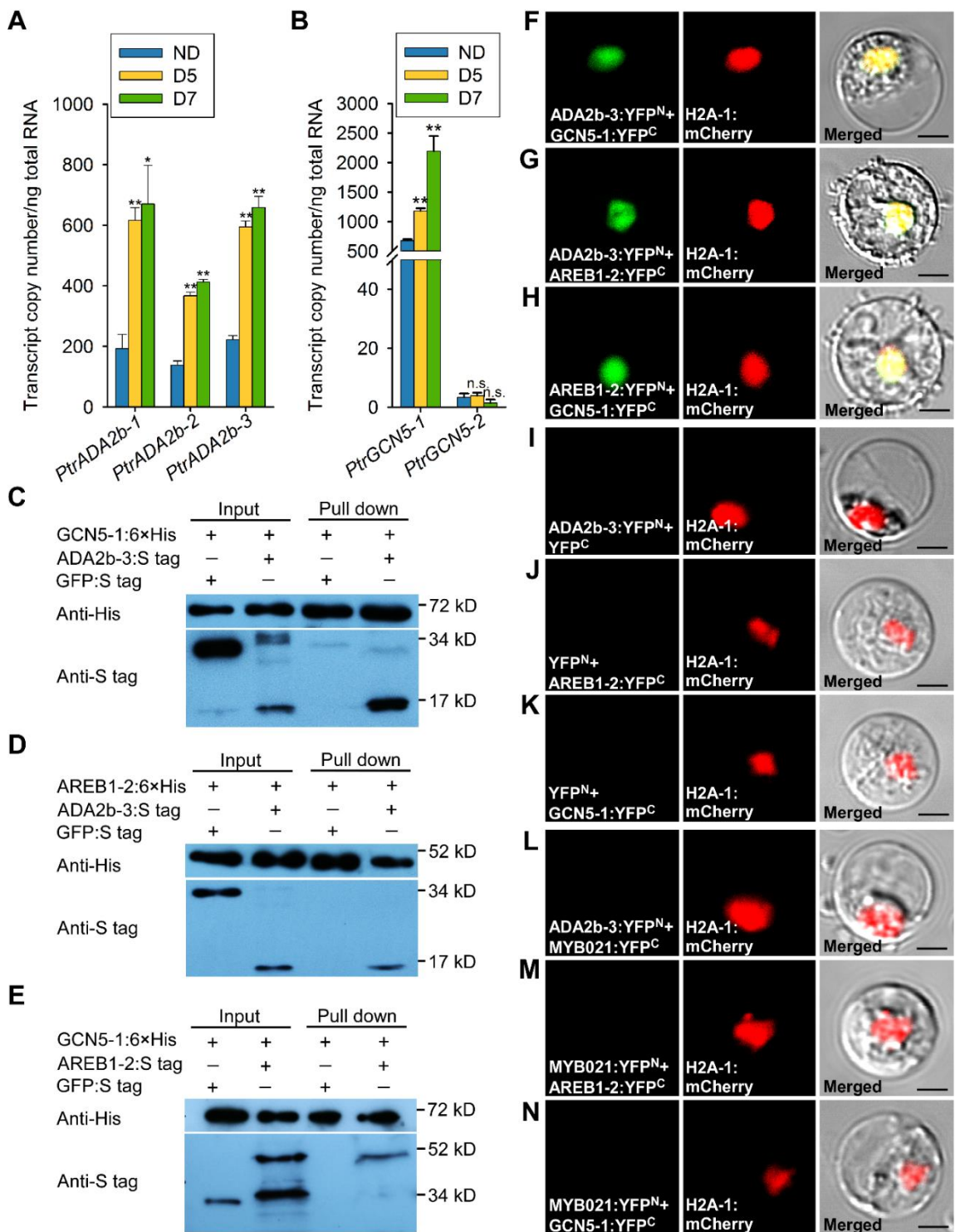


Figure 6. PtrAREB1-2 Interacts with the Histone Acetyltransferase Complex PtrADA2b-3-PtrGCN5-1. (A) and (B) Abundance of alternatively spliced transcripts of *PtrADA2b-1*, *PtrADA2b-2*, and *PtrADA2b-3* (A), and *PtrGCN5-1* and *PtrGCN5-2* (B) determined by RT-qPCR in the xylem of *P. trichocarpa* under well-watered and drought conditions. Error bars indicate one SE of three biological replicates in (A), and six biological replicates in (B) from independent pools of *P. trichocarpa* stem differentiating xylem (SDX) tissues. Asterisks indicate significant difference between control (ND) and the drought-treated (D5; D7) samples for each gene (* $P < 0.05$; ** $P < 0.01$, Student's *t*-test), and n.s. denotes no significant difference. (C-E) Interactions of *PtrADA2b-3*, *PtrGCN5-1*, and *PtrAREB1-2* with each other determined by pull-down. His-tagged *PtrGCN5-1* and *PtrAREB1-2*, and S-tagged *PtrADA2b-3* and *PtrAREB1-2* purified from *E. coli* were used for pull-down assays, and GFP was used as a negative control. (F-N) BiFC assays in *P. trichocarpa* SDX protoplasts showing that *PtrADA2b-3*, *PtrGCN5-1*, and *PtrAREB1-2* proteins interact with each other in the nucleus (F-H). Cotransfection of each protein of interest with empty plasmid was served as a control (I-K). *PtrMYB021*, an unrelated TF expressed in the nucleus (Li et al., 2012), was used as another negative control (L-N). Neither negative control gave any YFP signal. Green shows the YFP signals from protein interaction, red indicates the nuclear marker H2A-1:mCherry, and yellow represents the merged signals from YFP and mCherry. Bars=10 μ m. Images from two other biological replicates are shown in Supplemental Figure 13.

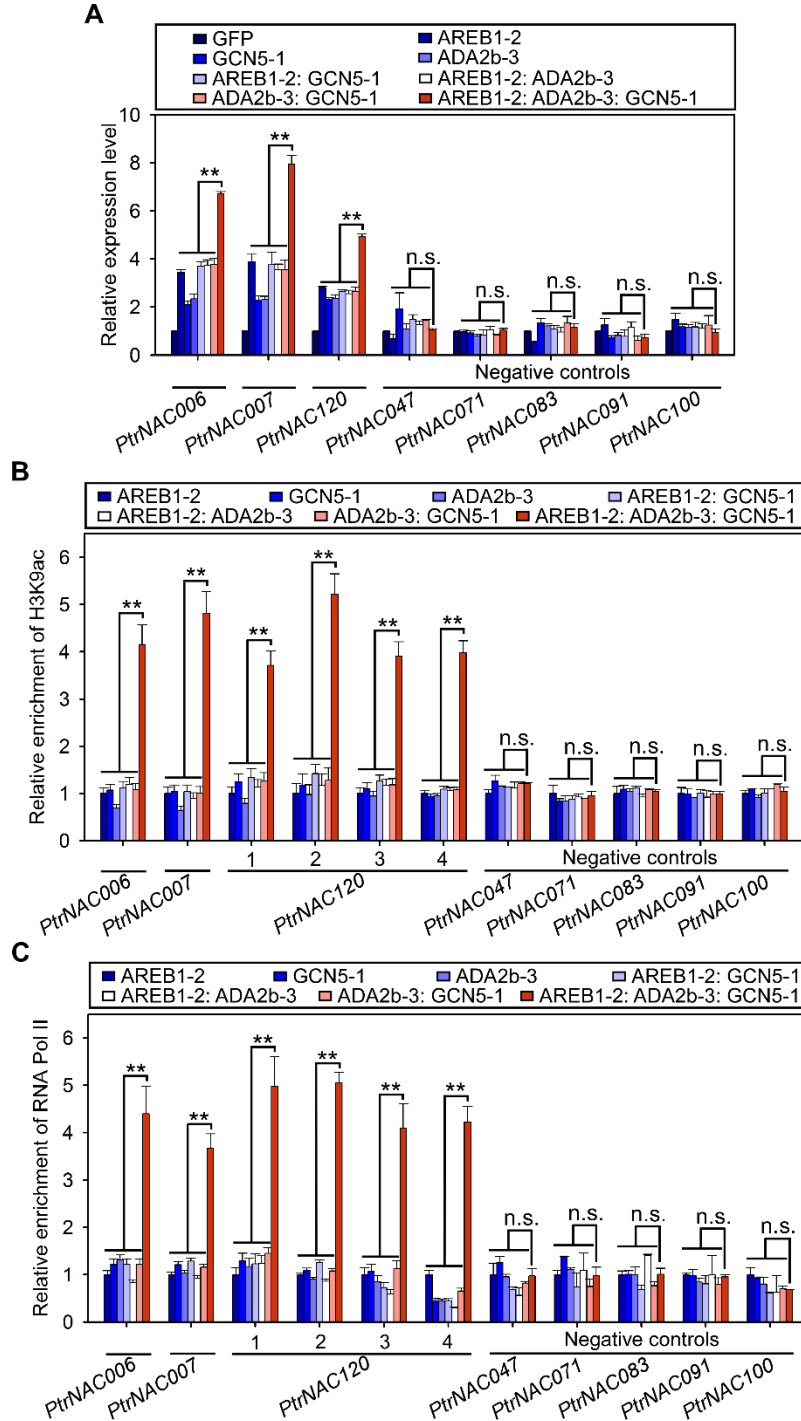


Figure 7. PtrADA2b-3 and PtrGCN5-1 Together Enhance PtrAREB1-2-Mediated Transcriptional Activation of *PtrNAC* Genes by Increasing H3K9ac Level and RNA Polymerase II Recruitment at Their Promoters.

(A) Quantitative PCR detection of *PtrNAC006*, *PtrNAC007*, and *PtrNAC120* transcripts in *P. trichocarpa* stem differentiating xylem (SDX) protoplasts overexpressing *GFP* (control), *PtrAREB1-2*, *PtrGCN5-1*, *PtrADA2b-3*, *PtrAREB1-2:PtrGCN5-1*, *PtrAREB1-2:PtrADA2b-3*, *PtrADA2b-3:PtrGCN5-1*, or *PtrAREB1-2:PtrADA2b-3:PtrGCN5-1* in the presence of external 50 μ M ABA. Five genes without ABRE motifs were used as negative controls, none of which had activated expression. The control values in **(A)** were set as 1. Error bars represent one SE of three biological replicates (three independent batches of SDX protoplast transfections). Asterisks indicate significant difference between the ternary complex and each monomeric or dimeric protein for each gene (** $P < 0.01$, Student's *t*-test), and n.s. denotes no significant difference. **(B)** and **(C)** ChIP-qPCR showing that co-overexpression of *PtrAREB1-2*, *PtrADA2b-3*, and *PtrGCN5-1* increased H3K9ac **(B)** and RNA polymerase II (Pol II) **(C)** enrichment at the promoters of *PtrNAC006*, *PtrNAC007*, and *PtrNAC120*. SDX protoplasts overexpressing *PtrAREB1-2*, *PtrGCN5-1*, *PtrADA2b-3*, *PtrAREB1-2:PtrGCN5-1*, *PtrAREB1-2:PtrADA2b-3*, *PtrADA2b-3:PtrGCN5-1*, *PtrAREB1-2:PtrADA2b-3:PtrGCN5-1*, or *GFP* (control) were used for ChIP assay with anti-H3K9ac **(B)** and anti-RNA Pol II **(C)** antibodies, and the precipitated DNA was quantified by qPCR. None of the five negative control genes had enhanced H3K9ac **(B)** or RNA Pol II **(C)** levels at their promoters. Enrichment values represent the relative fold change compared to the protoplasts overexpressing *PtrAREB1-2*. Error bars indicate one SE of three biological replicates (three independent batches of SDX protoplast transfections). Asterisks in **(B)** and **(C)** indicate significant difference between the ternary complex and each monomeric or dimeric protein for each fragment containing the ABRE motif (** $P < 0.01$, Student's *t*-test), and n.s. denotes no significant difference.

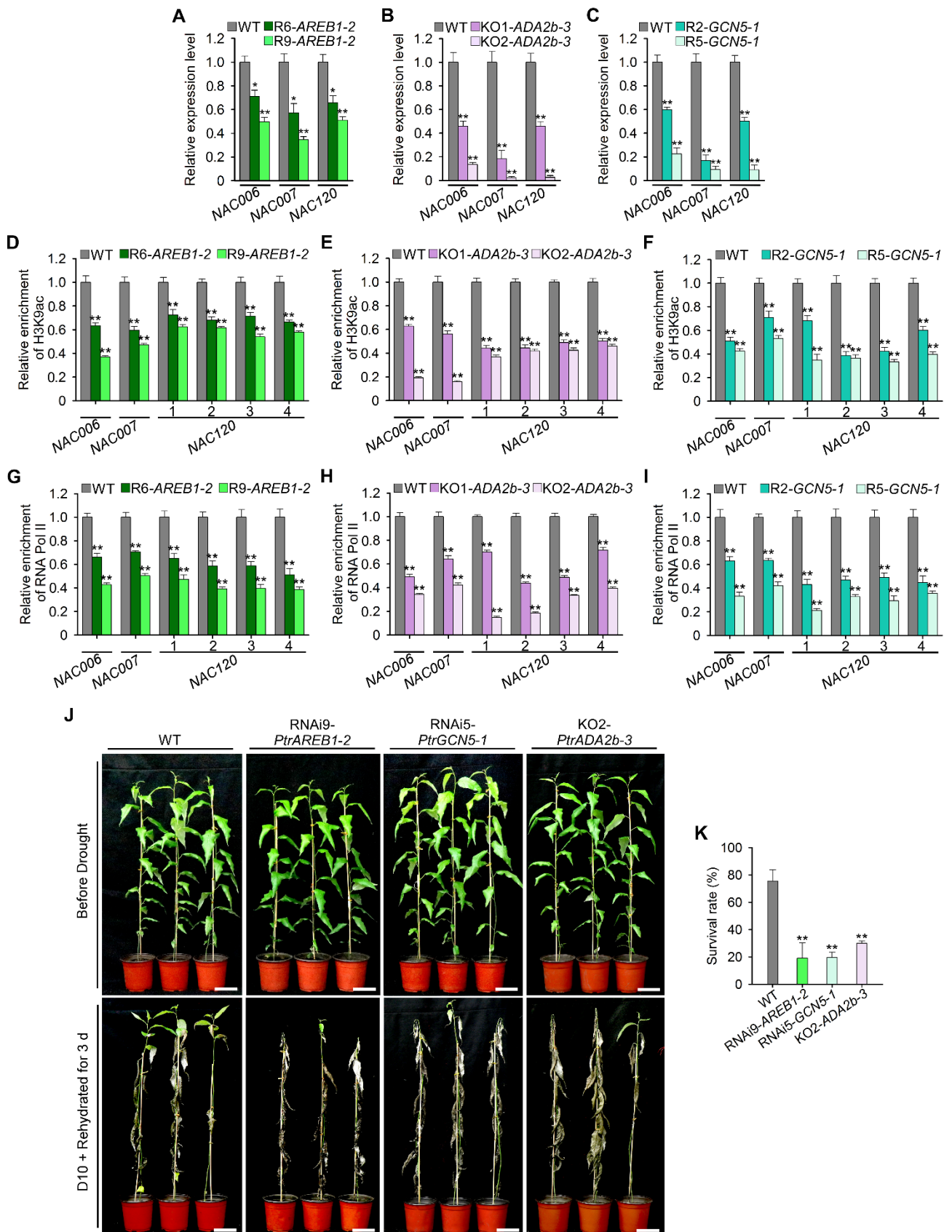


Figure 8. Reduced or Deleted Expression of *PtrAREB1-2*, *PtrADA2b-3*, or *PtrGCN5-1* in *P. trichocarpa* Decreases H3K9ac and RNA Polymerase II Enrichment on *PtrNAC* Genes, Expression of These *NAC* Genes, and Plant Drought Tolerance.

(A-C) Quantitative PCR detection of *PtrNAC006*, *PtrNAC007*, and *PtrNAC120* transcripts in wild-type (WT), RNAi-*PtrAREB1-2* (R6 and R9 = lines 6 and 9) (A), KO-*PtrADA2b-3* (KO1 and KO2 = knock-out mutants 1 and 2) (B) and RNAi-*PtrGCN5-1* (R2 and R5 = lines 2 and 5) (C) transgenic plants following drought treatment for 5 days. Error bars in (A-C) indicate one SE of three biological replicates from independent pools of *P. trichocarpa* stem differentiating xylem (SDX) tissues, and asterisks indicate significant difference between each transgenic line and WT plants for each *PtrNAC* gene, * $P < 0.05$, ** $P < 0.01$ (Student's *t*-test).

(D-F) ChIP quantitative PCR (ChIP-qPCR) detection of H3K9ac at promoters of *PtrNAC* genes in WT, RNAi-*PtrAREB1-2* **(D)**, KO-*PtrADA2b-3* **(E)** and RNAi-*PtrGCN5-1* **(F)** transgenic plants following drought treatment for 5 days. **(G-I)** ChIP-qPCR detection of RNA polymerase II (Pol II) enrichment at promoters of *PtrNAC* genes in WT, RNAi-*PtrAREB1-2* **(G)**, KO-*PtrADA2b-3* **(H)**, and RNAi-*PtrGCN5-1* **(I)** transgenic plants following drought treatment for 5 days. ChIP assays were performed using antibodies against H3K9ac **(D-F)** and RNA Pol II **(G-I)**, and the precipitated DNA was quantified by qPCR. Enrichment values represent the relative fold change compared to WT plants. Numbers in **(D-I)** indicate ABRE motif sites in *PtrNAC120*. Each experiment had three biological replicates showing similar results. Error bars indicate one SE of three technical replicates, and asterisks indicate significant difference from WT plants, ** $P < 0.01$ (Student's *t*-test). **(J)** Drought-sensitive phenotype of RNAi9-*PtrAREB1-2*, RNAi5-*PtrGCN5-1*, and KO2-*PtrADA2b-3* transgenic plants. Three-month-old plants (before drought, upper panel) were dehydrated for 10 days and then rehydrated for 3 days (D10 + Rehydrated for 3 d, lower panel). Bars=10 cm. **(K)** Statistical analysis of survival rates after drought treatment and recovery (D10 + Rehydrated for 3 d). Error bars represent one SE of three independent experiments with at least 12 plants of each genotype in each replicate, and asterisks indicate significant difference between the transgenics of each gene construct and WT plants. ** $P < 0.01$ (Student's *t*-test).

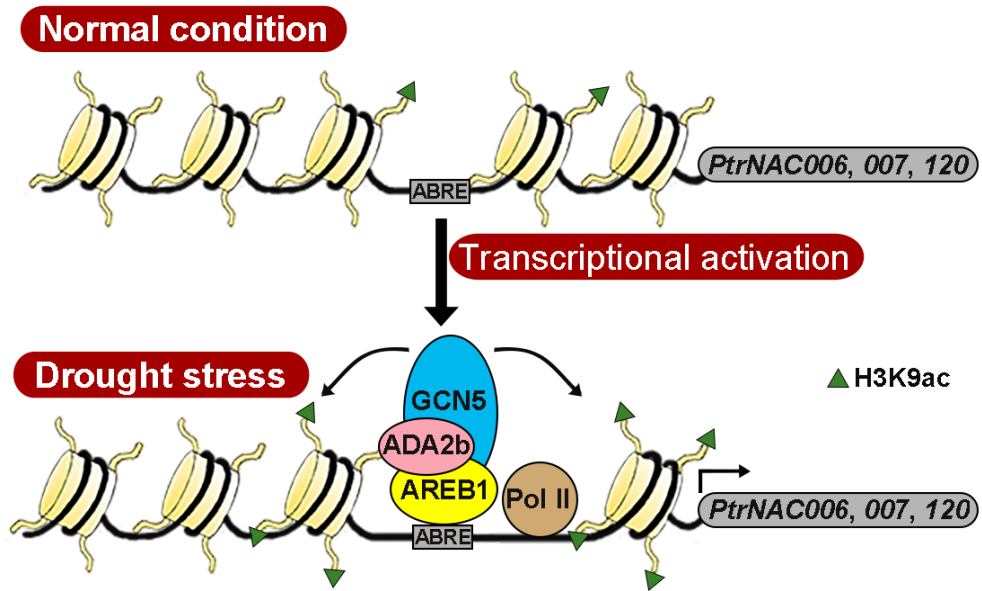


Figure 9. Proposed Model of AREB1-Mediated Histone Acetylation in Regulation of Drought Stress-Responsive *PtrNAC* Genes.

Under drought stress conditions, the expression of the AREB1 transcription factor is induced. AREB1 interacts with the ADA2b-GCN5 histone acetyltransferase complex and recruits the proteins to *PtrNAC006*, *PtrNAC007*, and *PtrNAC120* genes through binding to ABRE motifs, resulting in enhanced H3K9ac and RNA polymerase II (Pol II) enrichment for activating expression of the *PtrNAC006*, *PtrNAC007*, and *PtrNAC120* genes.

Parsed Citations

Arango-Velez, A., Zwiazek, J.J., Thomas, B.R., and Tyree, M.T. (2011). Stomatal factors and vulnerability of stem xylem to cavitation in poplars. *Physiol. Plant.* 143: 154-165.

Pubmed: [Author and Title](#)

Google Scholar: [Author Only](#) [Title Only](#) [Author and Title](#)

Ascenzil, R., and Gantt, J.S. (1999). Molecular genetic analysis of the drought-inducible linker histone variant in *Arabidopsis thaliana*. *Plant Mol. Biol.* 41: 159-169.

Pubmed: [Author and Title](#)

Google Scholar: [Author Only](#) [Title Only](#) [Author and Title](#)

Aubert, Y., Vile, D., Pervent, M., Aldon, D., Ranty, B., Simonneau, T., Vavasseur, A., and Galaud, J.P. (2010). RD20, a stress-inducible caleosin, participates in stomatal control, transpiration and drought tolerance in *Arabidopsis thaliana*. *Plant Cell Physiol.* 51: 1975-1987.

Pubmed: [Author and Title](#)

Google Scholar: [Author Only](#) [Title Only](#) [Author and Title](#)

Balasubramanian, R., Pray-Grant, M.G., Selleck, W., Grant, P.A., and Tan, S. (2002). Role of the Ada2 and Ada3 transcriptional coactivators in histone acetylation. *J. Biol. Chem.* 277: 7989-7995.

Pubmed: [Author and Title](#)

Google Scholar: [Author Only](#) [Title Only](#) [Author and Title](#)

Barber, V.A., Juday, G.P., and Finney, B.P. (2000). Reduced growth of Alaskan white spruce in the twentieth century from temperature-induced drought stress. *Nature.* 405: 668-673.

Pubmed: [Author and Title](#)

Google Scholar: [Author Only](#) [Title Only](#) [Author and Title](#)

Barbosa, E.G.G., Leite, J.P., Marin, S.R.R., Marinho, J.P., Carvalho, J.D.C., Fuganti-Pagliarini, R., Farias, J.R.B., Neumaier, N., Marcelino-Guimaraes, F.C., de Oliveira, M.C.N., Yamaguchi-Shinozaki, K., Nakashima, K., Maruyama, K., Kanamori, N., Fujita, Y., Yoshida, T., and Nepomuceno, A.L. (2013). Overexpression of the ABA-Dependent AREB1 Transcription Factor from *Arabidopsis thaliana* Improves Soybean Tolerance to Water Deficit. *Plant. Mol. Biol. Rep.* 31: 719-730.

Pubmed: [Author and Title](#)

Google Scholar: [Author Only](#) [Title Only](#) [Author and Title](#)

Berger, S.L. (2007). The complex language of chromatin regulation during transcription. *Nature.* 447: 407-412.

Pubmed: [Author and Title](#)

Google Scholar: [Author Only](#) [Title Only](#) [Author and Title](#)

Berta, M., Giovannelli, A., Sebastiani, F., Camussi, A., and Racchi, M.L. (2010). Transcriptome changes in the cambial region of poplar (*Populus alba* L.) in response to water deficit. *Plant biology.* 12: 341-354.

Pubmed: [Author and Title](#)

Google Scholar: [Author Only](#) [Title Only](#) [Author and Title](#)

Bogeat-Triboulot, M.B., Brosche, M., Renaut, J., Jouve, L., Le Thiec, D., Fayyaz, P., Vinocur, B., Witters, E., Laukens, K., Teichmann, T., Altman, A., Hausman, J.F., Polle, A., Kangasjarvi, J., and Dreyer, E. (2007). Gradual soil water depletion results in reversible changes of gene expression, protein profiles, ecophysiology, and growth performance in *Populus euphratica*, a poplar growing in arid regions. *Plant Physiol.* 143: 876-892.

Pubmed: [Author and Title](#)

Google Scholar: [Author Only](#) [Title Only](#) [Author and Title](#)

Bonnet, J., Wang, C.Y., Baptista, T., Vincent, S.D., Hsiao, W.C., Stierle, M., Kao, C.F., Tora, L., and Devys, D. (2014). The SAGA coactivator complex acts on the whole transcribed genome and is required for RNA polymerase II transcription. *Genes Dev.* 28: 1999-2012.

Pubmed: [Author and Title](#)

Google Scholar: [Author Only](#) [Title Only](#) [Author and Title](#)

Brownell, J.E., Zhou, J., Ranalli, T., Kobayashi, R., Edmondson, D.G., Roth, S.Y., and Allis, C.D. (1996). Tetrahymena histone acetyltransferase A: a homolog to yeast Gcn5p linking histone acetylation to gene activation. *Cell.* 84: 843-851.

Pubmed: [Author and Title](#)

Google Scholar: [Author Only](#) [Title Only](#) [Author and Title](#)

Charron, J.B., He, H., Elling, A.A., and Deng, X.W. (2009). Dynamic landscapes of four histone modifications during deetiolation in *Arabidopsis*. *Plant Cell.* 21: 3732-3748.

Pubmed: [Author and Title](#)

Google Scholar: [Author Only](#) [Title Only](#) [Author and Title](#)

Choat, B., Jansen, S., Brodribb, T.J., Cochard, H., Delzon, S., Bhaskar, R., Bucci, S.J., Feild, T.S., Gleason, S.M., Hacke, U.G., Jacobsen, A.L., Lens, F., Maherali, H., Martinez-Vilalta, J., Mayr, S., Mencuccini, M., Mitchell, P.J., Nardini, A., Pittermann, J., Pratt, R.B., Sperry, J.S., Westoby, M., Wright, I.J., and Zanne, A.E. (2012). Global convergence in the vulnerability of forests to drought. *Nature.* 491: 752-755.

Pubmed: [Author and Title](#)

Google Scholar: [Author Only](#) [Title Only](#) [Author and Title](#)

Evert, R.F. (2006). *Esau's Plant Anatomy: Meristems, Cells, and Tissues of the Plant Body: Their Structure, Function, and Development*, 3rd ed. (Hoboken, NJ: John Wiley & Sons).

Pubmed: [Author and Title](#)

Google Scholar: [Author Only Title Only Author and Title](#)

Fisher, J.B., Goldstein, G., Jones, T.J., and Cordell, S. (2007). Wood vessel diameter is related to elevation and genotype in the Hawaiian tree *Metrosideros polymorpha* (Myrtaceae). *Am. J. Bot.* 94: 709-715.

Pubmed: [Author and Title](#)

Google Scholar: [Author Only Title Only Author and Title](#)

Fujita, M., Fujita, Y., Maruyama, K., Seki, M., Hiratsu, K., Ohme-Takagi, M., Tran, L.S., Yamaguchi-Shinozaki, K., and Shinozaki, K. (2004). A dehydration-induced NAC protein, RD26, is involved in a novel ABA-dependent stress-signaling pathway. *Plant J.* 39: 863-876.

Pubmed: [Author and Title](#)

Google Scholar: [Author Only Title Only Author and Title](#)

Fujita, Y., Fujita, M., Satoh, R., Maruyama, K., Parvez, M.M., Seki, M., Hiratsu, K., Ohme-Takagi, M., Shinozaki, K., and Yamaguchi-Shinozaki, K. (2005). AREB1 is a transcription activator of novel ABRE-dependent ABA signaling that enhances drought stress tolerance in *Arabidopsis*. *Plant Cell.* 17: 3470-3488.

Pubmed: [Author and Title](#)

Google Scholar: [Author Only Title Only Author and Title](#)

Fujita, Y., Fujita, M., Shinozaki, K., and Yamaguchi-Shinozaki, K. (2011). ABA-mediated transcriptional regulation in response to osmotic stress in plants. *J. Plant Res.* 124: 509-525.

Pubmed: [Author and Title](#)

Google Scholar: [Author Only Title Only Author and Title](#)

Furihata, T., Maruyama, K., Fujita, Y., Umezawa, T., Yoshida, R., Shinozaki, K., and Yamaguchi-Shinozaki, K. (2006). Abscisic acid-dependent multisite phosphorylation regulates the activity of a transcription activator AREB1. *Proc. Natl. Acad. Sci. USA* 103: 1988-1993.

Pubmed: [Author and Title](#)

Google Scholar: [Author Only Title Only Author and Title](#)

Grant, P.A., Duggan, L., Cote, J., Roberts, S.M., Brownell, J.E., Candau, R., Ohba, R., Owen-Hughes, T., Allis, C.D., Winston, F., Berger, S.L., and Workman, J.L. (1997). Yeast Gcn5 functions in two multisubunit complexes to acetylate nucleosomal histones: characterization of an Ada complex and the SAGA (Spt/Ada) complex. *Genes Dev.* 11: 1640-1650.

Pubmed: [Author and Title](#)

Google Scholar: [Author Only Title Only Author and Title](#)

Hark, A.T., Vlachonasiou, K.E., Pavangadkar, K.A., Rao, S., Gordon, H., Adamakis, I.D., Kaldis, A., Thomashow, M.F., and Triezenberg, S.J. (2009). Two *Arabidopsis* orthologs of the transcriptional coactivator ADA2 have distinct biological functions. *Biochim. Biophys. Acta.* 1789: 117-124.

Pubmed: [Author and Title](#)

Google Scholar: [Author Only Title Only Author and Title](#)

Hickman, R., Hill, C., Penfold, C.A., Breeze, E., Bowden, L., Moore, J.D., Zhang, P., Jackson, A., Cooke, E., Bewicke-Copley, F., Mead, A., Beynon, J., Wild, D.L., Denby, K.J., Ott, S., and Buchanan-Wollaston, V. (2013). A local regulatory network around three NAC transcription factors in stress responses and senescence in *Arabidopsis* leaves. *Plant J.* 75: 26-39.

Pubmed: [Author and Title](#)

Google Scholar: [Author Only Title Only Author and Title](#)

Hochberg, U., Bonel, A.G., David-Schwartz, R., Degu, A., Fait, A., Cochard, H., Peterlunger, E., and Herrera, J.C. (2017). Grapevine acclimation to water deficit: the adjustment of stomatal and hydraulic conductance differs from petiole embolism vulnerability. *Planta.* 245: 1091-1104.

Pubmed: [Author and Title](#)

Google Scholar: [Author Only Title Only Author and Title](#)

Hu, H., Dai, M., Yao, J., Xiao, B., Li, X., Zhang, Q., and Xiong, L. (2006). Overexpressing a NAM, ATAF, and CUC (NAC) transcription factor enhances drought resistance and salt tolerance in rice. *Proc. Natl. Acad. Sci. USA* 103: 12987-12992.

Pubmed: [Author and Title](#)

Google Scholar: [Author Only Title Only Author and Title](#)

Hu, R., Qi, G., Kong, Y., Kong, D., Gao, Q., and Zhou, G. (2010). Comprehensive analysis of NAC domain transcription factor gene family in *Populus trichocarpa*. *BMC Plant Biol.* 10: 145.

Pubmed: [Author and Title](#)

Google Scholar: [Author Only Title Only Author and Title](#)

Jaenisch, R., and Bird, A. (2003). Epigenetic regulation of gene expression: how the genome integrates intrinsic and environmental signals. *Nat. Genet.* 33: 245-254.

Pubmed: [Author and Title](#)

Google Scholar: [Author Only Title Only Author and Title](#)

Kim, D., Perte, G., Trapnell, C., Pimentel, H., Kelley, R., and Salzberg, S.L. (2013). TopHat2: accurate alignment of transcriptomes in the presence of insertions, deletions and gene fusions. *Genome Biol.* 14: R36.

Pubmed: [Author and Title](#)

Google Scholar: [Author Only](#) [Title Only](#) [Author and Title](#)

Kim, J.M., To, T.K., Ishida, J., Matsui, A., Kimura, H., and Seki, M. (2012). Transition of chromatin status during the process of recovery from drought stress in *Arabidopsis thaliana*. *Plant Cell Physiol.* 53: 847-856.

Pubmed: [Author and Title](#)

Google Scholar: [Author Only](#) [Title Only](#) [Author and Title](#)

Kim, J.M., To, T.K., Ishida, J., Morosawa, T., Kawashima, M., Matsui, A., Toyoda, T., Kimura, H., Shinozaki, K., and Seki, M. (2008). Alterations of lysine modifications on the histone H3 N-tail under drought stress conditions in *Arabidopsis thaliana*. *Plant Cell Physiol.* 49: 1580-1588.

Pubmed: [Author and Title](#)

Google Scholar: [Author Only](#) [Title Only](#) [Author and Title](#)

Kornet, N., and Scheres, B. (2009). Members of the GCN5 histone acetyltransferase complex regulate PLETHORA-mediated root stem cell niche maintenance and transit amplifying cell proliferation in *Arabidopsis*. *Plant cell.* 21: 1070-1079.

Pubmed: [Author and Title](#)

Google Scholar: [Author Only](#) [Title Only](#) [Author and Title](#)

Koutelou, E., Hirsch, C.L., and Dent, S.Y. (2010). Multiple faces of the SAGA complex. *Curr. Opin. Cell Biol.* 22: 374-382.

Pubmed: [Author and Title](#)

Google Scholar: [Author Only](#) [Title Only](#) [Author and Title](#)

Kouzarides, T. (2007). Chromatin modifications and their function. *Cell.* 128: 693-705.

Pubmed: [Author and Title](#)

Google Scholar: [Author Only](#) [Title Only](#) [Author and Title](#)

Kurdistani, S.K., Tavazoie, S., and Grunstein, M. (2004). Mapping global histone acetylation patterns to gene expression. *Cell.* 117: 721-733.

Pubmed: [Author and Title](#)

Google Scholar: [Author Only](#) [Title Only](#) [Author and Title](#)

Langmead, B., and Salzberg, S.L. (2012). Fast gapped-read alignment with Bowtie 2. *Nat. Methods.* 9: 357-U354.

Pubmed: [Author and Title](#)

Google Scholar: [Author Only](#) [Title Only](#) [Author and Title](#)

Lee, D.K., Chung, P.J., Jeong, J.S., Jang, G., Bang, S.W., Jung, H., Kim, Y.S., Ha, S.H., Choi, Y.D., and Kim, J.K. (2017). The rice OsNAC6 transcription factor orchestrates multiple molecular mechanisms involving root structural adaptations and nicotianamine biosynthesis for drought tolerance. *Plant Biotechnol. J.* 15: 754-764.

Pubmed: [Author and Title](#)

Google Scholar: [Author Only](#) [Title Only](#) [Author and Title](#)

Lee, D.Y., Hayes, J.J., Dmitry, P., and Wolffe, A.P. (1993). A positive role for histone acetylation in transcription factor access to nucleosomal DNA. *Cell.* 72: 73-84.

Pubmed: [Author and Title](#)

Google Scholar: [Author Only](#) [Title Only](#) [Author and Title](#)

Li, Q., Lin, Y.C., Sun, Y.H., Song, J., Chen, H., Zhang, X.H., Sederoff, R.R., and Chiang, V.L. (2012). Splice variant of the SND1 transcription factor is a dominant negative of SND1 members and their regulation in *Populus trichocarpa*. *Proc. Natl. Acad. Sci. USA* 109: 14699-14704.

Pubmed: [Author and Title](#)

Google Scholar: [Author Only](#) [Title Only](#) [Author and Title](#)

Li, W., Lin, Y.C., Li, Q., Shi, R., Lin, C.Y., Chen, H., Chuang, L., Qu, G.Z., Sederoff, R.R., and Chiang, V.L. (2014). A robust chromatin immunoprecipitation protocol for studying transcription factor-DNA interactions and histone modifications in wood-forming tissue. *Nat. Protoc.* 9: 2180-2193.

Pubmed: [Author and Title](#)

Google Scholar: [Author Only](#) [Title Only](#) [Author and Title](#)

Li, W., Liu, H., Cheng, Z.J., Su, Y.H., Han, H.N., Zhang, Y., and Zhang, X.S. (2011). DNA methylation and histone modifications regulate de novo shoot regeneration in *Arabidopsis* by modulating WUSCHEL expression and auxin signaling. *PLoS Genet.* 7: e1002243.

Pubmed: [Author and Title](#)

Google Scholar: [Author Only](#) [Title Only](#) [Author and Title](#)

Lin, Y.C., Li, W., Chen, H., Li, Q., Sun, Y.H., Shi, R., Lin, C.Y., Wang, J.P., Chen, H.C., Chuang, L., Qu, G.Z., Sederoff, R.R., and Chiang, V.L. (2014). A simple improved-throughput xylem protoplast system for studying wood formation. *Nat. Protoc.* 9: 2194-2205.

Pubmed: [Author and Title](#)

Google Scholar: [Author Only](#) [Title Only](#) [Author and Title](#)

Lin, Y.C., Li, W., Sun, Y.H., Kumari, S., Wei, H., Li, Q., Tunlaya-Anukit, S., Sederoff, R.R., and Chiang, V.L. (2013). SND1 transcription factor-directed quantitative functional hierarchical genetic regulatory network in wood formation in *Populus trichocarpa*. *Plant Cell.* 25: 4324-4341.

Pubmed: [Author and Title](#)

Google Scholar: [Author Only](#) [Title Only](#) [Author and Title](#)

Mao, Y., Pavangadkar, K.A., Thomashow, M.F., and Triezenberg, S.J. (2006). Physical and functional interactions of *Arabidopsis* ADA2

transcriptional coactivator proteins with the acetyltransferase GCN5 and with the cold-induced transcription factor CBF1. *Biochim Biophys. Acta.* 1759: 69-79.

Pubmed: [Author and Title](#)

Google Scholar: [Author Only](#) [Title Only](#) [Author and Title](#)

McLeay, R.C., and Bailey, T.L. (2010). Motif Enrichment Analysis: a unified framework and an evaluation on ChIP data. *BMC Bioinformatics.* 11: 165.

Pubmed: [Author and Title](#)

Google Scholar: [Author Only](#) [Title Only](#) [Author and Title](#)

Mi, H., Muruganujan, A., Casagrande, J.T., and Thomas, P.D. (2013). Large-scale gene function analysis with the PANTHER classification system. *Nat. Protoc.* 8: 1551-1566.

Pubmed: [Author and Title](#)

Google Scholar: [Author Only](#) [Title Only](#) [Author and Title](#)

Monclus, R., Dreyer, E., Villar, M., Delmotte, F.M., Delay, D., Petit, J.M., Barbaroux, C., Le Thiec, D., Brechet, C., and Brignolas, F. (2006). Impact of drought on productivity and water use efficiency in 29 genotypes of *Populus deltoides* x *Populus nigra*. *New Phytol.* 169: 765-777.

Pubmed: [Author and Title](#)

Google Scholar: [Author Only](#) [Title Only](#) [Author and Title](#)

Msanne, J., Lin, J., Stone, J.M., and Awada, T. (2011). Characterization of abiotic stress-responsive *Arabidopsis thaliana* RD29A and RD29B genes and evaluation of transgenes. *Planta.* 234: 97-107.

Pubmed: [Author and Title](#)

Google Scholar: [Author Only](#) [Title Only](#) [Author and Title](#)

Nakashima, K., Yamaguchi-Shinozaki, K., and Shinozaki, K. (2014). The transcriptional regulatory network in the drought response and its crosstalk in abiotic stress responses including drought, cold, and heat. *Front Plant Sci.* 5: 170.

Pubmed: [Author and Title](#)

Google Scholar: [Author Only](#) [Title Only](#) [Author and Title](#)

Norton, V.G., Imai, B.S., Yau, P., and Bradbury, E.M. (1989). Histone acetylation reduces nucleosome core particle linking number change. *Cell.* 57: 449-457.

Pubmed: [Author and Title](#)

Google Scholar: [Author Only](#) [Title Only](#) [Author and Title](#)

Quinlan, A.R., and Hall, I.M. (2010). BEDTools: A flexible suite of utilities for comparing genomic features. *Bioinformatics.* 26: 841-842.

Pubmed: [Author and Title](#)

Google Scholar: [Author Only](#) [Title Only](#) [Author and Title](#)

Ragauskas, A.J., Williams, C.K., Davison, B.H., Britovsek, G., Cairney, J., Eckert, C.A, Frederick, W., Hallett, J., Leak, D., Liotta, C., Mielenz, J., Murphy, R., Templar, R., and Tschaplinski, T. (2006). The path forward for biofuels and biomaterials. *Science.* 311: 484-489.

Pubmed: [Author and Title](#)

Google Scholar: [Author Only](#) [Title Only](#) [Author and Title](#)

Ramegowda, V., Gill, U.S., Sivalingam, P.N., Gupta, A, Gupta, C., Govind, G., Nataraja, K.N., Pereira, A, Udayakumar, M., Mysore, K.S., and Senthil-Kumar, M. (2017). GBF3 transcription factor imparts drought tolerance in *Arabidopsis thaliana*. *Sci. Rep.* 7: 9148.

Pubmed: [Author and Title](#)

Google Scholar: [Author Only](#) [Title Only](#) [Author and Title](#)

Robinson, M.D., McCarthy, D.J., and Smyth, G.K. (2010). edgeR: a Bioconductor package for differential expression analysis of digital gene expression data. *Bioinformatics.* 26: 139-140.

Pubmed: [Author and Title](#)

Google Scholar: [Author Only](#) [Title Only](#) [Author and Title](#)

Roeder, R.G. (1996). The role of general initiation factors in transcription by RNA polymerase II. *Trends Biochem Sci.* 21: 327-335.

Pubmed: [Author and Title](#)

Google Scholar: [Author Only](#) [Title Only](#) [Author and Title](#)

Shahbazian, M.D., and Grunstein, M. (2007). Functions of site-specific histone acetylation and deacetylation. *Annu. Rev. Biochem.* 76: 75-100.

Pubmed: [Author and Title](#)

Google Scholar: [Author Only](#) [Title Only](#) [Author and Title](#)

Shen, L., Shao, N.Y., Liu, X., Maze, I., Feng, J., and Nestler, E.J. (2013). diffReps: detecting differential chromatin modification sites from ChIP-seq data with biological replicates. *PLoS One.* 8: e65598.

Pubmed: [Author and Title](#)

Google Scholar: [Author Only](#) [Title Only](#) [Author and Title](#)

Skirycz, A., and Inze, D. (2010). More from less: plant growth under limited water. *Curr. Opin. Biotechnol.* 21: 197-203.

Pubmed: [Author and Title](#)

Google Scholar: [Author Only](#) [Title Only](#) [Author and Title](#)

Song, J., Lu, S., Chen, Z.Z., Lourenco, R., and Chiang, V.L. (2006). Genetic transformation of *Populus trichocarpa* genotype Nisqually-1: a functional genomic tool for woody plants. *Plant Cell Physiol.* 47: 1582-1589.

- Pubmed: [Author and Title](#)
Google Scholar: [Author Only Title Only Author and Title](#)
- Song, L., Huang, S.C., Wise, A., Castanon, R., Nery, J.R., Chen, H., Watanabe, M., Thomas, J., Bar-Joseph, Z., and Ecker, J.R. (2016).** A transcription factor hierarchy defines an environmental stress response network. *Science*. 354: aag1550.
Pubmed: [Author and Title](#)
Google Scholar: [Author Only Title Only Author and Title](#)
- Stockinger, E.J., Mao, Y., Regier, M.K., Triezenberg, S.J., and Thomashow, M.F. (2001).** Transcriptional adaptor and histone acetyltransferase proteins in *Arabidopsis* and their interactions with CBF1, a transcriptional activator involved in cold-regulated gene expression. *Nucleic acids research*. 29: 1524-1533.
Pubmed: [Author and Title](#)
Google Scholar: [Author Only Title Only Author and Title](#)
- Tran, L.S., Nakashima, K., Sakuma, Y., Simpson, S.D., Fujita, Y., Maruyama, K., Fujita, M., Seki, M., Shinozaki, K., and Yamaguchi-Shinozaki, K. (2004).** Isolation and functional analysis of *Arabidopsis* stress-inducible NAC transcription factors that bind to a drought-responsive cis-element in the early responsive to dehydration stress 1 promoter. *Plant Cell*. 16: 2481-2498.
Pubmed: [Author and Title](#)
Google Scholar: [Author Only Title Only Author and Title](#)
- Tyree, M.T., and Sperry, J.S. (1989).** Vulnerability of Xylem to Cavitation and Embolism. *Annu. Rev. Plant Physiol. Plant Mol. Biol.* 1: 19-36.
Pubmed: [Author and Title](#)
Google Scholar: [Author Only Title Only Author and Title](#)
- Ueta, R., Abe, C., Watanabe, T., Sugano, S.S., Ishihara, R., Ezura, H., Osakabe, Y., and Osakabe, K. (2017).** Rapid breeding of parthenocarpic tomato plants using CRISPR/Cas9. *Sci. Rep.* 7: 507.
Pubmed: [Author and Title](#)
Google Scholar: [Author Only Title Only Author and Title](#)
- Vlachonasios, K.E. (2003).** Disruption mutations of *ADA2b* and *GCN5* transcriptional adaptor genes dramatically affect *Arabidopsis* growth, development, and gene expression. *Plant Cell*. 15: 626-638.
Pubmed: [Author and Title](#)
Google Scholar: [Author Only Title Only Author and Title](#)
- Wang, S., Sun, H., Ma, J., Zang, C., Wang, C., Wang, J., Tang, Q., Meyer, C.A., Zhang, Y., and Liu, X.S. (2013).** Target analysis by integration of transcriptome and ChIP-seq data with BETA. *Nat. Protoc.* 8: 2502-2515.
Pubmed: [Author and Title](#)
Google Scholar: [Author Only Title Only Author and Title](#)
- Weiste, C., and Droge-Laser, W. (2014).** The *Arabidopsis* transcription factor bZIP11 activates auxin-mediated transcription by recruiting the histone acetylation machinery. *Nat. Commun.* 5: 3883.
Pubmed: [Author and Title](#)
Google Scholar: [Author Only Title Only Author and Title](#)
- Wickham, H. (2009).** ggplot2: Elegant Graphics for Data Analysis. Springer Science & Business Media.
Pubmed: [Author and Title](#)
Google Scholar: [Author Only Title Only Author and Title](#)
- Widiez, T., Symeonidi, A., Luo, C., Lam, E., Lawton, M., and Rensing, S.A. (2014).** The chromatin landscape of the moss *Physcomitrella patens* and its dynamics during development and drought stress. *Plant J.* 79: 67-81.
Pubmed: [Author and Title](#)
Google Scholar: [Author Only Title Only Author and Title](#)
- Wu, Y., Deng, Z., Lai, J., Zhang, Y., Yang, C., Yin, B., Zhao, Q., Zhang, L., Li, Y., Yang, C., and Xie, Q. (2009).** Dual function of *Arabidopsis* ATAF1 in abiotic and biotic stress responses. *Cell Res.* 19: 1279-1290.
Pubmed: [Author and Title](#)
Google Scholar: [Author Only Title Only Author and Title](#)
- Yoshida, T., Fujita, Y., Sayama, H., Kidokoro, S., Maruyama, K., Mizoi, J., Shinozaki, K., and Yamaguchi-Shinozaki, K. (2010).** AREB1, AREB2, and ABF3 are master transcription factors that cooperatively regulate ABRE-dependent ABA signaling involved in drought stress tolerance and require ABA for full activation. *Plant J.* 61: 672-685.
Pubmed: [Author and Title](#)
Google Scholar: [Author Only Title Only Author and Title](#)
- Zentner, G.E., and Henikoff, S. (2013).** Regulation of nucleosome dynamics by histone modifications. *Nature Struct. Mol. Biol.* 20: 259-266.
Pubmed: [Author and Title](#)
Google Scholar: [Author Only Title Only Author and Title](#)
- Zhou, J., Wang, X., He, K., Charron, J.B., Elling, A.A., and Deng, X.W. (2010).** Genome-wide profiling of histone H3 lysine 9 acetylation and dimethylation in *Arabidopsis* reveals correlation between multiple histone marks and gene expression. *Plant. Mol. Biol.* 72: 585-595.
Pubmed: [Author and Title](#)
Google Scholar: [Author Only Title Only Author and Title](#)

Zhou, S., Jiang, W., Long, F., Cheng, S., Yang, W., Zhao, Y., and Zhou, D.X. (2017). Rice homeodomain protein WOX11 recruits a histone acetyltransferase complex to establish programs of cell proliferation of crown root meristem. *Plant Cell*. 29: 1088-1104.

Pubmed: [Author and Title](#)

Google Scholar: [Author Only](#) [Title Only](#) [Author and Title](#)

Histone Acetylation Cooperating with AREB1 Transcription Factor Regulates Drought Response and Tolerance in *Populus trichocarpa*

Shuang Li, Ying-Chung Jimmy Lin, Pengyu Wang, Baofeng Zhang, Meng Li, Su Chen, Rui SHI, Sermsawat Tunlaya-Anukit, Xinying Liu, Zhifeng Wang, Xiufang Dai, Jing Yu, Chenguang Zhou, Baoguang Liu, Jack P. Wang, Vincent L. Chiang and Wei Li
Plant Cell; originally published online December 11, 2018;
DOI 10.1105/tpc.18.00437

This information is current as of December 27, 2018

Supplemental Data	/content/suppl/2018/12/11/tpc.18.00437.DC1.html
Permissions	https://www.copyright.com/ccc/openurl.do?sid=pd_hw1532298X&issn=1532298X&WT.mc_id=pd_hw1532298X
eTOCs	Sign up for eTOCs at: http://www.plantcell.org/cgi/alerts/ctmain
CiteTrack Alerts	Sign up for CiteTrack Alerts at: http://www.plantcell.org/cgi/alerts/ctmain
Subscription Information	Subscription Information for <i>The Plant Cell</i> and <i>Plant Physiology</i> is available at: http://www.aspb.org/publications/subscriptions.cfm